OSCILLATING-FIELD CURRENT-DRIVE SCHEMES FOR TOKAMAKS

Thesis by

Mark Alan Schalit

In Partial Fulfillment of the Requirements

for the Degree of

Doctor of Philosophy

California Institute of Technology

1989

(Submitted February 16, 1989)

This work is dedicated to my parents

and to my wonderful sister Laurie,

for their love and support.

ACKNOWLEDGEMENTS

I would like to thank my advisor, Professor Paul Bellan, for his skillful guidance, and for the personal encouragement I received during my graduate studies. It was a privilege to be a member of Professor Bellan's plasma physics group, an enriching experience that I will never forget. I have benefited from personal discussions with a number of Caltech faculty members, all of whom I admire greatly: Professor Noel Corngold, Professor Eugene Cowan, Professor Roy Gould, Professor Herbert Keller, and Professor Phillip Saffman. Special thanks to Dr. Michael Brown for carefully reading this thesis and for sharing his infectious enthusiasm for plasma physics. Thanks go to Dr. Jon McChesney, (soon to be Dr.'s) Hoanh Vu, and Andrew Bailey for many stimulating discussions. Special thanks to my friend Paula Samazan for a healthy dose of warm humor and philosophy.

I am grateful for financial support provided by the Rockwell International Corporation and the Hughes Aircraft Fellowship Program.

ABSTRACT

A novel current-drive scheme for steady-state tokamak operation is investigated in which external coils are applied to induce time-periodic fluid-type, fluctuations within the plasma; a nonlinear interaction between these fluctuations results in a time-averaged EMF, which maintains the large-scale magnetic field against Ohmic dissipation. Analytical and numerical modeling of this current-drive scheme is presented for low-frequency schemes (where the nonlinear $< \vec{u} \times \vec{b} >$ EMF is dominant) and for higher-frequency schemes (where the $< \vec{j} \times \vec{b} >$ Hall EMF is dominant). The Hall EMF is dominant at frequencies well above the ion-cyclotron frequency (referred to the strength of the static axial field) — except in the case of the rotamak, where the oscillating electric field is in the same direction as the static axial field.

A figure-of-merit for these current-drive schemes is the ratio of the strength of the static axial current to the strength of the oscillating current. This ratio is always much less than unity in all standard MHD calculations. As the electron-ion collision frequency vanishes, the ratio approaches infinity for the case of the rotamak. The ratio also approaches infinity for the $m = 1$ analogue of the rotamak — but only in the restrictive case where the static axial field becomes vanishingly small and where the DC magnetic fields are a small fraction of the AC magnetic fields. For the $m = 1$ analogue, the currents are confined to a skin layer as the axial field becomes very large, with the ratio of DC current strength to the oscillating current strength approaching unity.

The analysis presented here is compared and contrasted with existing theories and to a number of recent experiments.

TABLE OF CONTENTS

Acknowledgements iii

Abstract iv

Table of Contents v

Figures vii

Chapter 1. Introduction 1

Chapter 2. The Search for an MHD Dynamo 10

2.1 Dynamical Model of Bellan 12

2.2 Mode-Beating Model With Finite Pressure 15

2.3 Exact Solutions With Helical Symmetry 19

2.4 An Antidynamo Argument 27

Chapter 3. Models Based on Hall MHD Equations 31

3.1 Basic Equations and Boundary Conditions 44

3.1.1 Boundary Conditions at $r = r_c$ 52

3.1.2 Boundary Conditions at $r = 1$ 54

3.1.3 Boundary Conditions as $r \to 0$ 55

3.1.4 Boundary Conditions: Summary 56

3.2 Description of Numerical Methods 57

3.3 Role of Flux-Conserving Velocity Fields 60

3.4 Definition and Manipulation of a-type and b-type Vectors 63

3.5 DC Flux-Conserving Motions 65

3.6 Solutions of System S_1 as $\epsilon \to 0$ 72

3.6.1 The Limit $\alpha \to 0$, $k < 1$, B_a = fixed 77

3.6.2 The Limit $\alpha \to 0$, k = fixed, $B_a \to 0$ 79

3.6.3 The Limit α = fixed, k = fixed, $B_a \to \infty$ 81

3.7 Validity of the System S_1 85

3.8 Conservation Laws 88

3.8.1 Energy Conservation and Poynting Theorem 89

3.8.2 Magnetic Helicity Conservation 91

3.8.3 Momentum Conservation and Current-Drive Efficiency 94

3.9 Comparison With Experiment 96

Chapter 4. Summary and Conclusions 99

Appendix 1. Regularity Rules of Ralph Lewis 106

Appendix 2. Comments on the Calculation of Dutch and McCarthy 111

Appendix 3. Solution of System S_1 for Large Resistivity 112

References 114

FIGURES

Fig. 1.1 Endless loop of plasma with poloidal and toroidal directions indicated. 2

Fig. 1.2 Idealized sketch of an inductively driven tokamak. 2

Fig. 1.3 Sketch of the rhythmac configuration. 2

Fig. 1.4 Thesis format. 9

Fig. 2.1 Radial velocity and poloidal magnetic field for a low-β plasma. 17

Fig. 2.2 Toroidal plasma undergoing $m = 0$ MHD activity. 28

Fig. 3.1(a) Idealized sketch of the rotamak. 32

Fig. 3.1(b) Compact torus configuration. 32

Fig. 3.2(a) Nonzero k analogue of the rotamak 32

Fig. 3.2(b) Rhythmac configuration 32

Fig. 3.3 Basic Equations and Boundary Conditions for Hall MHD model. 45

Fig. 3.4 Schematic representation of the Hall MHD perturbation scheme. 70

Fig. 3.5 Plot of steady currents, J_θ and J_z. 78

Fig. 3.6 Analytical and numerical solutions of S_1 for the case $B_a = 0$, $\alpha = 0.2$. 80

Fig. 3.7 Contour plots of $I_z(k, B_a)$ 84

Fig. 3.8 Schematic representation of major thesis results 103

Chapter 1. Introduction

This thesis addresses the problem of how to drive a steady electrical current in an endless loop of plasma [Fig.(1.1)]. A tokamak fusion reactor is an example of an endless loop of plasma: A hot plasma of deuterium or tritium is contained within a toroidal vessel by magnetic fields that run in both the poloidal and toroidal directions. External coils wrapped around the torus in the poloidal direction produce a strong toroidal magnetic field within the plasma, which is needed for plasma stability. A strong toroidal current within the plasma itself produces poloidal magnetic field lines that serve to maintain pressure equilibrium. The toroidal current is also needed to heat the plasma.

The most common way to drive a toroidal current in a tokamak is to make the torus the secondary of a transformer [Fig.(1.2)]. The time-changing flux through the center of the torus generates a toroidal electric field, which drives a toroidal current. This arrangement suffers the disadvantage of requiring pulsed operation, with the plasma being created and destroyed with each pulse of the transformer. As outlined in the work of Fisch[1], there are a number of reasons that pulsed reactor operation is undesirable. For example, heat stress and mechanical stress associated with pulsed operation shortens the lifetime of reactor materials. Plasmas are often stable only in a limited parameter range. During pulsed operation, the plasma must go through a sequence of parameter regimes, some of which may cause undesirable disruptions; continuous operation, on the other hand, permits a single, stable operating regime. The apparatus for continuous operation is likely to be less unwieldy, and will free the center of the torus for other applications. Finally, there is less downtime in a steady-state reactor since there is no need to reset a transformer. For all of these

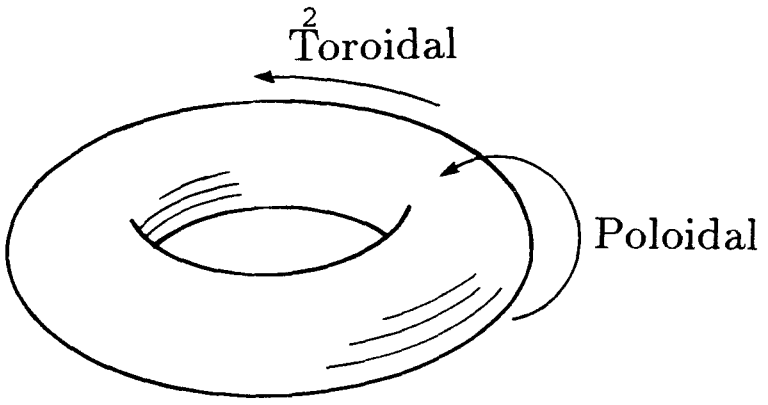

Figure 1.1. An endless loop of plasma with the toroidal and poloidal directions indicated.

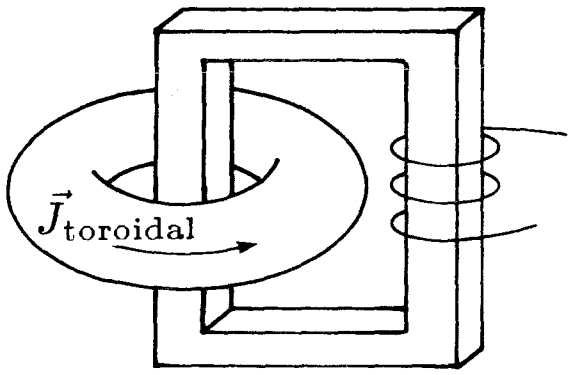

Figure 1.2. Idealized sketch of an inductively driven tokamak. The torus is the secondary of a transformer.

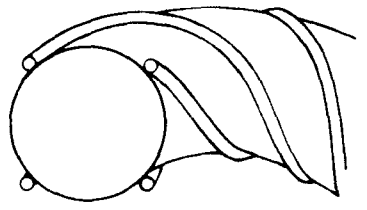

Figure 1.3. The $m = 1$, $k \neq 0$ rhythmac configuration. The current is the same at each point along a given helical filament. The current in adjacent filaments is phased 90° apart.

reasons, the goal of achieving steady-state tokamak current-drive is of enormous importance to fusion technology.

A number of other steady-state schemes — neutral beam injection, RF current-drive at the lower-hybrid and electron-cyclotron frequency — have been proposed and have been demonstrated successfully in the laboratory[1]. In lower-hybrid RF current-drive, the incident radiation transfers momentum to electrons by a process known as Landau damping. Only plasma electrons moving at near the phase velocity of the lower-hybrid wave receive momentum from the wave. In electron-cyclotron current-drive, the incident radiation is tuned in frequency to correspond to an electron-cyclotron resonance condition. A common point in these RF schemes is that the current is carried by only a subgroup of electrons in the velocity distribution that happen to fulfill a resonance condition. The electrons that carry the current have velocities well in excess of the electron thermal velocity.

Another class of noninductive, steady-state current-drive schemes is explored here. In these schemes, the plasma is envisioned as an interpenetrating *fluid* of ions and electrons. External coils with time-periodic currents are used to induce small fluid-type fluctuations within the plasma; a nonlinear interaction between these fluctuations results in a net DC EMF, which is used to maintain the large-scale magnetic field against Ohmic dissipation. In contrast to the RF schemes referred to above, the incident radiation imparts momentum to the entire electron fluid rather than to a subgroup of electrons that are resonant with the wave. The dynamo theory of cosmic bodies, such as the earth or sun, relies on a similar mechanism, where fluid motions deep within these spinning bodies generate and maintain a large-scale magnetic field. An example of such a scheme is the "rhythmac[3,4]," shown in

Fig.(1.3), which relies on helical external coils, phased 90° apart, to generate both poloidal and toroidal currents. The label "oscillating field current drive (OFCD)" was originally coined by a group at Los Alamos[5,6] to describe their current-drive experiments on the reversed field pinch (RFP). However, in this thesis, the term OFCD will take on a broader meaning and will refer to any scheme that relies on the application of time-periodic external coils to drive a net DC current.

One might adopt the point of view that a new plasma device is borne if external coils are wrapped around the torus and if the Ohmic heating transformer is removed. Although this is a matter of semantics, it is not clear whether one then has a tokamak employing a novel current drive scheme or a new fusion device, altogether. In this thesis, we are searching for small-amplitude field oscillations capable of sustaining the large-scale fields of a tokamak discharge. The oscillating fields are envisioned as tiny perturbations superimposed over the large zero-order tokamak fields; the favorable stability properties of the tokamak configuration are hopefully preserved. In this sense, it is probably more appropriate to say that we are searching for a new tokamak current-drive scheme, rather than for a new toroidal plasma device, altogether.

Many of the OFCD schemes are guided by considerations of the input and dissipation of magnetic helicity. The quantity $\int \vec{A} \cdot \vec{B}\, d^3x$ (where $\vec{B}$ is the magnetic field , $\nabla \times \vec{A} = \vec{B}$ and $\vec{A} \cdot \vec{B}$ is the magnetic helicity density) is a measure of the structural complexity of the magnetic field topology [see Ref.(23), Sec.(2.1)]. For example, magnetic flux tubes that are twisted into interlinking knots carry a higher helicity content than flux tubes that are not linked. From Faraday's law and

$\nabla \cdot \vec{B} = 0$ *alone*, it follows that the helicity density obeys the conservation law,

$$\frac{\partial}{\partial t}\left(\vec{A}\cdot\vec{B}\right) + \nabla\cdot\left(\phi\vec{B} + \vec{E}\times\vec{A}\right) + 2\vec{E}\cdot\vec{B} = 0 \ .$$

[This equation is derived and discussed in Sec.(3.8.2)]. The surface flux of helicity is given by $\phi\vec{B} + \vec{E}\times\vec{A}$, and $\vec{E}\cdot\vec{B}$ represents the volume dissipation (or source) of magnetic helicity. It should be noted that the helicity density $\vec{A}\cdot\vec{B}$ is not gauge-invariant; however, the helicity conservation equation stated above is valid for any choice of gauge. It should be reiterated that the helicity conservation equation given above is a manifestation of Faraday's law and $\nabla\cdot\vec{B} = 0$ alone; the equation has nothing to do with the underlying dynamics of the system under study. It is possible to inject magnetic helicity into a vacuum region, into a simple conductor, or into a plasma. For the case where the system under study obeys a form of Ohm's law [e.g., $\vec{E} = \eta\vec{J}$ (conductor), $\vec{E} + \vec{U}\times\vec{B} = \eta\vec{J}$ (standard MHD), $\vec{E} - \frac{1}{ne}\vec{J}\times\vec{B} = \eta\vec{J}$ (Hall MHD)], the helicity dissipation term becomes $2\eta\vec{J}\cdot\vec{B}$. For a tokamak with a DC toroidal current $\vec{J}_0$ parallel to a large toroidal field $\vec{B}_0$, some method must be devised to replace the resulting helicity dissipation, $2\eta\vec{J}_0\cdot\vec{B}_0$.

As proposed by Bevir and Gray[7] and by others[2,8], the time-averaged helicity flux $< \vec{e}\times\vec{a} >$ at the plasma surface can, in principle, be used to replenish the helicity dissipation $2\eta\vec{J}_0\cdot\vec{B}_0$ within the torus (throughout this thesis, lower-case variables will generally denote time-periodic quantities, whereas upper-case variables will denote DC quantities). This process is referred to as "AC helicity injection." However, it must be noted that the injection of magnetic helicity alone does not imply that a useful DC current will emerge. For example, suppose that a circularly polarized EM wave impinges on a slab of copper ($\vec{E} = \eta\vec{J}$). The circularly polarized wave carries with it a net magnetic helicity flux, which enters the

copper slab and is deposited within a skin layer. However, a net DC current cannot arise here since there is no nonlinear interaction to couple the oscillating fields. The point here is that the helicity dissipation term $\eta < \vec{J} \cdot \vec{B} >$ can be decomposed into a DC dissipation term $2\eta \vec{J}_0 \cdot \vec{B}_0$ and an AC dissipation term $2\eta < \vec{j} \cdot \vec{b} >$; in the case of a simple conductor, all of the incident helicity is consumed by the oscillating fields (this feature of the helicity conservation equation is further discussed in the work of Bellan[10]). For OFCD schemes to be realized, one must have AC injection of helicity with predominantly DC dissipation. The amount of AC vs. DC dissipation obtained is beyond the scope of the magnetic helicity conservation equation and can be explored only by considering the dynamics of the system under study.

In addition to magnetic helicity, it is of vital interest to consider the injection of momentum into the plasma in a description of OFCD schemes. From Maxwell's equations *alone*, the momentum conservation equation reads, in MKS units,

$$\frac{\partial}{\partial t}\left(\epsilon_0 \vec{E} \times \vec{B}\right) + \nabla \cdot \left\{ \left(\frac{B^2}{2\mu_0} + \frac{\epsilon_0 E^2}{2} \right) \bar{\bar{I}} - \left(\frac{\vec{B}\vec{B}}{\mu_0} + \epsilon_0 \vec{E}\vec{E} \right) \right\} + \rho \vec{E} + \vec{J} \times \vec{B} = 0 \ ,$$

where the tensor in the curly brackets is the Maxwell stress tensor. The stress tensor has units of a momentum flux (momentum per unit area per unit time). Consider a straight cylindrical surface surrounding a plasma, centered about the z axis. Suppose that a traveling EM wave of the form $e^{i(kz-\omega t)}$ is maintained at the cylindrical surface. Klima[11] has shown from the stress tensor alone that

$$(z - \text{component of injected momentum}) = \frac{k}{\omega} (\text{injected power}) \ .$$

[Klima's result is discussed further in Sec.(3.8.3)]. This result states that all traveling waves impart momentum (assuming that power is being injected), regardless

of the detailed dynamics of the plasma. It has been observed experimentally (on devices such as the "rotamak[12]," the "synchromac[13,14]," and the "rhythmac[3,4,15,16]) " that maintaining a traveling wave at the plasma surface results in a net DC current. Schemes that rely, instead, on a standing wave pattern are capable of injecting magnetic helicity — but not momentum.

However, one must note that the injected momentum can also be consumed by the oscillating fields (because of the AC momentum dissipation term, $< \vec{j} \times \vec{b} >$); there is again a competition between DC momentum dissipation and AC momentum dissipation. As an example, maintaining a traveling wave at the surface of a copper cylinder ($\vec{E} = \eta \vec{J}$) will not result in a net DC current; the injected momentum is consumed by the oscillating fields. An interesting situation occurs if the medium under consideration satisfies the Hall form of Ohm's law, $\vec{E} - (1/ne)\vec{J} \times \vec{B} = \eta \vec{J}$. At the same time, it is consistent to assume that the charge density ρ vanishes, since quasi-neutrality is usually assumed in MHD models. The momentum dissipation term now becomes becomes $ne(\vec{E} - \eta \vec{J})$. As we shall see in Chapter 3, we can rule out the possibility of generating static electric fields (a consequence of the geometry and boundary conditions) leaving only $< -ne\eta \vec{J} >$ as the time-averaged momentum dissipation term. It follows that the net injected momentum must generate a static DC current. The resulting absence of a nonlinear dissipation term explains the success of Hall MHD models, which are discussed in Chapter 3.

The OFCD schemes can be divided broadly into two categories: (1) "laminar," and (2) "turbulent." The latter category makes use of the Taylor[17] principle, which states that a plasma relaxes spontaneously to a state of minimum energy while conserving magnetic helicity. This is a simple way to account for the complicated

plasma dynamics. If the helicity flux is known at the plasma surface and if the plasma is assumed to relax to the Taylor state, then one can predict the necessary external currents and parameters for OFCD operation. This is the basis for OFCD schemes for the RFP (also called $F - \Theta$ pumping) proposed by Schoenberg[5,6] et al., Finn[18], Strauss and Harned[19] and Nebel[20] et al. . In laminar theories, one searches for coherent wave motion capable of sustaining magnetic fields against Ohmic dissipation through a nonlinear interaction in Ohm's law. All of the schemes explored in this work are laminar theories.

The format of this thesis is outlined in tree-diagram form in Fig.(1.4). All of the models used in this thesis are ultimately derived from the two-fluid plasma equations, Eqs.(3.3)-(3.4). For low frequencies and long wavelengths, the standard MHD equations provide an adequate approximation to the full two-fluid equations. At these low frequencies, the $< \vec{u} \times \vec{b} >$ EMF in Ohm's law is the dominant current-drive mechanism [LHS of tree in Fig.(1.4)]; at higher frequencies, the $< \vec{j} \times \vec{b} >$ Hall EMF is the dominant nonlinear current-drive mechanism [RHS of tree in Fig.(1.4)]. The range of frequencies for the validity of each regime is discussed in detail in Chapter 3. In the low-frequency regime, current-drive schemes with azimuthal symmetry ($m = 0$, $k = 0$) and with helical symmetry ($m \neq 0$, $k \neq 0$) are analyzed in detail. Like a rat in a maze, we found that all paths on the LHS of the tree in Fig.(1.4) lead to a dead-end; we were unable to uncover a viable low-frequency current-drive scheme based on the standard MHD equations. However, the higher-frequency schemes, based on the $< \vec{j} \times \vec{b} >$ Hall EMF, show promise theoretically and in the laboratory. This thesis represents the most complete analytical and numerical work to date on the $< \vec{j} \times \vec{b} >$ current-drive schemes for nonzero k.

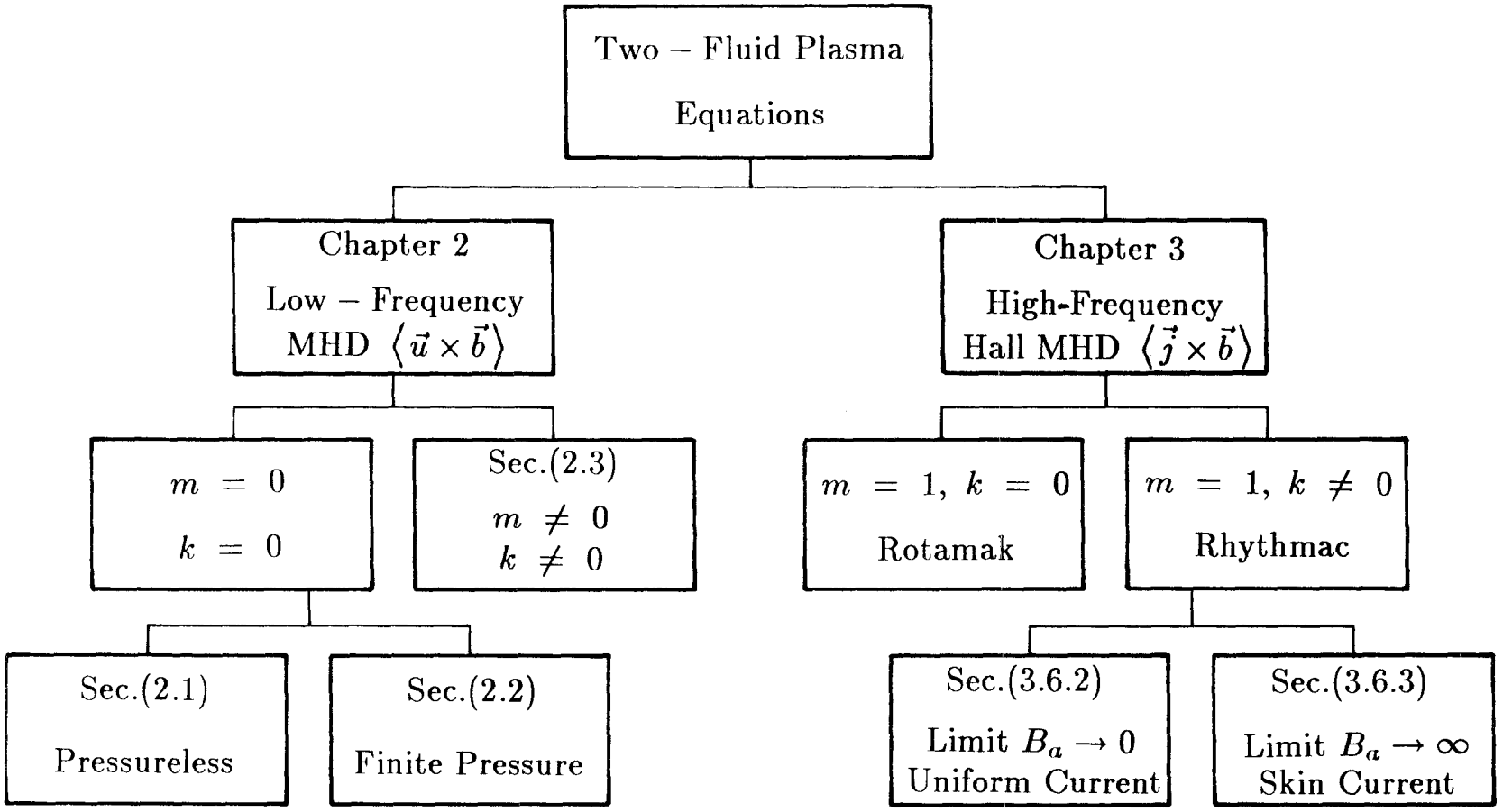

Figure 1.4. Thesis format. All models are ultimately derived from the two-fluid plasma equations. Low-frequency schemes (LHS of tree) rely on the $< \vec{u} \times \vec{b} >$ EMF in Ohm's law, whereas higher-frequency schemes (RHS of tree) rely on the $< \vec{j} \times \vec{b} >$ Hall EMF.

Chapter 2. The Search For an MHD Dynamo

This chapter is devoted to MHD laminar models of OFCD. We begin in Sec.(2.1) by examining an $m = 0$ scheme proposed by Bellan[21], in which the toroidal and poloidal fields of a tokamak are modulated 90° out of phase. Modulation of the toroidal field results in a radial compression of the plasma; the radial velocity u_r associated with this compressional Alfvenic motion interacts with the oscillating poloidal field b_p (which resides in a skin layer) to produce a time-averaged toroidal EMF, $< u_r b_p >$. The resulting EMF resides in a narrow skin layer near the wall, and Bellan's original model is very sensitive to assumptions made regarding the plasma/wall interaction. Three different models have been proposed to describe the plasma dynamics near the wall. In the original model, the radial fluid velocity does not vanish at the wall and a source of plasma must exist to maintain a finite flux of plasma to and from the wall. Liewer[22] et al. have studied an alternate model in which a vacuum region exists, separating the plasma from the wall; it was found that the motion of the plasma/vacuum interface significantly reduces the toroidal EMF. Bellan[10] has explained the adverse effect of a moving plasma boundary by applying the magnetic helicity conservation equation with a Lagrangian term that takes into account the movement of the plasma surface. In Sec.(2.2) a third model is presented, which includes finite pressure. In this case it is possible to eliminate the movement of the plasma boundary entirely and yet still have dynamo action within a skin layer near the plasma surface. However, the conclusions are as pessimistic as those of Liewer, and it is again found that the driven DC poloidal magnetic field is a small fraction of the oscillating poloidal field.

Investigators in dynamo theory have found that too much symmetry precludes

dynamo action[23]. In Sec.(2.4), MHD models that possess $m = 1$ structure are analyzed. The model has three potential advantages: (1) Only $m = 1$ modes can have a finite, time-averaged EMF at the magnetic axis (a consequence of the "regularity rules" discussed in Appendix.1); (2) the model breaks the symmetry that may have precluded dynamo action in the earlier models; and (3) the resulting velocity field contains helicity ($\vec{U} \cdot \nabla \times \vec{U}$) which, according to kinematic dynamo theory, is necessary for dynamo action [see Chapter 7 of Ref.(23)].

Here we give a brief overview of the mathematical techniques used in Secs.(2.1)-(2.3). The standard MHD equations are taken as the fundamental set of equations. In each case, the equations are linearized about a zero-order equilibrium that includes a uniform, static magnetic field. Linearizing is appropriate here since, as mentioned before, we envision the case where the oscillating fields are a small perturbation superimposed over a large, zero-order field. Taking a static, uniform magnetic field to zero-order is not as realistic as one might wish since tokamaks have considerable magnetic shear; however, the uniform field is adopted to make the mathematics tractable. Adding magnetic shear results in an interesting problem mathematically (a challenging fourth-order WKB problem) but serves only to clutter the physical ideas. The linearized equations are next Fourier-analyzed to achieve a set of ODE's. After the perturbed fields are evaluated, the EMF $< \vec{u} \times \vec{b} >$ is calculated.

Sec.(2.4) is devoted to the argument given by Professor Roy Gould[24], based on Faraday's law, which shows that time-periodic MHD models preclude significant dynamo action. This analysis seems to account for the weak dynamo effect found in the previous models.

2.1 Dynamical Model of Bellan

Bellan[21] has suggested a dynamical MHD model that relies on a nonlinear interaction between a resistive diffusion mode and an Alfvenic mode to sustain a toroidal current. In practice, the Alfvenic mode can be created by oscillating the toroidal field coils, resulting in a radial compression of the plasma. The resistive diffusion mode can be created by modulating the Ohmic heating transformer; the resulting oscillating poloidal field penetrates a distance equal to the classical skin depth. We begin the description of this model by stating the MHD equations, in a dimensionless form that will be used throughout this chapter:

$$\frac{\partial \rho}{\partial t} = -\nabla \cdot \rho \vec{U} \quad ,$$

$$\frac{dP}{dt} = -\gamma P \nabla \cdot \vec{U} \quad ,$$

$$\frac{\partial \vec{B}}{\partial t} = \eta \nabla^2 \vec{B} + \nabla \times \left(\vec{U} \times \vec{B} \right) \quad ,$$

$$\rho \frac{d\vec{U}}{dt} = -\nabla \left(P + B^2/2 \right) + \vec{B} \cdot \nabla \vec{B} \quad .$$

This mode-beating model can be illustrated with a simple slab model ($\nabla = \hat{x} \frac{\partial}{\partial x}$), where the coordinates (x, y, z) represent the "radial," "poloidal," and "toroidal" directions, respectively. The MHD equations are linearized about a uniform equilibrium, $B_a \hat{z}$, ρ_0, P_0, $\vec{U} = 0$, yielding,

$$\frac{\partial \rho}{\partial t} = -\rho_0 \frac{\partial u}{\partial x} \quad , \tag{2.1}$$

$$\frac{\partial p}{\partial t} = -\gamma P_0 \frac{\partial u}{\partial x} \quad , \tag{2.2}$$

$$\rho_0 \frac{\partial u}{\partial t} = -\frac{\partial}{\partial x} \left(p + B_a b_z \right) \quad , \tag{2.3}$$

$$\frac{\partial b_z}{\partial t} = -B_a \frac{\partial u}{\partial x} + \eta \frac{\partial^2 b_z}{\partial x^2} \quad , \tag{2.4}$$

$$\frac{\partial b_y}{\partial t} = \eta \frac{\partial^2 b_y}{\partial x^2} \quad , \tag{2.5}$$

where u is the $\hat{x}$ component of the velocity field. For a low-beta plasma, the pressure can be neglected in Eq.(2.3). The resistive term on the RHS of Eq.(2.4) can be neglected for the case of low resistivity. Eqs.(2.3)-(2.5) then form a closed system for the variables u, b_y, and b_z. Assuming $e^{i(kx-\omega t)}$ dependence then yields

$$-i\omega\rho_0 u = -ikB_a b_z \quad , \tag{2.6}$$

$$-i\omega b_z = -ikB_a u \quad , \tag{2.7}$$

$$-i\omega b_y = -k^2 \eta b_y \quad . \tag{2.8}$$

The poloidal field, given by Eq.(2.8), decouples from all other fields and vanishes outside a resistive skin layer,

$$b_y = \tilde{b}_y \ \mathrm{Re}\ e^{i(\kappa x-\omega t)} \quad , \tag{2.9}$$

where $\kappa = \sqrt{(i\omega)/\eta}$. Combining Eqs.(2.6)-(2.7) gives the dispersion for Alfven waves,

$$\omega = kv_a \quad , \qquad v_a^2 = \frac{B_a^2}{\rho_0} \quad . \tag{2.10}$$

The velocity field associated with this compressional Alfven wave is given by

$$u = \tilde{u} \ \mathrm{Re}\ e^{i[(\omega/v_a)x-\omega t]} \quad . \tag{2.11}.$$

For simplicity, it is assumed that plasma exists to the right of a rigid boundary located at $x = 0$. Within a skin layer of width $\sim 1/\kappa$, the EMF generated through

the interaction of the resistive mode and the Alfvenic mode is roughly $\sim \tilde{u}\tilde{b}_y$. The driven toroidal current then scales as $J_z^{\text{driven}} \sim (\tilde{u}\tilde{b}_y)/\eta$, and the poloidal field driven by this current is roughly $B_y^{\text{driven}} \sim J_z^{\text{driven}}/\kappa$, or

$$B_y^{\text{driven}} \sim \frac{\tilde{u}\tilde{b}_y}{\sqrt{\omega\eta}} \quad . \tag{2.12}$$

From Eq.(2.7), $\tilde{u} \sim v_a(\tilde{b}_z/B_a)$ and substitution into Eq.(2.12) yields

$$\frac{B_y^{\text{driven}}}{\tilde{b}_y} \sim \frac{v_a}{\sqrt{\omega\eta}}\frac{\tilde{b}_z}{B_a} \quad . \tag{2.13}$$

For a tokamak plasma, the oscillating fields must be a fraction of the steady toroidal and poloidal fields (i.e., $B_y^{\text{driven}}/\tilde{b}_y \gg 1$, $\tilde{b}_z/B_a \ll 1$); according to Eq.(2.13), this can occur for low driving frequencies and low resistivity.

From Eq.(2.11) it is apparent that the radial velocity does not vanish at the rigid boundary located at $x = 0$. A source of plasma must therefore be delivered at $x = 0$ in order to maintain the finite flux of plasma to the wall. Such a model may be unrealistic and Liewer[22] et al. have studied an extension of the model in which a vacuum region exists, separating the plasma from the wall; the plasma/vacuum interface must then quiver in the radial direction. As shown by Liewer, this movement reduces the resulting current-drive mechanism significantly. Bellan[10] has explained the adverse effect of a moving plasma boundary in terms of the magnetic helicity conservation equation. In conclusion, the mode-beating model described in this section may provide a useful mechanism — but only if plasma is created and destroyed at the wall in such a way that the resistivity can be considered uniform at all locations and at all times. If, instead, it is more realistic to envision a vacuum region that separates the plasma from the wall, then the current-drive scheme will fail.

2.2 Mode-Beating Model with Finite Pressure

It was shown in the last section that an MHD dynamo could result through the interaction of a compressional Alfven mode and a resistive diffusion mode. The model was very sensitive to assumptions regarding the plasma behavior near the wall. If a vacuum region separates the plasma from the wall, then the position of the plasma/vacuum interface must quiver in the radial direction; Liewer showed that the driven current is significantly reduced in this case. As illustrated here, the radial motion of the boundary can be eliminated by adding finite pressure in the MHD equations (this is yet another way to model the plasma behavior at the wall).

In slab geometry, the pressureless MHD equation of motion reads,

$$\rho \frac{dU}{dt} = JB \ ,$$

where U is the x component of the velocity, J is the y-component of the current density, and B is the z-component of the magnetic field. Ohm's law reads,

$$E - UB = \eta J \ ,$$

where E is the y-component of the electric field. If the fluid velocity is to vanish at $x = 0$, then the Lorentz force JB must also vanish at $x = 0$ since a fluid element at the wall cannot move. If both J and U vanish at $x = 0$, then from Ohm's law it follows that E vanishes at the wall. *The slab system without pressure therefore precludes the possibility of magnetic helicity injection since the helicity flux at $x = 0$ is proportional to the electric field.*

By including finite pressure in the MHD equations, it is possible to set $U = 0$ at the wall and yet still prescribe the electric field; the slab system can then be

used to study the injection of magnetic helicity. Assuming $e^{i(kx-\omega t)}$ dependence in Eqs.(2.1)-(2.5) (with ω real) for all perturbed quantities gives

$$\frac{\rho}{\rho_0} = \frac{k}{\omega} u \ , \tag{2.14}$$

$$\frac{p}{P_0} = \gamma \frac{k}{\omega} u \ , \tag{2.15}$$

$$-\omega \rho_0 u + k(p + B_a b_z) = 0 \ , \tag{2.16}$$

$$\frac{b_z}{B_a} = \frac{k}{\omega + i\eta k^2} u \ , \tag{2.17}$$

$$i\omega b_y = \eta k^2 b_y \ . \tag{2.18}$$

The poloidal field, given by Eq.(2.18), decouples from all other fields and vanishes outside a resistive skin layer,

$$b_y = \tilde{b}_y \mathrm{Re}\, e^{i(\kappa x - \omega t)} \ ,$$

where $\kappa = \sqrt{(i\omega)/\eta}$. Combining Eqs.(2.15)-(2.17) gives the dispersion,

$$k^4 \left(\frac{i\eta c_s^2}{\omega}\right) + k^2 (v_A^2 + c_s^2 - i\eta\omega) - \omega^2 = 0 \ ,$$

where $c_s^2 = (\gamma P_0)/\rho_0$ (sound speed), $v_A^2 = B_a^2/\rho_0$ (Alfven speed). For small η , the dispersion admits two solutions, which we shall label "resistive"(res) and "ideal":

$$k_{\mathrm{ideal}} = \frac{\omega}{\sqrt{v_A^2 + c_s^2}} \qquad k_{\mathrm{res}} = \sqrt{\frac{i\omega}{\eta}} \sqrt{1 + \beta^{-1}} \ ,$$

where $\beta^{-1} = v_A^2/c_s^2$. We can now construct a velocity field that vanishes at $x = 0$:

$$u = \tilde{u} \mathrm{Re} \left[e^{i(k_{\mathrm{res}} x - \omega t)} - e^{i(k_{\mathrm{ideal}} x - \omega t)} \right] . \tag{2.19}$$

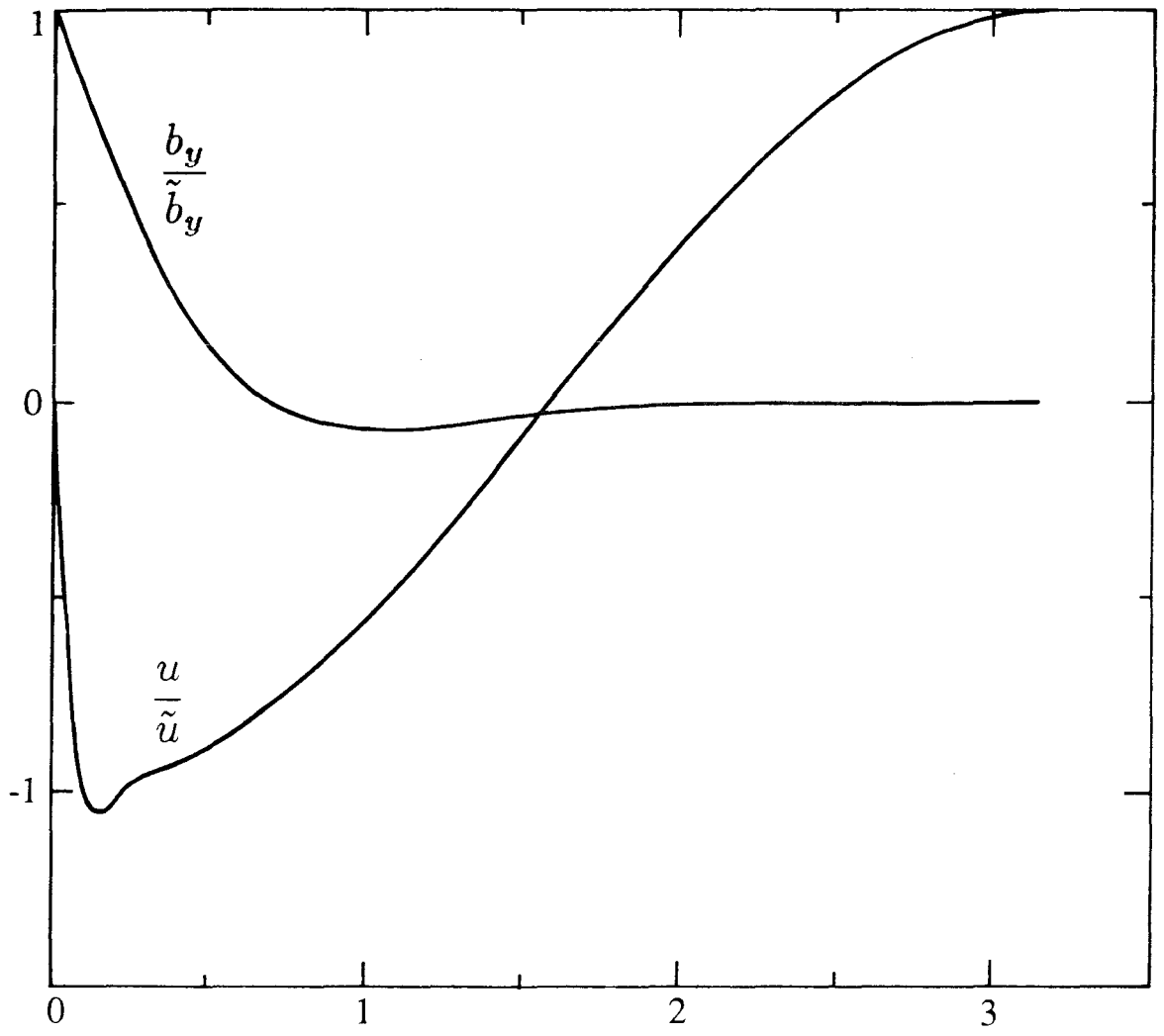

Figure 2.1. Plot of radial velocity $u/\tilde{u}$ and poloidal magnetic field $b_y/\tilde{b}_y$ for a low-β plasma ($\eta = 0.1, \omega = 1$, $c_s^2 = 0.02$, $v_a^2 = 1$).

Fig.(2.1) contains a plot of u and b_y for a low- β plasma. The velocity goes to zero in a boundary of width $\sim 1/k_{\rm res}$. The poloidal field vanishes outside a boundary layer of width $\sim 1/\kappa$. For a low- β plasma, $k_{\rm res} \gg \kappa$.

Inside the layer of width $1/\kappa$, the induced EMF is roughly $\sim \tilde{u}\tilde{b}_y$ (plasma exists up to the wall so that there is no need to consider a moving plasma boundary, as in the previous model). The driven toroidal current density is then $J_{\rm driven} \sim (\tilde{u}\tilde{b}_y)/\eta$. The poloidal field driven by this current is roughly $B_y^{\rm driven} \sim J_{\rm driven}/\kappa$, or

$$B_y^{\rm driven} \sim \frac{\tilde{u}\tilde{b}_y}{\sqrt{\omega\eta}} \ . \tag{2.20}$$

From Eqs.(2.14) and (2.19), one finds,

$$\frac{\rho}{\rho_0} = \tilde{u}\ {\rm Re}\Big[\frac{k_{\rm res}}{\omega} e^{i(k_{\rm res}x-\omega t)} - \frac{k_{\rm ideal}}{\omega} e^{i(k_{\rm ideal}x-\omega t)}\Big] \ .$$

Inside the layer $\sim 1/k_{\rm res}$, where $k_{\rm res} \gg k_{\rm ideal}$, one finds $\rho/\rho_0 \sim \tilde{u}(k_{\rm res}/w) \sim (\tilde{u}/\sqrt{\omega\eta})\sqrt{1+\beta^{-1}}$. Solving for $\tilde{u}$ gives

$$\tilde{u} \sim \frac{\rho}{\rho_0}\frac{\sqrt{\omega\eta}}{\sqrt{1+\beta^{-1}}} \ . \tag{2.21}$$

Combining Eqs.(2.20)-(2.21) gives

$$\frac{B_y^{\rm driven}}{\tilde{b}_y} \sim \frac{\rho/\rho_0}{\sqrt{1+\beta^{-1}}} \ .$$

The driven poloidal field is thus a small fraction of the perturbed poloidal field if $\rho/\rho_0 \ll 1$ and $\beta \ll 1$.

In summary, the radial motion of the plasma/vacuum interface — which was an important issue in the previous model — can be eliminated by including finite pressure in the MHD equations. However, in this case, again it is not possible to drive a substantial current.

2.3 Exact Solutions With Helical Symmetry

It was natural for the earliest investigators of the dynamo theory of the earth to search for mathematically tractable theories with a high degree of symmetry. The earth, after all, resembles a spinning sphere, and the earliest search for kinematic dynamos therefore focused on velocity fields with azimuthal symmetry. However, the surprising result was found, that velocity fields with too much symmetry are incapable of sustaining a large-scale magnetic field against Ohmic decay; the formal proof of this statement for velocity fields with azimuthal symmetry is given by the Cowling[25] antidynamo theorem. In this section we focus attention on MHD waves with helical symmetry. Exact solutions will be given for the linearized, pressureless MHD equations for the case where the zero-order magnetic field is uniform (no magnetic shear). A number of authors[26,27] have investigated the spectrum of resistive MHD, using WKB techniques and asymptotic matching; the exact solutions given here may provide a useful check for their work.

The resistive, pressureless MHD equations are first linearized about the zero-order fields $B_0 = B_a\hat{z}$, $U_0 = 0$. Letting lower-case variables denote perturbed quantities, the linearized MHD equations become

$$\rho_0 \frac{\partial \vec{u}}{\partial t} = -\nabla\left(\vec{B}_0 \cdot \vec{b}\right) + \vec{B}_0 \cdot \nabla\vec{b} \ ,$$

$$\frac{\partial \vec{b}}{\partial t} = \nabla \times \left(\vec{u} \times \vec{B}_0\right) + \eta\nabla^2\vec{b} \ .$$

The Alfven velocity in this system of dimensionless units is $v_a^2 = B_a^2/\rho_0$. Assuming that all perturbed fields are proportional to $\sim e^{i(\omega t + m\theta + kz)}$ yields a system of ordinary differential equations in the independent variable, r. The three components

of the induction equation yield

$$\omega b_r = kB_a u_r - i\eta \left\{ \frac{1}{r}\left(r b_r'\right)' - \left(k^2 + \frac{m^2+1}{r^2}\right) b_r - \frac{2imb_\theta}{r^2} \right\} , \qquad (2.22)$$

$$\omega b_\theta = kB_a u_\theta - i\eta \left\{ \frac{1}{r}\left(r b_\theta'\right)' - \left(k^2 + \frac{m^2+1}{r^2}\right) b_\theta + \frac{2imb_r}{r^2} \right\} , \qquad (2.23)$$

$$\omega b_z = \frac{B_a}{r}\left[i(r u_r)' - m u_\theta \right] - i\eta \left\{ \frac{1}{r}\left(r b_z'\right)' - \left(k^2 + \frac{m^2}{r^2}\right) b_z \right\} . \qquad (2.24)$$

The three components of the equation of motion yield

$$\omega \rho_0 u_r = B_a \left[k b_r + i b_z' \right] , \qquad (2.25)$$

$$\omega \rho_0 u_\theta = B_a \left[k b_\theta - \frac{m b_z}{r} \right] , \qquad (2.26)$$

$$u_z = 0 . \qquad (2.27)$$

Much of the following analysis can be simplified by defining the "rotating" coordinates,

$$u_\pm = u_r \pm i u_\theta ,$$

$$b_\pm = b_r \pm i b_\theta .$$

Multiplying Eq.(2.23) by $\pm i$ and adding to Eq.(2.22) give

$$\omega b_\pm = kB_a u_\pm - i\eta \left\{ \frac{1}{r}\left(r b_\pm'\right)' - \left(k^2 + \frac{m^2+1}{r^2}\right) b_\pm \mp 2m b_\pm \right\} . \qquad (2.28)$$

Multiplying Eq.(2.26) by $\pm i$ and adding to Eq.(2.25) gives

$$\omega \rho_0 u_\pm = kB_a b_\pm + iB_a \left(b_z' \mp \frac{m b_z}{r} \right) . \qquad (2.29)$$

We next define the following dimensionless parameters:

$$x = kr ,$$

$$\epsilon = \frac{\eta\omega}{v_a^2} \ ,$$

$$\xi = \frac{\omega/k}{v_a} \ ,$$

$$\gamma^2 = \frac{\xi^2}{1+i\epsilon} - 1 \ ,$$

$$\beta^2 = i\frac{1}{\epsilon}(1-\xi^2) - 1 \ .$$

A useful identity is

$$\gamma^2 - \beta^2 = \frac{i}{\epsilon}\gamma^2 \ . \tag{2.30}$$

Next, write the Bessel operator in the shorthand form,

$$\mathcal{L}(\alpha^2, n^2) = x^2\frac{d^2}{dx^2} + x\frac{d}{dx} + \alpha^2 x^2 - n^2 \ .$$

Solving Eq.(2.29) for $u_\pm$ and inserting into Eq.(2.28) gives

$$\mathcal{L}\left[\beta^2, (m\pm 1)^2\right] b_\pm = \frac{1}{\epsilon} x\left(x b_z' \mp m b_z\right) \ , \tag{2.31}$$

where primes denote $\frac{d}{dx}$ above, and in all that follows. Solving Eqs.(2.25)-(2.26) for u_r, u_θ and inserting into Eq.(2.24) yields

$$\mathcal{L}\left[\gamma^2, m^2\right] b_z = 0 \ . \tag{2.32}$$

The solution to Eq.(2.32) is

$$b_z = \tilde{b}_z J_m(\gamma x) \ , \tag{2.33}$$

where $\tilde{b}_z$ is a complex constant. The solution $Y_m(\gamma x)$ is rejected, since the solution must not diverge at $r = 0$. Substituting Eq.(2.33) into the RHS of Eq.(2.31) yields

$$\text{RHS of Eq.(2.31)} = \frac{1}{\epsilon} x\tilde{b}_z\left[x\frac{d}{dx}J_m(\gamma x) \mp m J_m(\gamma x)\right] \ ,$$

which can be simplified using a standard Bessel identity, $x\frac{d}{dx}J_m(x) \mp mJ_m(x) = \mp xJ_{m\pm1}(x)$. Eq.(2.31) then becomes

$$\mathcal{L}\left[\beta^2,(m\pm1)^2\right]b_\pm = \mp\gamma\frac{1}{\epsilon}\tilde{b}_z x^2 J_{m\pm1}(\gamma x) \ . \tag{2.34}$$

The general solution to Eq.(2.34), which is well-behaved at the origin, is given by

$$b_\pm = \pm\frac{\tilde{b}_z}{i\gamma}J_{m\pm1}(\gamma x) + \tilde{b}_\pm J_{m\pm1}(\beta x) \ , \tag{2.35}$$

where $b_\pm$ are complex constants. Using

$$b_r = \frac{1}{2}(b_+ + b_-) \ , \qquad b_\theta = \frac{1}{2i}(b_+ - b_-) \ ,$$

together with the Bessel identities,

$$\frac{1}{2}(J_{m-1} - J_{m+1}) = \frac{d}{dx}J_m \ , \qquad \frac{1}{2}(J_{m+1} + J_{m-1}) = \frac{m}{x}J_m \ ,$$

yields

$$b_r = \frac{i\tilde{b}_z}{\gamma}\frac{d}{d(\gamma x)}J_m(\gamma x) + \frac{\tilde{b}+}{2}J_{m+1}(\beta x) + \frac{\tilde{b}_-}{2}J_{m-1}(\beta x) \ ,$$

$$b_\theta = -\frac{\tilde{b}_z}{\gamma}\frac{m}{(\gamma x)}J_m(\gamma x) + \frac{\tilde{b}_+}{2i}J_{m+1}(\beta x) - \frac{\tilde{b}_-}{2i}J_{m-1}(\beta x) \ .$$

Using $\nabla\cdot\vec{b} = 0$ gives the condition $\tilde{b}_+ = \tilde{b}_-$. Using this and Bessel identities mentioned above yields the general solution,

$$\begin{aligned}\vec{b} = {} & \tilde{b}_z\left\{\frac{i}{\gamma}\frac{d}{d(\gamma x)}J_m(\gamma x) \ , \ -\frac{m}{\gamma}\frac{1}{(\gamma x)}J_m(\gamma x) \ , \ J_m(\gamma x)\right\} \\ & + \tilde{b}_\perp\left\{\frac{m}{(\beta x)}J_m(\beta x) \ , \ i\frac{d}{d(\beta x)}J_m(\beta x) \ , \ 0\right\} \ ,\end{aligned} \tag{2.36}$$

where $\tilde{b}_z$ and $\tilde{b}_\perp$ are arbitrary complex constants.

For small resistivity, the solution given by Eq.(2.36) is again the superposition of an Alfvenic mode (first term on the RHS) and a resistive mode (second term on the RHS). The resistive mode is confined to a skin layer — except in the special case where the phase velocity happens to match the Alfven velocity ($\xi = 1$). We have already investigated the interaction of the resistive mode with the Alfvenic mode, and here we are interested in exploring the EMF that is due to the Alfvenic mode alone, which can be written as

$$b_r = \frac{i}{\gamma}\frac{d}{d(\gamma x)}b_z \ , \quad b_\theta = -\frac{m}{\gamma}\frac{1}{(\gamma x)}b_z \ , \quad b_z = \tilde{b}_z J_m(\gamma x) \ . \tag{2.37}$$

There are several features of the Alfvenic mode that are of potential interest for OFCD: (1) The velocity field, like the magnetic field, possesses helical symmetry and therefore carries helicity, $\vec{u} \cdot \nabla \times \vec{u}$; (2) the EMF will no longer be confined to a narrow skin layer near the plasma surface; and (3) for $m = 1$ the EMF will be finite on axis. If the applied field is tuned so that the phase velocity matches the Alfven speed ($\xi = 1$), then, for $\epsilon \ll 1$, one has $\gamma^2 \approx -i\epsilon$. Using the small argument expansion for Bessel functions, $J_1(z) \sim (1/2)z$ as $z \to 0$ in Eq.(2.37) yields, for $m = 1$,

$$\vec{b} \approx \tilde{b}(1, i, 0), \quad \vec{j} \approx ik\hat{z} \times \vec{b} = k\tilde{b}(1, i, 0) \ , \quad (\omega/k = v_a) \ ,$$

where $\tilde{b}$ is a complex constant. Hence, for $\epsilon \ll 1$, Eq.(2.37) yields $m = 1$ circularly polarized waves propagating in the toroidal direction. The oscillating vectors $\vec{j}$ and $\vec{b}$ are *in phase* so that there is a uniform helicity dissipation $2\eta k\tilde{b}^2$. Here, the DC helicity dissipation will turn out to be equal and opposite to the AC helicity dissipation.

The time-averaged toroidal EMF is given by

$$< \text{EMF} > = \frac{1}{2}\text{Re}\ (u_r b_\theta^* - u_\theta^* b_r) \quad . \tag{2.38}$$

Using Eqs.(2.25)-(2.26) to eliminate u_r and u_θ from Eq.(2.38) then gives

$$< \text{EMF} > = \frac{kB_a}{2\omega\rho_0}\text{Re}\ \left\{ i\frac{db_z}{dx} b_\theta^* + \frac{m}{x} b_r b_z^* \right\} \quad .$$

Eliminating b_θ and b_r, using Eq.(2.37) and rearranging gives

$$< \text{EMF} > = \frac{kB_a}{2\omega\rho_0}\frac{m}{x}\text{Re}\ \left(\frac{i}{\gamma^2}\right)\frac{d}{dx}|b_z|^2 \quad . \tag{2.39}$$

Now,

$$< \text{EMF} > = \eta J_z^{\text{driven}} = \eta\frac{1}{r}\frac{d}{dr}\left(rB_\theta^{\text{driven}}\right) \quad . \tag{2.40}$$

Combining Eqs.(2.39)-(2.40), and integrating with respect to x yields

$$B_\theta^{\text{driven}} = \frac{B_a}{2\omega\rho_0\eta}\text{Re}\ \left(\frac{i}{\gamma^2}\right)\frac{m}{x}|b_z|^2 \quad . \tag{2.41}$$

From Eq.(2.37) it follows that $\frac{m}{x}|b_z| = |\gamma^2||b_\theta|$. Using this to eliminate $|b_z|$ from Eq.(2.41) yields, after some algebra,

$$\frac{B_\theta^{\text{driven}}}{|b_\theta|} = -\frac{\xi^2}{2\left(1+\epsilon^2\right)}\frac{x}{m}\frac{|b_\theta|}{B_a} \quad . \tag{2.42}$$

For a fusion reactor with parameters $B_a \sim 50\text{kG}$, $n \sim 10^{14}\text{cm}^{-3}$, $T \sim 10$ kev, the parameter ϵ will be very small ($\sim 10^{-9}$) and $\epsilon^2 \ll 1$ in Eq.(2.42). The parameter ξ is the ratio of the phase velocity to the Alfven speed. Suppose that we wish to have $B_\theta^{\text{driven}}\ /\ |b_\theta| \sim 10$, $|b_\theta|\ /\ B_a \sim 1/100$, so that $\xi^2 \sim 10^3$. The required frequency would be roughly 100 MHz, near the ion cyclotron frequency. The standard MHD equations break down at frequencies higher than this. For phase velocities lower

than the Alfven speed (a more attractive regime from a practical standpoint), the driven DC field is a small fraction of the oscillating field. However, it should be noted that in the experimental work of Hotta[16] et al., our MHD theory underestimates the driven current by a factor of roughly 100 [see Sec.(3.9)].

Ohkawa[28] also presents a brief calculation of the EMF that is due to circularly polarized Alfven waves. There are several features of Ohkawa's work that deserve special mention. In Ohkawa's work, all waves are uniform in the transverse direction: $\vec{A}(\vec{x},t) = A_0(1,i,0)e^{i(kz-\omega t)}$, where ω is real and k is complex. The quantities ω and k are not independent; instead, they are related through a dispersion relation. In our calculation, all waves are of the form $\vec{A}(\vec{x},t) = \vec{A}(r)e^{i(\theta+kz-\omega t)}$, where ω and k are both *real*. The quantities ω and k are determined by the driving frequency and the geometry of the external coils. We feel that our model is more realistic for two reasons: (1) A torus can be modeled by a periodic cylinder, and any disturbance can be decomposed into Fourier components proportional to $e^{i(m\theta+kz)}$ with $k = 2\pi n/L$ real; and (2) the EMF generated by a wave that propagates and decays in the z direction produces a steady current of the form $\vec{J} = \hat{z}J(z)$. Such a steady current is not divergence-free and, by charge conservation, must lead to an infinite build-up of charge.

Ohkawa has proposed launching circularly polarized waves that propagate and decay spatially in the toroidal direction. Since the circularly polarized waves carry a uniform, constant helicity flux, the helicity of the wave must be transferred to the plasma. Based on this argument, Ohkawa predicts that the ratio of the power absorbed to the Ohmic power dissipated is given by $P_{\text{absorbed}}/P_{\text{Ohmic}} = q_0 kR$, where q_0 is the safety factor, k is the wavevector, and R is the major radius. However,

Ohkawa's favorable current-drive efficiency is strictly an upper bound, since it is assumed that all of the helicity flux is consumed by the DC fields. In fact, Ohkawa's scheme leads to poor current-drive efficiency unless a very strong anisotropic resistivity is assumed (where $\eta_\perp/\eta_\parallel \sim (B_a/b)^2$). If a strongly anisotropic resistivity can be formed (e.g., by minority ion-cyclotron damping), then our helical MHD scheme will also produce favorable current-drive efficiencies.

In summary, the EMF generated by helical MHD waves has been calculated. If the phase velocity is below the Alfven speed, then the dynamo action is weak, with the driven DC fields a small fraction of the AC fields. The current-drive efficiency quoted by Ohkawa should be considered an upper bound, since magnetic helicity can be consumed by the oscillating fields.

2.4 An Antidynamo Argument

Professor Roy Gould[24] has emphasized the importance of Faraday's law in the analysis of laminar MHD models. Gould's argument is outlined here.

Consider, for the moment, a toroidal plasma with azimuthal symmetry. The plasma is quivering in the radial direction because of MHD activity, but maintains azimuthal symmetry at all times. The motion is strictly time-periodic. Imagine dividing the torus into an infinite number of circular filaments of radius r and cross-sectional area dA. A single filament is drawn in Fig.(2.2). The filament is expanding and contracting because of MHD activity, and the closed contour c is moving with the filament. From Faraday's law,

$$\int_c \vec{E}' \cdot d\vec{l} = \frac{d\phi}{dt} \ , \tag{2.43}$$

where $\vec{E}' = \vec{E} + \vec{U} \times \vec{B}$ is the electric field as seen in the moving frame and ϕ is the magnetic flux linking c. Since all quantities are assumed to be time-periodic, it follows that $< d\phi/dt >= 0$. If the plasma satisfies the MHD Ohm's law,

$$\vec{E} + \vec{U} \times \vec{B} = \eta \vec{J} \ , \tag{2.44}$$

with η =const., then inserting Eq.(2.44) into Eq.(2.43) yields

$$\left\langle \int_c \vec{J} \cdot d\vec{l} \right\rangle = 0 \ . \tag{2.45}$$

The instantaneous current within the filament will be defined as

$$dI = \frac{\int_c \vec{J} \cdot d\vec{l}}{2\pi r} \, dA$$

[note that dI has the dimensions of (current density) (area)]. If r and dA do not depend on time, then $< dI >$ must vanish according to Eq.(2.45). If r and dA

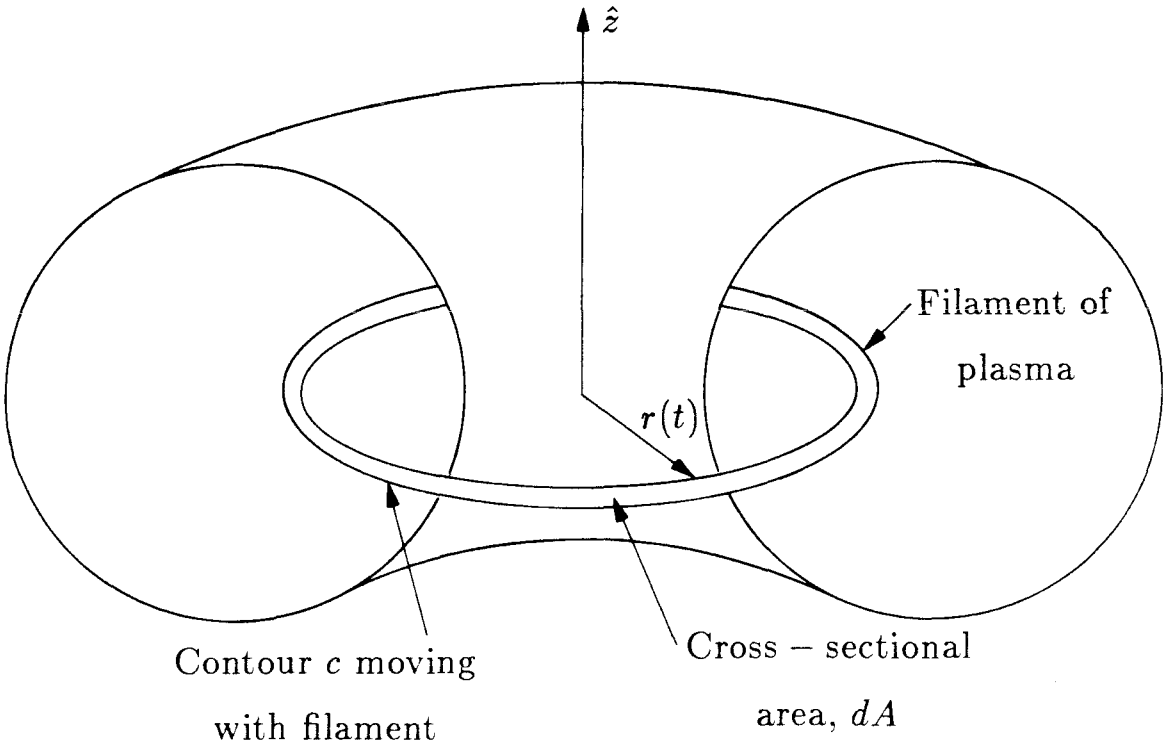

Figure 2.2. Sketch of a toroidal plasma undergoing $m = 0$, $k = 0$ MHD activity. The plasma is divided into an infinite number of filaments of cross-sectional area dA and radius $r(t)$. The contour c is quivering in the radial direction, moving with the filament.

depend on time (the cross-sectional area may change with time for a compressible plasma), then dI can have a small, but finite, time average. In any event, the dynamo mechanism must be very weak because of Eq.(2.45).

At higher frequencies, the Hall term may be important, and Ohm's law becomes

$$\vec{E} + \vec{U} \times \vec{B} - \frac{1}{ne}\vec{J} \times \vec{B} = \eta \vec{J} \ . \tag{2.46}$$

Inserting Eq.(2.46) into Eq.(2.43) yields

$$\left\langle \int_c \vec{J} \cdot d\vec{l} \right\rangle = -\frac{1}{ne\eta} \left\langle \int_c (\vec{J} \times \vec{B}) \cdot d\vec{l} \right\rangle \ .$$

It is now possible to sustain a significant current through the interaction of time-periodic fields. Since the motion is assumed to be time-periodic, it is always true that $< \int_c \vec{E'} \cdot d\vec{l} >= 0$, which states that the loop-voltage taken around each filament must vanish on time-averaging.

The argument above assumes azimuthal symmetry. However, it appears that the argument can be extended to other situations in which the filaments writhe and undulate in complicated — but *time-periodic* — patterns.

We have made a systematic search in an effort to uncover a useful laminar MHD dynamo for tokamak current-drive. We have studied cases that possess azimuthal symmetry as well as cases that possess helical symmetry. In all cases, it was found that the resulting dynamo mechanism is too weak to be of practical interest, with the driven fields always a small fraction of the oscillating fields. It may be necessary to invoke more complicated MHD activity, such as turbulence and/or magnetic tearing and reconnection, to achieve a useful dynamo mechanism. The reader is referred to the work of Finn[18] and Strauss and Harned[19] for more discussion.

We now turn to a higher-frequency, current-drive scheme in Chapter 3, which is based on the $< \vec{j} \times \vec{b} >$ Hall EMF in Ohm's law.

Chapter 3. Models Based on the Hall MHD Equations

In this chapter, a higher-frequency OFCD scheme is explored, which relies on the $< \vec{j} \times \vec{b} >$ Hall EMF in Ohm's law. This scheme owes its heritage to the rotamak, a device that relies on a transverse rotating magnetic field to generate and maintain the symmetrical, nested flux surfaces of a compact torus configuration [Fig.(3.1)]. The rotamak along with related schemes, now has a large body of literature all its own, and the reader is referred to the work of Jones[31] for a general overview.

An idealized picture of the rotamak appears in Fig.(3.1a), where $\frac{\partial}{\partial z} = 0$, and where external coils are arranged to approximate a current sheet of the form $\vec{J}^{ext} \sim \delta(r-R)e^{i(\theta-\omega t)}$. In addition, azimuthal coils are applied to generate a static axial field, $B_a\hat{z}$. In vacuum, the external coils generate a rotating magnetic field in the plane perpendicular to the z-axis:

$$\vec{B} = B_\omega \cos(\omega t)\hat{x} + B_\omega \sin(\omega t)\hat{y} + B_a\hat{z} \ , \tag{3.1}$$

$$\vec{E} = \omega B_\omega \left[x\cos(\omega t) + y\sin(\omega t)\right]\hat{z} \ . \tag{3.2}$$

The rotating vacuum field is straight and uniform at any given instant of time, but the direction of the field rotates with angular frequency, ω. The frequency of oscillation is assumed to be large enough so that the more massive ions cannot respond to the applied field. As will become clear below, the rotating field is capable of setting the plasma electrons into rotation in the azimuthal direction (a traveling wave in the θ-direction is maintained at the surface, injecting momentum in the azimuthal direction). If the applied field is of sufficient strength, then a saturation point is reached, where the entire electron cloud rotates synchronously with the applied field. In rotamak experiments, the resulting azimuthal current reverses the direction of the static field on axis, creating a compact torus [Fig.(3.1b)].

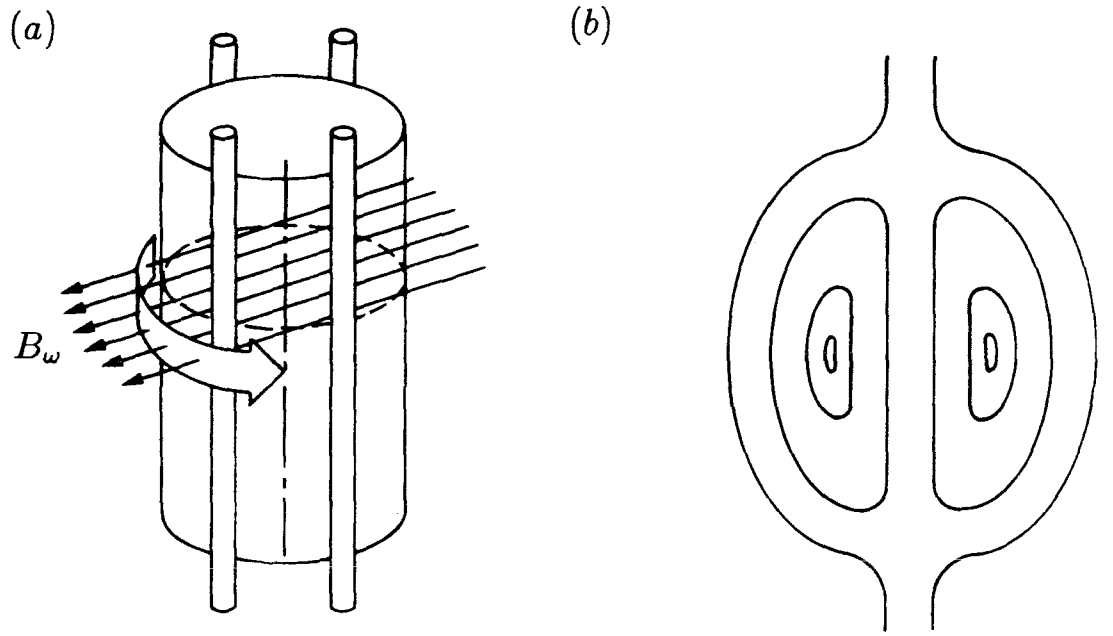

Figure 3.1. (a) Idealized sketch ($\partial/\partial z = 0$) of the rotamak showing external $m = 1$, $k = 0$ coils and transverse rotating field, B_ω. A static axial field is also applied (not drawn). (b) Flux contours of the compact torus configuration.

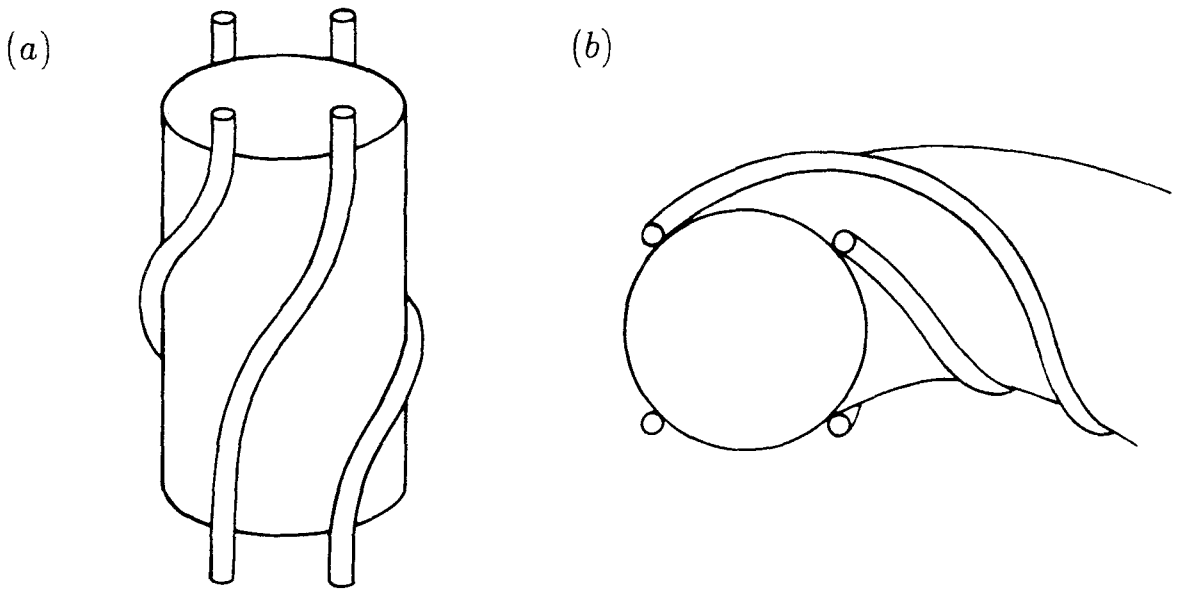

Figure 3.2. (a) Nonzero k analogue of the rotamak. External coils approximate a current distribution of the form $J^{ext} \propto e^{i(\theta+kz-\omega t)}$. (b) rhythmac configuration ($m = 1, k \neq 0$).

In order to understand the dynamics of the $< \vec{j} \times \vec{b} >$ current-drive scheme, imagine starting from an equilibrium plasma and applying a rotating magnetic field. The vacuum fields given by Eqs.(3.1)-(3.2) penetrate into the plasma cylinder a distance equal to the classical skin depth, which may be a small fraction of the plasma radius for low resistivity. The oscillating electric field given by Eq.(3.2) sets the electrons oscillating in the z-direction (again, we assume that the ions cannot respond appreciably to the high-frequency fields). The oscillating electron velocity v_z interacts with the radial-vacuum, magnetic field b_r to generate a time-averaged azimuthal force, $< v_z b_r >$ (the phase of the electron fluid velocity v_z with respect to the radial field b_r depends on the amount of resistivity present). Electrons rotating in this skin layer see a doppler-shifted frequency $\omega^* = \omega - V_\theta/r$ and therefore an increase in the effective skin depth, leading to further penetration of the applied field. Increasing the strength of the applied field leads eventually to a saturation point where all the electrons rotate synchronously with the field and where the effective skin depth becomes infinite.

At any given instant of time, the rotamak has open field lines in the radial direction, raising the question of whether particles can escape along open field lines in the radial direction. If one considers the orbit of a charged particle immersed in the vacuum fields of Eqs.(3.1)-(3.2), it is possible to show that all orbits are bounded in the (x, y) plane, provided that the axial field B_a is sufficiently strong (of course, particles are free to escape in the z direction). This calculation becomes tractable by applying a transformation to rotating variables[32]. The radial field lines are open — but only for a transient period, and particles cannot escape in the radial direction.

Imagine now giving a helical twist to the external coils drawn in Fig.(3.1a), approximating an external current sheet of the form $\vec{J}^{ext} = \delta(r-R)e^{i(\theta+kz-\omega t)}$ [Fig.(3.2a)]. A traveling wave is now maintained in both the azimuthal and axial directions. If the coils are wrapped around a torus, then one obtains the "rhythmac" configuration of Dutch and McCarthy and Storer[3], shown in Fig.(3.2b).

A simple mathematical model will now be derived to describe the $< \vec{j} \times \vec{b} >$ current-drive scheme. We begin by considering the two-fluid equations of motion,

$$n_e m_e \frac{d\vec{v}_e}{dt} = -n_e e\left(\vec{E} + \vec{v}_e \times \vec{B}\right) - \nabla P_e - n_e m_e \nu_{ei}\left(\vec{v}_e - \vec{v}_i\right) \quad , \tag{3.3}$$

$$n_i m_i \frac{d\vec{v}_i}{dt} = +n_i e\left(\vec{E} + \vec{v}_i \times \vec{B}\right) - \nabla P_i - n_i m_i \nu_{ei}\left(\vec{v}_i - \vec{v}_e\right) \quad , \tag{3.4}$$

where subscripts i and e refer to ions and electrons, respectively.

As a first approximation, suppose that the plasma is cold and collisionless so that the pressure and collision terms can be neglected. Suppose further that the plasma is immersed in a static, uniform magnetic field: $\vec{B} = B_a\hat{z}$. The linearized fluid equations then become

$$n_\sigma m_\sigma \frac{\partial \vec{v}_\sigma}{\partial t} = n_\sigma q_\sigma \left(\vec{E} + \vec{v}_\sigma \times B_a\hat{z}\right) \quad \sigma = i,\ e \ . \tag{3.5}$$

A given disturbance can be decomposed into Fourier components of the form, $\vec{v}_\sigma(\vec{x},t) = \bar{v}_\sigma e^{i(\vec{k}\cdot\vec{x}-\omega t)}$, $\vec{E}(\vec{x},t) = \bar{E}e^{i(\vec{k}\cdot\vec{x}-\omega t)}$, where

$$\bar{v}_\sigma = \frac{iq_\sigma}{m_\sigma\omega}\bar{E}_\parallel + \frac{q_\sigma}{m_\sigma\left(\omega^2-\Omega_{c\sigma}^2\right)}\left[i\omega\bar{E}_\perp + \vec{\Omega}_{c\sigma}\times\bar{E}\right] \quad , \tag{3.6}$$

$$\vec{\Omega}_{c\sigma} = \hat{z}\frac{q_\sigma B_a}{m_\sigma} \quad ,$$

and where $\bar{E}_{\|}$, $\bar{E}_{\perp}$ are the components of $\bar{E}$ with respect to the z axis. For $\omega \ll \Omega_{ci}$, Eq.(3.6) yields

$$\bar{v}_\sigma \approx \frac{iq_\sigma}{m_\sigma \omega}\bar{E}_{\|} + \frac{1}{B_a^2}\bar{E} \times B_a\hat{z} \quad . \tag{3.7}$$

Thus, in the plane perpendicular to $\hat{z}$, the ions and electrons execute an identical $\vec{E} \times \vec{B}$ drift. For $\omega \gg \Omega_{ci}$, Eq.(3.6) yields

$$\bar{v}_\sigma \approx \frac{iq_\sigma}{m_\sigma \omega}\bar{E} \quad , \tag{3.8}$$

so that all components of the electron velocity are now much larger than the ion velocity, by a factor of a mass ratio. The important point here is that the ion motion can be neglected only at frequencies well above Ω_{ci} — the ion cyclotron frequency referred to the static magnetic field. A special case occurs when $B_a\hat{z}$ and $\bar{E}$ are parallel, in which case the static field decouples from the fluid motion. Note from Eqs.(3.1)-(3.2) that the standard rotamak (idealized such that $\frac{\partial}{\partial z} = 0$) conforms to this special case where $\vec{E}$ and $B_a\hat{z}$ are parallel.

Starting from the electron equation of motion [Eq.(3.3)], the following approximations are made:

• A cold-plasma approximation is adopted and the electron pressure term is neglected.

• Quasi-neutrality is assumed and the density is assumed uniform: $n = n_i = n_e =$ constant.

• The frequency of the applied field is assumed to be high enough so that ion motion can be neglected ($\vec{v}_i = 0$). The ions then form a uniform background of positive charge. The frequency regime for this approximation is discussed at length, below.

• The electron inertia term is neglected. This neglect is justified when $\omega \ll \nu_{ei}$. For fusion plasmas of very low resistivity, the inertia term should be retained, and this is a worthy goal for future studies.

Noting that $\vec{J} = -ne\vec{v}_e$ and $\eta = \frac{m_e \nu_{ei}}{ne^2}$, the electron equation of motion becomes

$$\vec{E} - \frac{1}{ne}\left(\vec{J} \times \vec{B}\right) = \eta \vec{J} \ . \tag{3.9}$$

Together with Faraday's law,

$$\nabla \times \vec{E} = -\frac{\partial \vec{B}}{\partial t} \ , \tag{3.10}$$

and Ampere's law,

$$\nabla \times \vec{B} = \mu_0 \vec{J} \ , \tag{3.11}$$

this system forms a complete description of the time-evolution of the fields $\vec{E}$, $\vec{B}$, and $\vec{J}$. This nonlinear model has been adopted by other authors to describe the operation of the rotamak[33,34,35] ($k = 0$) and the rhythmac[36,37] ($k \neq 0$).

The above model [Eqs.(3.9)-(3.11)] is relatively simple (in comparison to standard MHD), because the ion motion is not included. As indicated above, the role played by the ion fluid depends on the frequency of the applied field and the orientation of the oscillating electric field with respect to the static axial magnetic field. Note again that the rotamak and rhythmac employ a rotating magnetic field of strength B_ω, in addition to a static axial field of strength B_a; the cyclotron frequencies associated with these fields will be labeled ω_c and Ω_c, respectively. It has been quoted many times in the literature that Eqs.(3.9)-(3.11) are valid, provided that

$$\omega_{ci} \ll \omega \ll \omega_{ce} \ , \tag{3.12}$$

where all cyclotron frequencies are referred to the strength of the applied field, B_ω. It is claimed that $\omega \gg \omega_{ci}$ is necessary so that the rotating field does not impart momentum to the ions and $\omega \ll \omega_{ce}$ so that the electrons can be considered "tied" to the field lines. It is claimed that Eq.(3.12) is the proper frequency range for the rotamak or the rhythmac[3,15].

Hugrass[38] is apparently the only author, at the time of this writing, who has made a serious attempt to assess the correct frequency range for steady-state rotamak operation ($k = 0$). In Ref.(38), Hugrass returns to the full, two-fluid equations [Eqs.(3.3)-(3.4)]. Hugrass notes that electron-ion collisions will eventually set the ion fluid into synchronous rotation with the electron fluid, quenching the driven azimuthal current. In order to achieve a steady-state current in his calculations, Hugrass introduces an "artificial" frictional force $-n_i m_i \nu^* \vec{v}_i$ on the RHS of Eq.(3.4), which preferentially slows down the ions but not the electrons. Hugrass claims that the effective collision frequency ν^* can represent the role of charge-exchange processes or ionization-recombination. Next, Hugrass assumes that the electron and ion fluid motion consist of a steady azimuthal drift together with a oscillating component, strictly in the $\hat{z}$ direction. The results of Hugrass's analysis in Ref.(38) are summarized below:

- In order to achieve a steady current, the artificial collision frequency ν^* must be of sufficient strength, such that

$$\chi = \frac{m_i}{m_e}\frac{\nu^*}{\nu_{ei}} > 1 \ .$$

- In order to achieve full penetration of the rotating field, the applied field must be

of sufficient strength, such that

$$\epsilon = \frac{\nu_{ei}}{\omega_{ce}} \ll 1 \ . \qquad \text{[Eq.(57) in Ref.(38)]}$$

• The rotating field does not impart significant momentum to the ions, provided that

$$\omega > \sqrt{\chi}\,\omega_{ci} \ . \qquad \text{[Eq.(56) in Ref.(38)]}$$

• The electron cloud rotates synchronously with the applied field, provided that

$$\omega \ll \frac{1}{\epsilon}\omega_{ce} \ . \qquad \text{[Eq.(58) in Ref.(38)]}$$

Hugrass therefore predicts that steady rotamak ($k = 0$) operation will occur when

$$\sqrt{\chi}\,\omega_{ci} \ll \omega \ll \frac{1}{\epsilon}\omega_{ce} \ , \qquad (3.13)$$

which is quite different from the frequency range given in Eq.(3.12). Note that Eq.(3.13) gives the frequency range in terms of the applied field strength, B_ω, not in terms of the axial field strength, B_a; this is not unexpected because the symmetry of the idealized $\frac{\partial}{\partial z} = 0$ rotamak ensures that the oscillating electric field is always parallel to the static axial field, B_a. The static field therefore decouples from the fluid motion.

The results of Ref.(38) depend crucially on the high degree of symmetry found in the rotamak. There is apparently no evidence to suggest that Eq.(3.12) or Eq.(3.13) applies to the rhythmac ($k \neq 0$). For $k \neq 0$, it is safe to assume that Eqs.(3.9)-(3.11) are valid in the frequency range,

$$\Omega_{ci} \ll \omega \ll \nu_{ei} \ . \qquad (3.14)$$

We require $\omega \gg \Omega_{ci}$ to ignore the ion motion and $\omega \ll \nu_{ei}$ to ignore electron inertia. The system is therefore valid for resistive plasmas of relatively low field strengths. The small-scale experiments performed in Australia[4] are of this type, where $B_\omega \approx$ 50 G, $B_a \approx 300$ G. For an argon plasma, $\Omega_{ci} \approx 12$ kHz, which is well below the applied frequency of $\omega/(2\pi) \approx 300$ kHz.

The displacement current was dropped in Eq.(3.11), and we shall discuss the implications of this approximation. Inside the plasma, this is justified for the case of low resistivity and low frequency. As in standard MHD, neglect of the displacement current is justified when $v/c \ll 1$, where v is a typical fluid velocity. In the model to be described in the following sections, a vacuum region exists, separating the plasma from the external current sheet. The displacement current can also be neglected in the vacuum region, provided that $\omega/k \ll c$, where ω/k is the phase velocity of the applied traveling wave. From Eq.(3.11), it follows immediately that $\nabla \cdot \vec{J} = 0$; from Gauss's law, this implies that radial currents must vanish at the plasma/vacuum boundary.

The complete nonlinear system given by Eqs.(3.9)-(3.11) can be solved to obtain the field quantities $\vec{E}$, $\vec{B}$, and $\vec{J}$. The charge density ρ does not appear as one of the independent variables since ρ was eliminated through the assumption of quasi-neutrality. Nevertheless, $\nabla \cdot \vec{E} = 0$ is not imposed as an additional constraint and, in fact, solutions with $\nabla \cdot \vec{E} \neq 0$ will emerge in solutions of Eqs.(3.9)-(3.11). If Poisson's equation is used to compute the charge density, then a number of paradoxical results emerge:

• Time-dependent and static charge-densities appear within the plasma, contradicting the assumption of charge-neutrality.

• Charge conservation is not necessarily satisfied, since the displacement current was dropped: Time-dependent charge-density fluctuations can occur within the plasma — and yet $\nabla \cdot \vec{J} = 0$ was assumed. Time-dependent surface charges can appear — and yet it was assumed that J_r vanishes at the boundary.

This apparent discrepancy also arises in standard MHD work (see Krall and Trivelpiece[39], page 96, or Bateman[40] page 42). The correct way to interpret the equations is as follows:

• The fields $\vec{E}$, $\vec{B}$, $\vec{J}$ are first calculated from Eqs.(3.9)-(3.11).

• Poisson's equation is used to calculate the charge-density ρ to *verify* the original assumption of quasi-neutrality (i.e., that $n_i - n_e$ is "small").

• The equation $\frac{\partial \rho}{\partial t} + \nabla \cdot \vec{J} = 0$ is used to determine what *additional* currents are needed to satisfy charge conservation; one can then verify that the currents needed to satisfy charge-conservation are negligibly small in comparison to the currents calculated from Eqs.(3.9)-(3.11).

Taking the curl of Eq.(3.9) and using Faraday's law to eliminate $\nabla \times \vec{E}$, give an equation for the time-evolution of the magnetic field,

$$\frac{\partial \vec{B}}{\partial t} = \frac{\eta}{\mu_0} \nabla^2 \vec{B} - \frac{1}{ne} \nabla \times \left(\vec{J} \times \vec{B} \right) \quad , \tag{3.15}$$

$$\nabla \times \vec{B} = \mu_0 \vec{J} \quad .$$

One should note the similarity of this equation to other induction-type equations, such as the equation for vorticity $\vec{\omega}$,

$$\frac{\partial \vec{\omega}}{\partial t} = \frac{\mu}{\rho} \nabla^2 \vec{\omega} + \nabla \times \left(\vec{U} \times \vec{\omega} \right) \quad , \tag{3.16}$$

$$\nabla \times \vec{U} \;=\; \vec{\omega} \;\;,$$

from hydrodynamics, and the induction equation form standard MHD,

$$\frac{\partial \vec{B}}{\partial t} \;=\; \frac{\eta}{\mu_0}\nabla^2\vec{B} \;+\; \nabla \times \left(\vec{U} \times \vec{B}\right) \;\;, \tag{3.17}$$

$$\vec{U} \text{ satisfies eq. of motion} \;\;.$$

All of these equations combine convection and diffusion — and yet Eq.(3.15) is fundamentally different. Eliminating the diffusion term in Eq.(3.16) or Eq.(3.17) lowers the number of spatial derivatives on the RHS; for small, but finite, amounts of diffusivity, leading to boundary layers and the possibility of using WKB techniques. Setting $\eta = 0$ in Eq.(3.15) does not lower the number of spatial derivatives of $\vec{B}$. Nevertheless, it will be shown in Sec.(3.5) that the behavior of Eq.(3.15) in the limit as $\epsilon \rightarrow 0$ can be markedly different from the behavior when $\epsilon = 0$, exactly.

Both Dutch and McCarthy[3] and Bertram[36,37] look for steady-state helical solutions of Eq.(3.15) of the form,

$$\vec{B} \;=\; \sum_{m=-\infty}^{\infty} \vec{b}_m(r)\; e^{im(\theta+kz-\omega t)} \;\;.$$

This ansatz creates an infinite system of coupled ODE's. Both of the authors mentioned above truncate the resulting system by eliminating all harmonics for which $m \geq 2$. For large resistivity, the nonlinear $\vec{J} \times \vec{B}$ term in Eq.(3.15) enters as a perturbation; higher-order harmonics are then diminished by factors of $\left(\frac{1}{\eta}\right)^m$. However, truncating the system is hard to justify in the more important case of low resistivity, since it is then the *linear* term that enters as a perturbation. In this work, the neglect of higher-order harmonics will be justified, whenever possible.

In the work of Dutch and McCarthy[3], it is assumed that solutions of the truncated system exist for which $j_r = 0$ (lower-case variables denote oscillating quantities and upper-case variables denote DC fields). This was true for the case of the rotamak ($k = 0$), since then the rotating vacuum field had only an electric field component in the z-direction. However, when $k \neq 0$, the rotating vacuum field has electric field components in all three directions, and it is not possible to find solutions for which $j_r = 0$. It is shown in Appendix (2) that the assumption $j_r = 0$ leads to an inconsistency in Ref.3.

Bertram [Ref.(37)] has done a numerical study of the truncated system in which he allows radial screening currents. It is suggested in Ref.(37) that, for $k \neq 0$, there is an analogue of the standard rotamak solution in which a steady, uniform, toroidal current is found as $\eta \rightarrow 0$. However, it is shown in this thesis that Bertram's solution is attained only when the static axial field vanishes and when the the DC fields are a small fraction of the AC fields. Instead, it will be shown that the steady current, for nonzero k, is confined to a skin layer. Bertram[36] was first to identify a similar skin effect, in an analytical calculation done in slab geometry.

Sec.(3.1) of this work contains a description of the basic equations, geometry, and boundary conditions used to model the Hall MHD, current-drive scheme. Sec.(3.2) is devoted to a description of the numerical methods used to study the truncated systems. The special role of flux-conserving velocity fields is examined in Secs.(3.3)-(3.5). Numerical and analytical solutions of the first truncated system are presented in Sec.(3.6), followed by a justification for truncating the system in Sec.(3.7). The conservation laws of momentum, energy, and magnetic helicity are derived and discussed in Sec.(3.8). Finally, a comparison of theory and experimental

work is presented in Sec.(3.9).

3.1 Basic Equations and Boundary Conditions

The goal of the following sections is a mathematical description of the response of an infinite plasma cylinder to an applied rotating magnetic field of $m = 1$ structure.

Three-dimensional space is divided into three regions, as drawn in Fig.(3.3). Region I ($r < R$) contains the plasma cylinder and the fields within region I are described by the Hall MHD equations,

$$\nabla \times \vec{B} = \mu_0 \vec{J} \ ,$$

$$\nabla \cdot \vec{B} = 0 \ ,$$

$$\nabla \times \vec{E} = -\frac{\partial \vec{B}}{\partial t} \ ,$$

$$\vec{E} = \eta \vec{J} + \frac{1}{ne} \vec{J} \times \vec{B} \ .$$

As mentioned earlier, the density n and the resistivity η are assumed uniform. External coils with $m = 1$ structure are located at $r = r_c$ $(r_c \geq R)$. The current in the external coil is of the form of a traveling helical wave, $I \propto e^{i(\theta + kz - \omega t)}$. Region II $(R < r < r_c)$ is a vacuum region where growing and decaying fields are permitted; region III $(r > r_c)$ is a vacuum region where only decaying fields are permitted. In the vacuum regions, the fields obey

$$\nabla \times \vec{B} = 0 \ ,$$

$$\nabla \cdot \vec{B} = 0 \ ,$$

$$\nabla \times \vec{E} = -\frac{\partial \vec{B}}{\partial t} \ ,$$

$$\nabla \cdot \vec{E} = 0 \ .$$

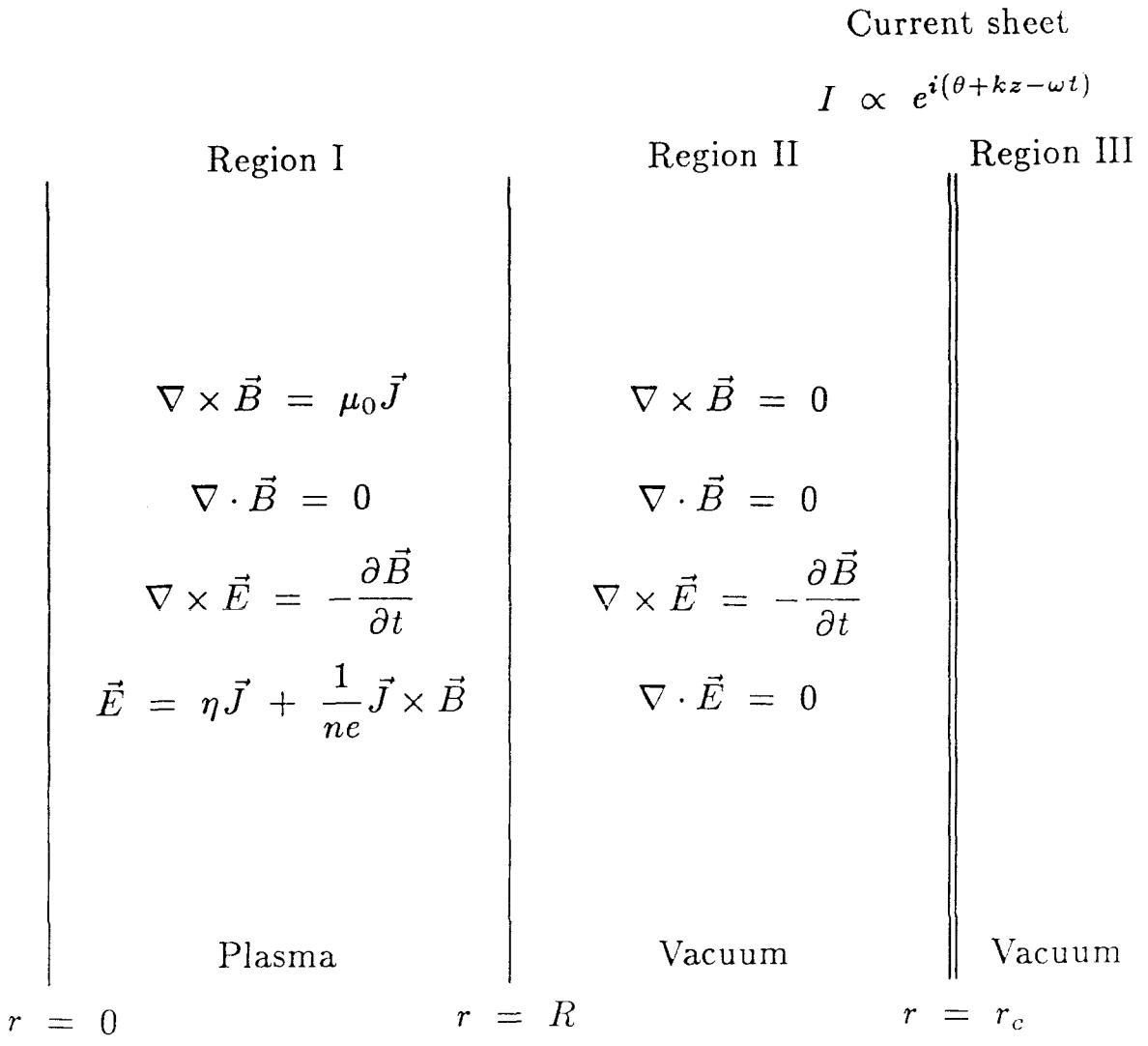

Figure 3.3 Straight cylindrical geometry for Hall MHD model. In region I, the plasma is assumed to satisfy the Hall MHD equations. Region II is a vacuum region where growing and decaying solutions are allowed; in region III, only decaying solutions are permitted. A helical sheet current is applied at $r = r_c$. The magnetic field is continuous everywhere — except at $r = r_c$ where the sheet current generates discontinuities in B_θ and B_z.

We now define a system of dimensionless units that will be used in all subsequent calculations. We will redefine the variables $\vec{B}$, $\vec{E}$, etc,... rather than choose a new set of variables. In dimensionless units, the fields within region I obey

$$\nabla \times \vec{B} = \alpha \vec{J} \ ,$$

$$\nabla \cdot \vec{B} = 0 \ ,$$

$$\nabla \times \vec{E} = -\frac{\partial \vec{B}}{\partial \tau} \ ,$$

$$\vec{E} = \epsilon \vec{J} + \vec{J} \times \vec{B} \ .$$

In this set of dimensionless units, $\vec{B}$ is normalized to B_ω (the strength of the applied rotating field); $\vec{J}$ is normalized to $ne\omega R$ (where n is the uniform density, e is the electron charge, ω is the frequency of the applied field, R is the plasma column radius); lengths are normalized to R (i.e., region I is the domain $r < 1$); $\vec{E}$ is normalized to $\omega R B_\omega$; $\epsilon = \frac{\eta n e}{B_w} = \frac{\nu_{ei}}{\omega_{ce}}$ (where ω_{ce} is the electron cyclotron frequency with respect to the applied rotating field strength); $\tau = \omega t$; $\alpha = (ne\omega R)(\mu_0 R)/B_w$. The current in the external coils is proportional to $e^{i\psi}$, where $\psi = \theta + kz - \tau$. The wave vector k is normalized to $1/R$. These definitions are summarized below:

Dimensionless Units

$\vec{B}$ normalized to B_ω

$\vec{J}$ normalized to $ne\omega R$

$\vec{r}$ normalized to R

k normalized to $1/R$

$$\vec{E} \text{ normalized to } \omega R B_w$$

$$\epsilon = \frac{\eta n e}{B_w} = \frac{\nu_{ei}}{\omega_{ce}}$$

$$\tau = \omega t$$

$$\alpha = \frac{(ne\omega R)(\mu_0 R)}{B_w}$$

$$\psi = \theta + kz - \tau \quad .$$

Two of these dimensionless parameters deserve special mention. The parameter ϵ, used as a basic perturbation parameter throughout these calculations, is the inverse of the Hall magnetic Reynolds number; ϵ gives a measure of the ratio of diffusion to convection. As will be emphasized later, the electron fluid becomes flux-conserving in the limit of small ϵ. The quantity $ne\omega R$ is the current-density associated with the rigid-rotor solution of the standard rotamak. The quantity $(ne\omega R)(\mu_0 R)$ is therefore a measure of the axial DC magnetic field driven by the rigid-rotor current. Since B_w is the strength of the applied rotating field, it follows that

$$\alpha \sim \frac{\text{DC magnetic field}}{\text{AC magnetic field}} \quad .$$

For tokamak current-drive, it is essential that the oscillating fields be kept as small as possible; hence $\alpha \gg 1$ is necessary for fusion applications.

The current in the external coils is of the form of a traveling helical wave, $\sim e^{i(\theta+kz-\tau)}$. In steady state, one would expect similar traveling waves to be induced within the plasma in response to the applied field. However, the nonlinear Hall term couples the harmonics, giving rise to all harmonics of the applied field. We therefore look for steady-state solutions of the form,

$$\vec{B} = \sum_{m=-\infty}^{\infty} \vec{b}_m(r)\, e^{im(\theta+kz-\tau)} \quad , \tag{3.18}$$

where $\vec{b}_m(r)$ is a complex function of r and $\vec{b}_m^* = \vec{b}_{-m}$. The ansatz given by Eq.(3.18) transforms the original PDE into an infinite system of coupled, nonlinear ODE's. The system of equations obtained by retaining only harmonics m such that $|m| \leq M$ will be labeled "the truncated system S_M."

The truncated system S_M can be written as a system of first-order ODE's of the general form,

$$\frac{d}{dr} y_i = f_i(y_1, y_2, \ldots y_N, r) \qquad i = 1, \ldots N \ , \tag{3.19}$$

where there are N independent variables $y_1(r) \ldots y_N(r)$ (N will depend on the number of harmonics retained). Boundary conditions are given at $r = 0$ and $r = 1$, forming a two-point, boundary-value problem. It is of interest to write the system S_M in the general form of Eq.(3.19) for use in numerical work and for counting the number of boundary conditions needed.

The θ and z components of Faraday's law yield, for a given harmonic m,

$$\frac{d}{dr}(re_\theta^m) = im(rb_z^m + e_r^m) \ , \tag{3.20}$$

$$\frac{d}{dr}(e_z^m) = im(ke_r^m - b_\theta^m) \ , \tag{3.21}$$

and the θ, z components of Ampere's law yield

$$\frac{d}{dr}(rb_\theta^m) = \alpha r j_z^m + imb_r^m \ , \tag{3.22}$$

$$\frac{d}{dr}(b_z^m) = imkb_r^m - \alpha j_\theta^m \ . \tag{3.23}$$

For $m = 0$, there are four real independent variables: re_θ^0, e_z^0, rb_θ^0, b_z^0. For a given harmonic m, $m \geq 1$, there are four complex independent variables: re_θ^m, e_z^m,

rb_θ^m, b_z^m. It is unnecessary to include negative values of m, since $\vec{b}_{-m} = \vec{b}_m^*$. It follows that the system S_M has $4M$ complex, independent variables and four real, independent variables.

Two of the independent variables can be eliminated from the system. When $m = 0$, Eqs.(3.20)-(3.21) yield $(re_\theta^0)' = 0$, $(e_z^0)' = 0$. Since e_θ^0 must not diverge as $r \to 0$, then it follows that e_θ^0 must vanish throughout the plasma. We shall impose the boundary condition that $(e_\theta^0,\ e_z^0)$ vanishes in the vacuum regions; the electrostatic field $(e_\theta^0,\ e_z^0)$ then vanishes everywhere. The system S_M is reduced to $4M$ complex independent variables and two real independent variables.

In order to obtain the form of Eq.(3.19), the "auxiliary" variables e_r^m, b_r^m, j_z^m, j_θ^m on the RHS of Eqs.(3.20)-(3.23) must be written solely in terms of the independent variables identified above (it is, of course, possible to define a different set of independent variables — the choice given here is the most straightforward). This can be accomplished by using the radial components of Faraday's law and Ampere's law,

$$b_r^m = \frac{1}{r} e_z^m - k e_\theta^m \ , \tag{3.24}$$

$$j_r^m = \frac{im}{\alpha} \left[\frac{1}{r} b_z^m - k b_\theta^m \right] \ , \tag{3.25}$$

together with the components of Ohm's law,

$$e_r^m = \epsilon j_r^m + j_\theta^p b_z^{m-p} - j_z^p b_\theta^{m-p} \ , \tag{3.26}$$

$$e_\theta^m = \epsilon j_\theta^m + j_z^p b_r^{m-p} - j_r^p b_z^{m-p} \ , \tag{3.27}$$

$$e_z^m = \epsilon j_z^m + j_r^p b_\theta^{m-p} - j_\theta^p b_r^{m-p} \ , \tag{3.28}$$

where repeated superscripts denote an implied sum, from $-M,\ldots,+M$. Solving Eqs.(3.24)-(3.28) for the auxiliary variables requires some matrix algebra, and the details are deferred until Sec.(3.2).

In the vacuum regions, $\nabla \times \vec{B} = 0$, and the magnetic field can be written as the gradient of a scalar function:

$$\vec{b}_m(r)e^{im\psi} = \nabla\left[\phi_m(r)e^{im\psi}\right] \quad (\ m \geq 1\ )\ . \tag{3.29}$$

Using $\nabla \cdot \vec{B} = 0$, Eq.(3.29) yields

$$\nabla^2\left[\phi_m(r)e^{im\psi}\right] \ = \ 0\ . \tag{3.30}$$

Eq.(3.30) leads to the modified Bessel equation,

$$r^2\frac{d^2\phi_m}{dr^2} \ + \ r\frac{d\phi_m}{dr} \ - \ (m^2 + m^2k^2r^2)\phi_m \ = \ 0\ ,$$

with solutions $I_m(mkr)$ (growing) and $K_m(mkr)$ (decaying). The vacuum fields are given by a superposition of growing and decaying modes,

$$\left\{\dot{I}_m\ ,\ \frac{i}{kr}I_m\ ,\ iI_m\right\}\ e^{im\psi}\ \text{(growing)}\ ,$$

$$\left\{\dot{K}_m\ ,\ \frac{i}{kr}K_m\ ,\ iK_m\right\}\ e^{im\psi}\ \text{(decaying)}\ ,$$

where the argument of all Bessel functions is (kmr) and where

$$\dot{I}_m(x) = \frac{d}{dx}I_m(x)\ .$$

Notice that dots will be used to indicate the derivative with respect to argument. This choice is unconventional but will unclutter the notation in future sections, where primes will be needed to denote $\frac{d}{dr}$.

In region II ($1 < r < r_c$), the solution consists of a linear combination of growing and decaying modes and for a given mode m, $m \geq 1$,

$$\vec{b}_m(r) = \gamma_m \left\{ \dot{K}_m , \frac{i}{kr} K_m , iK_m \right\} + \beta_m \left\{ \dot{I}_m , \frac{i}{kr} I_m , iI_m \right\} .$$

In region III ($r > r_c$), only decaying modes are allowed. For a given mode m, $m \geq 1$,

$$\vec{b}_m(r) = \alpha_m \left\{ \dot{K}_m , \frac{i}{kr} K_m , iK_m \right\} .$$

3.1.1 Boundary Conditions at $r = r_c$

At $r = r_c$ the radial magnetic field is continuous, yielding

$$\left(\gamma_m \dot{K}_m + \beta_m \dot{I}_m\right) - \alpha_m \dot{K}_m = 0 \ . \tag{3.31}$$

Let $[\![b_\theta^m]\!]$, $[\![b_z^m]\!]$ indicate the jump in b_θ , b_z at $r = r_c$ that is due to the external currents. One then has

$$\frac{i}{kr_c}\left[(\gamma_m K_m + \beta_m I_m) - \alpha_m K_m\right] = [\![b_\theta^m]\!] \ , \tag{3.32}$$

$$i\left[(\gamma_m K_m + \beta_m I_m) - \alpha_m K_m\right] = [\![b_z^m]\!] \ . \tag{3.33}$$

The argument of all Bessel functions in Eqs.(3.31)-(3.33) is (kmr_c). From Eqs.(3.32)-(3.33), one sees immediately that

$$kr_c[\![b_\theta^m]\!] = [\![b_z^m]\!] \ .$$

Thus, the jump in b_θ is not independent of the jump in b_z. Multiplying Eq.(3.31) by K_m gives

$$K_m\left[(\gamma_m \dot{K}_m + \beta_m \dot{I}_m) - \alpha_m \dot{K}_m\right] = 0 \ . \tag{3.34}$$

Multiplying Eq.(3.32) by $\dot{K}_m$ and rearranging gives

$$\dot{K}_m\left[(\gamma_m K_m + \beta_m I_m) - \alpha_m K_m\right] = \frac{kr_c}{i}\dot{K}_m[\![b_\theta^m]\!] \ . \tag{3.35}$$

Subtracting Eq.(3.34) from Eq.(3.35) yields

$$\beta_m\left(\dot{K}_m I_m - K_m \dot{I}_m\right) = \frac{kr_c}{i}\dot{K}_m[\![b_\theta^m]\!] \ .$$

The above can be simplified using the Wronskian,

$$I_m(x)\frac{d}{dx}K_m(x) - K_m(x)\frac{d}{dx}I_m(x) = -\frac{1}{x} \ ,$$

yielding

$$\beta_m \;=\; i(kr_c)^2 m \dot{K}_m [\![b_\theta^m]\!] \;\; . \tag{3.36}$$

It follows that the coefficients β_m are determined uniquely by the jump in $[\![b_\theta^m]\!]$ — and therefore by the prescribed current in the external coil, whereas the decaying solutions are fixed by currents in the plasma.

Since the current in the external coil is proportional to $e^{i(\theta+kz-\tau)}$, it follows that $\beta_m = 0$ for $|m| \neq 1$. We will choose the normalization,

$$\beta_m \;=\; \begin{cases} 0 & |m| \neq 1 \;\; , \\ \frac{1}{2\dot{I}_1(k)} & |m| = 1 \;\; . \end{cases} \tag{3.37}$$

This choice of normalization ensures that the vacuum field (in dimensionless units) is always order unity at $r = 1$ for *any* value of k, large or small. The growing solution in region II is then given by

$$\vec{b}^{\,\text{growing}} \;=\; \frac{1}{2\dot{I}_1(k)} \left\{ \dot{I}_1(kr) \;,\; \frac{i}{kr} I_1(kr) \;,\; i I_1(kr) \right\} \; e^{i(\theta+kz-\tau)} \;+\; \text{c.c.} \;\; .$$

For small argument, $I_1(x) \sim \frac{1}{2}x$ as $x \to 0$. Hence, as $k \to 0$,

$$\vec{b}^{\,\text{growing}} \;\sim\; \{\cos(\theta-\tau) \;,\; -\sin(\theta-\tau) \;,\; 0\} \qquad (k \to 0) \;\; .$$

Hence, the normalization given by Eq.(3.37) yields the standard rotamak vacuum field in the limit $k \to 0$. The standard rotamak solution must therefore be recovered, in all subsequent work, in the limit as $k \to 0$.

If one is interested in calculating the needed prescribed external current, then it is necessary to return to Eq.(3.36).

3.1.2 Boundary Conditions at $r = 1$

At $r = 1$, all components of the magnetic field are continuous. Just inside the plasma surface, the fields are given by

$$b_r^m = \gamma_m \dot{K}_m + \beta_m \dot{I}_m \ , \tag{3.38}$$

$$b_\theta^m = \frac{i}{k} (\gamma_m K_m + \beta_m I_m) \ , \tag{3.39}$$

$$b_z^m = i(\gamma_m K_m + \beta_m I_m) \ , \tag{3.40}$$

where the argument of all Bessel functions is now (km). From Eqs.(3.39)-(3.40) one finds the boundary condition,

$$b_z^m = k b_\theta^m \quad (\ m \geq 1 \ ) \ . \tag{3.41}$$

Note that $j_r^m = \frac{im}{r} b_z^m - imk b_\theta^m \quad (m \geq 1)$ so that boundary condition (3.41) implies that $j_r^m \quad (m \geq 1)$ vanishes at $r = 1$. Multiplying Eq.(3.38) by K_m, multiplying Eq.(3.39) by $\frac{k}{i} \dot{K}_m$, subtracting, and using the Wronskian, give

$$K_m(km) \ b_r^m - \frac{k}{i} \dot{K}_m(km) \ b_\theta^m = \frac{\beta_m}{mk} \quad (\ m \geq 1 \ ) \ , \tag{3.42}$$

where β_m is given by Eq.(3.37). So far, $2M$ complex boundary conditions have been specified [Eqs.(3.41)-(3.42)].

3.1.3 Boundary Conditions as $r \to 0$.

Let $\{a_r^m, a_\theta^m, a_z^m\}e^{i\psi}$ represent any field quantity. Using the regularity rules (Appendix.1),

$$a_r^m \sim r^{m-1} \ , \quad a_\theta^m \sim r^{m-1} \ , \quad a_z^m \sim r^m \ , \qquad (m \geq 1) \ ,$$

as $r \to 0$. Taking the limit of Eq.(3.22) as $r \to 0$ gives

$$b_\theta^m \sim i b_r^m \qquad (m \geq 1) \ . \tag{3.43}$$

Since $a_z^m \sim r^m$ for $m \geq 1$, then

$$b_z^m \sim 0 \qquad (m \geq 1) \ . \tag{3.44}$$

For $m = 0$, the regularity rules (Appendix.1) yield

$$a_r^0 \sim r \ , \quad a_\theta^0 \sim r \ , \quad a_z^0 \sim \text{const.} \ .$$

Hence, for $m = 0$, we add the boundary conditions,

$$b_\theta^0 \sim 0 \ , \tag{3.45}$$

$$b_z^0 \sim B_a \ , \tag{3.46}$$

where B_a is an arbitrary constant. We have added $2M$ complex boundary conditions [Eqs.(3.43)-(3.44)] and two real boundary conditions [Eqs.(3.45)-(3.46)].

3.1.4 Boundary Conditions: Summary.

The number of boundary conditions must be equal to the total number of independent variables. For the system S_M, $4M$ complex boundary conditions and two real boundary conditions must be specified (as noted above, the electrostatic field e_θ^0, e_z^0 is assumed to vanish in all regions).

Boundary Conditions at $r = 1$

$$b_z^m - k b_\theta^m = 0 \quad (m \geq 1)$$

$$k\, K_m(km)\, b_r^m + i\, k^2\, \dot{K}_m(km)\, b_\theta^m = \begin{cases} \frac{1}{2\dot{I}_1(k)} & (m = 1) \\ 0 & (m \geq 2) \end{cases}$$

Boundary Conditions as $r \to 0$

$$b_\theta^m - i b_r^m = 0 \quad (m \geq 1) \ ,$$

$$b_z^m = 0 \quad (m \geq 1) \ ,$$

$$b_\theta^0 = 0 \ ,$$

$$b_z^0 = B_a \quad (\ B_a = \text{arbitrary constant}\ ) \ .$$

3.2 Description of Numerical Methods

The numerical methods used here are based on a two-point boundary-value code called PVCPR[44], given in the IMSL library of mathematical software. The routine solves systems of O.D.E.'s of the form,

$$\frac{d}{dr}y_i \;=\; f_i(y_1,\, y_2,\, \ldots y_N,\, r) \qquad i = 1, \ldots N \;\;,$$

where $y_1, \ldots y_N$ are real functions of the independent variable, r. A finite-difference equation is created (using the trapezoid rule) from the original O.D.E. and the resulting system of equations (which is nonlinear, in general) is solved by iteration. Naturally, the iteration converges rapidly if a nearby solution is given as an initial guess; a family of solutions can be obtained by starting from a known solution and gradually increasing a given parameter.

The code has two powerful features worthy of mention. First, the resolution of the mesh (the number of grid points) is increased adaptively to ensure that the local error is the same throughout the domain. This increase in resolution becomes important if boundary layers should appear. Secondly, the code features a deferred correction process, which uses the Jacobian,

$$J_{ij} \;=\; \frac{\partial}{\partial y_j} f_i(y_1, \ldots, y_N,\, r) \;\;,$$

to obtain higher-order discretizations. The absolute error can be reduced far below the $O(h^2)$ truncation error expected from the trapezoid rule.

The system S_M, given by Eqs.(3.20)-(3.23), is almost of the correct form for numerical work; what remains is to write the auxiliary variables e_r^m, b_r^m, j_z^m, j_θ^m in terms of the independent variables. The radial components of Faraday's law

[Eq.(3.24)] and Ampere's law [Eq.(3.25)] provide expressions for b_r^m and j_r^m in terms of the independent variables. Eliminating j_z^m from Eqs.(3.27)-(3.28) gives the matrix equation,

$$j_\theta^q \left\{ \epsilon \delta^{m-q} + \frac{1}{\epsilon} b_r^{m-p} b_r^{p-q} \right\} = e_\theta^m + j_r^p b_z^{m-p} + \frac{1}{\epsilon} b_r^{m-p} \left[-e_z^p + j_r^q b_\theta^{p-q} \right] \quad . \quad (3.47)$$

The expression in curly brackets represents a square Hermitian matrix with $(2M+1)^2$ entries. For $M = 1$ this matrix reads,

$$T = \begin{pmatrix} \epsilon + \frac{1}{\epsilon}|b_r^1|^2 & 0 & \frac{1}{\epsilon}\left(b_r^{-1}\right)^2 \\ 0 & \epsilon + \frac{2}{\epsilon}|b_r^1|^2 & 0 \\ \frac{1}{\epsilon}\left(b_r^1\right)^2 & 0 & \epsilon + \frac{1}{\epsilon}|b_r^1|^2 \end{pmatrix},$$

which can be inverted to yield

$$T^{-1} = \frac{1}{\epsilon^3 + 2\epsilon|b_r^1|^2} \begin{pmatrix} \epsilon^2 + |b_r^1|^2 & 0 & -\left(b_r^{-1}\right)^2 \\ 0 & \epsilon^2 & 0 \\ -\left(b_r^1\right)^2 & 0 & \epsilon^2 + |b_r^1|^2 \end{pmatrix}.$$

Multiplying Eq.(3.47) by T^{-1} yields an expression for j_θ^q. One can then return to Eq.(3.28) and Eq.(3.26) to evaluate the remaining auxiliary variables, j_z^m and e_r^m, respectively.

Even for the system truncated after a single harmonic, the Jacobian is an enormously complicated expression with 100 entries. For the numerical work presented here, a symbolic processor (MACSYMA) was used to compute the Jacobian analytically; the symbolic processor was then used to translate the Jacobian into FORTRAN code, which was then streamlined to speed execution time. As an experiment, the Jacobian was also calculated numerically by calculating $f_i(y_1, \ldots, y_N, r)$

at two nearby points. An algorithm to compute the numerical Jacobian is trivial to devise and the same simple algorithm applies for any number of harmonics. However, the deferred correction process assumes that J_{ij} is known to machine precision and the numerical Jacobian scheme occasionally failed (the iteration failed to converge). All the numerical work presented in this thesis was generated using analytical Jacobian scheme.

3.3 The Role of Flux-Conserving Velocity Fields

Returning temporarily to original units, the model adopted to describe the time evolution of the magnetic field reads,

$$\frac{\partial \vec{B}}{\partial t} = \frac{\eta}{\mu_0}\nabla^2\vec{B} - \frac{1}{ne}\nabla\times\left(\vec{J}\times\vec{B}\right) \quad . \tag{3.48}$$

As the resistivity becomes vanishingly small, Eq.(3.48) becomes

$$\nabla\times\left(\vec{E} + \vec{U}\times\vec{B}\right) = 0 \quad , \tag{3.49}$$

where $\vec{U}$ is the electron fluid velocity. As emphasized by Hugrass[41], Eq.(3.49) states that the electron velocity field conserves magnetic flux in the limit as $\eta \to 0$. This means that the flux $\int_c \vec{B}\cdot d\vec{S}$ through any closed contour c moving with the fluid is constant in time. This is equivalent to the well-known principle that magnetic field lines are "glued" to the fluid in the limit of high magnetic Reynolds number. The time evolution of the flux ϕ is given by

$$\begin{aligned}\frac{d\phi}{dt} &= \int_c \frac{\partial\vec{B}}{\partial t}\cdot d\vec{S} + \int_c \vec{B}\cdot\left(\vec{U}\times d\vec{l}\right) \\ &= \int_c \left(-\nabla\times\vec{E}\right)\cdot d\vec{S} + \int_c d\vec{l}\cdot\left(\vec{B}\times\vec{U}\right) \quad . \\ &= -\int_c \left(\vec{E} + \vec{U}\times\vec{B}\right)\cdot d\vec{l}\end{aligned}$$

Hence, the condition $\vec{E}+\vec{U}\times\vec{B} = \nabla\psi$ (where ψ is single-valued) ensures that flux is conserved ($\frac{d\phi}{dt} = 0$).

We are now ready to prove a lemma that describes helical solutions of the ideal Hall MHD induction equation,

$$-\frac{\partial\vec{B}}{\partial\tau} = \nabla\times\left(\vec{J}\times\vec{B}\right)$$

(we have now returned to dimensionless units). As noted earlier, a similar induction equation arises in hydrodynamics and standard MHD, so that the results here may find application in other contexts.

Consider a vector field $\vec{Q} = \vec{Q}(r, \psi)$ that depends only on the radial coordinate r and the helical coordinate $\psi = \theta + kz - \tau$. Suppose further that $\vec{Q}$ is divergence-free: $\nabla \cdot \vec{Q} = 0$. We are interested in finding the most general vector $\vec{J} = \vec{J}(r)$, $\nabla \cdot \vec{J} = 0$, which satisfies

$$-\frac{\partial \vec{Q}}{\partial \tau} = \nabla \times \left(\vec{J} \times \vec{Q} \right) \tag{3.50}$$

(i.e., we seek the most general DC flux-preserving motion). Since both $\vec{Q}$ and $\vec{J}$ are divergence-free, then Eq.(3.50) becomes

$$-\frac{\partial \vec{Q}}{\partial \tau} = \vec{Q} \cdot \nabla \vec{J} \; - \; \vec{J} \cdot \nabla \vec{Q} \quad . \tag{3.51}$$

Since $\nabla \cdot \vec{J} = 0$, the radial part of $\vec{J}$ must vanish: $\vec{J} = \hat{\theta} J_\theta(r) \; + \; \hat{z} J_z(r)$. One then finds

$$\vec{Q} \cdot \nabla \vec{J} \; = \; Q_r \vec{J}' \; - \; \hat{r} \frac{Q_\theta J_\theta}{r} \quad , \tag{3.52}$$

$$\vec{J} \cdot \nabla \vec{Q} \; = \; \left(k J_z + \frac{J_\theta}{r} \right) \frac{\partial \vec{Q}}{\partial \psi} \; - \; \hat{r} \frac{Q_\theta J_\theta}{r} \; + \; \hat{\theta} \frac{Q_r J_\theta}{r} \quad , \tag{3.53}$$

$$\frac{\partial \vec{Q}}{\partial \psi} \; = \; -\frac{\partial \vec{Q}}{\partial \tau} \quad , \tag{3.54}$$

where primes denote $\frac{d}{dr}$. Inserting Eqs(3.52)-(3.54) into Eq.(3.51) gives

$$\frac{\partial \vec{Q}}{\partial \psi}(1 + k J_z + \frac{J_\theta}{r}) \; + \; \hat{\theta} Q_r (\frac{J_\theta}{r} - J_\theta') \; - \; \hat{z} Q_r J_z' = 0 \quad .$$

If $\frac{\partial Q_r}{\partial \psi}$ and Q_r are nonzero, then Eq. (3.50) is satisfied, provided that

$$1 + k J_z + \frac{J_\theta}{r} = 0 \; , \quad \frac{J_\theta}{r} - J_\theta' = 0 \; , \quad J_z' = 0 \quad .$$

The solution to the above equations is given by

$$\vec{J} \;=\; -\hat{\theta}r(1+kJ_{z0}) \;+\; \hat{z}J_{z0} \quad ,$$

where J_{z0} is an arbitrary constant.

We summarize the above by stating the following lemma.

Lemma

Given $\vec{Q} = \vec{Q}(r,\psi)$, $\psi = \theta + kz - \tau$, $\nabla \cdot \vec{Q} = 0$, then,

$$-\frac{\partial \vec{Q}}{\partial \tau} \;=\; \nabla \times \left\{ [-\hat{\theta}r(1+kJ_{z0}) + \hat{z}J_{z0}] \;\times\; \vec{Q} \right\} \quad , \tag{3.55}$$

where J_{z0} is an arbitrary constant.

Thus, we have identified the most general family of DC flux-conserving currents. The bulk motion of the electron fluid consists of a uniform current in the z-direction and a current in the θ-direction, which is linear in r.

3.4 Definition and Manipulation of a-type and b-type Vectors

The boundary conditions described previously in Sec.(3.2) give rise to vacuum fields for which the radial magnetic field is 90° out of phase with the θ and z components. The structure of the vacuum field gives rise to a special algebra with a set of simple rules. Suppose that

$$\vec{q} = \left\{\hat{r}q_r(r) + \hat{\theta}q_\theta(r) + \hat{z}q_z(r)\right\} e^{i\psi} \quad , \tag{3.56}$$

$$\vec{Q} = \hat{\theta}Q_\theta(r) + \hat{z}Q_z(r) \quad , \tag{3.57}$$

where lower-case variables are complex, upper-case variables are real and $\psi = \theta + kz - \tau$. Then, by definition,

a-type vectors are of the form $\left\{\hat{r}(\text{real}) + \hat{\theta}(\text{imaginary}) + \hat{z}(\text{imaginary})\right\} e^{i\psi}$

b-type vectors are of the form $\left\{\hat{r}(\text{imaginary}) + \hat{\theta}(\text{real}) + \hat{z}(\text{real})\right\} e^{i\psi}$.

Clearly, any vector $\vec{q}$ of the form given by Eq.(3.56) can be decomposed into an a-type and a b-type vector. The following rules for manipulation of a-type and b-type vectors are trivial to prove by direct computation.

Rule (1)

If $\vec{q}$ is a-type, then $i\vec{q}$ is b-type.

If $\vec{q}$ is b-type, then $i\vec{q}$ is a-type.

Rule (2)

If $\vec{q}$ is a-type, then $\nabla \times \vec{q}$ is also a-type.

If $\vec{q}$ is b-type, then $\nabla \times \vec{q}$ is also b-type.

Rule (3)

If $\vec{q}$ is a-type, then $\vec{q} \times \vec{Q}$ is b-type.

If $\vec{q}$ is b-type, then $\vec{q} \times \vec{Q}$ is a-type.

Rule (4)

The product $\vec{q}_{a1} \times \vec{q}_{a2}$ is a-type.

The product $\vec{q}_{b1} \times \vec{q}_{b2}$ is a-type.

The product $\vec{q}_a \times \vec{q}_b$ is b-type.

3.5 DC Flux-Conserving Motions

In this section we proceed analytically, as far as possible, with the full Hall MHD system. We seek steady-state, helical solutions of the equation,

$$-\frac{\partial \vec{B}}{\partial \tau} \;=\; \epsilon \nabla \times \vec{J} \;+\; \nabla \times \left(\vec{J} \times \vec{B} \right) \quad , \tag{3.58}$$

valid in the limit $\epsilon \rightarrow 0$. When $\epsilon = 0$ exactly, it was shown in Sec.(3.4) that a bulk DC flux-conserving motion exists for which there is a uniform toroidal current. Similarly, in the work of Bertram[37], it is suggested that a solution of Eq.(3.58) exists for which there is a uniform toroidal current in the limit as $\epsilon \rightarrow 0$. The purpose of this section is to show that Bertram's result is valid only in the special case where the static toroidal field vanishes and where the DC fields are a small fraction of the oscillating fields.

To zero order in ϵ, $\vec{B} = \vec{B}_0 + \epsilon \vec{B}_1 \ldots$, Eq.(3.58) yields

$$-\frac{\partial \vec{B}_0}{\partial \tau} \;=\; \nabla \times \left(\vec{J}_0 \times \vec{B}_0 \right) \quad . \tag{3.59}$$

Once again, Eq.(3.59) states that $\vec{J}_0$ must be flux-conserving. We will assume in this section that $\vec{J}_0$ is a DC quantity — although this is by no means the only possibility.

Using the lemma of Sec.(3.4), an exact solution of Eq.(3.59) is given by

$$\vec{B}_0 \;=\; \left\{ 0 \;,\; \frac{1}{2} \alpha r J_{z0} \;,\; B_a + \frac{1}{2} \alpha r^2 (1 + k J_{z0}) \right\} \;+\; \vec{b}_v + \vec{b}_v^{\,*} \quad , \tag{3.60}$$

$$\vec{b}_v \;=\; \frac{1}{2 \dot{I}_1(k)} \left\{ \dot{I}_1(kr) \;,\; \frac{i}{kr} I_1(kr) \;,\; i I_1(kr) \right\} e^{i\psi} \quad , \quad \psi = \theta + kz - \tau \quad , \tag{3.61}$$

$$\vec{J}_0 \;=\; \{ 0 \;,\; -r(1 + k J_{z0}) \;,\; J_{z0} \} \quad ,$$

where B_a, J_{z0} are arbitrary constants.

The magnetic field $\vec{B}_0$ consists of a DC component and an oscillating helical vacuum field. The curl operation annihilates the vacuum field, and it is trivial to check to see that $\nabla \times \vec{B}_0 = \alpha \vec{J}_0$. The zero-order field given by Eq.(3.60) is a function only of (r, ψ) and therefore is of the correct form for the lemma. When $k \rightarrow 0$ and $J_{z0} \rightarrow 0$, one finds $\vec{J}_0 = -r\hat{\theta}$, which is the rigid-rotor solution of the standard rotamak. Bertram's solution for the rhythmac is obtained if $J_{z0} = -k/(2+k^2)$.

Eq.(3.60) represents an exact solution when $\epsilon = 0$, and we now perturb this solution and look for "nearby" solutions for small ϵ. To first order, one has,

$$-\frac{\partial \vec{B}_1}{\partial \tau} = \nabla \times \vec{J}_0 + \nabla \times \left(\vec{J}_0 \times \vec{B}_1 + \vec{J}_1 \times \vec{B}_0 \right) .$$

The LHS cancels with the second term on the RHS, using the lemma (note that $\vec{B}_1$ is again only a function of (r, ψ) and therefore of the correct form for the lemma). The first-order equation then becomes

$$\nabla \times \left(\vec{J}_0 + \vec{J}_1 \times \vec{B}_0 \right) = 0 . \tag{3.62}$$

To solve Eq.(3.62), we first write $\vec{B}_0$ as a sum of harmonics,

$$\vec{B}_0 = \vec{b}_0(r) + \left(\vec{b}_1(r) e^{i\psi} + b_{-1}(r) e^{-i\psi} \right) . \tag{3.63}$$

The first-order current $\vec{J}_1$ is also expanded into harmonics:

$$\vec{J}_1 = \vec{j}_0(r) + \left(\vec{j}_1(r) e^{i\psi} + \vec{j}_{-1} e^{-i\psi} \right) + \left(\vec{j}_2(r) e^{2i\psi} + j_{-2}(r) e^{-2i\psi} \right) + \ldots . \tag{3.64}$$

Substituting Eqs.(3.63)-(3.64) into Eq.(3.62) and gathering terms of the same harmonic gives,

$$\nabla \times \left[\vec{J}_0 + \vec{j}_1 \times \vec{b}_{-1} + \vec{j}_0 \times \vec{b}_0 + \vec{j}_{-1} \times \vec{b}_1 \right] = 0 , \tag{3.65}$$

$$\nabla \times \left[\vec{j}_2 \times \vec{b}_{-1} \; + \; \vec{j}_1 \times \vec{b}_0 \; + \; \vec{j}_0 \times \vec{b}_1 \right] \; = \; 0 \;\; , \tag{3.66}$$

$$\nabla \times \left[\vec{j}_3 \times \vec{b}_{-1} \; + \; \vec{j}_2 \times \vec{b}_0 \; + \; \vec{j}_1 \times \vec{b}_1 \right] \; = \; 0 \;\; , \tag{3.67}$$

etc .

Since $\nabla \times \left(\vec{j}_0 \times \vec{b}_0 \right) = 0$ (the radial components of $\vec{j}_0(r)$ and $\vec{b}_0(r)$ vanish), then Eq.(3.65) becomes

$$\nabla \times \left[\vec{J}_0 \; + \; 2\mathrm{Re}\left(\vec{j}_1 \times \vec{b}_v^{\,*} \right) \right] \; = \; 0 \;\; ,$$

and uncurling the above yields

$$\vec{J}_0 \; + \; 2\mathrm{Re} \; \left(\vec{j}_1 \times \vec{b}_v^{\,*} \right) \; = \; \nabla \phi(r) \;\; , \tag{3.68}$$

where $\phi(r)$ is an arbitrary scalar function. Noting that $\vec{b}_v$ is an a-type vector, and using the rules of Sec.(3.5), the (θ, z) components of Eq.(3.68) become

$$\vec{J}_0 \; + \; 2\vec{j}_{1b} \times \vec{b}_v^{\,*} \; = \; 0 \quad (\theta, \; z \; \text{only} \;) \;\; . \tag{3.69}$$

Letting

$$\vec{j}_{1b} = \{ j_r, j_\theta, j_z \} \;\; , \;\; \vec{J}_0 = \{ 0, J_\theta, J_z \} \;\; , \;\; \vec{b}_v = \frac{1}{2\dot{\tilde{I}}_1} \left\{ \dot{I}_1, \frac{i}{(kr)} I_1, i I_1 \right\} \;\; , \;\; \dot{\tilde{I}}_1 = \dot{I}_1(k) \;\; ,$$

the θ and z components of Eq.(3.69) give

$$J_\theta \; + \; \frac{1}{\dot{\tilde{I}}_1} \left(\dot{I}_1 j_z \; + \; i I_1 j_r \right) \; = \; 0 \;\; , \tag{3.70}$$

$$J_z \; + \; \frac{1}{\dot{\tilde{I}}_1} \left(-\frac{i I_1}{kr} j_r \; - \; \dot{I}_1 j_\theta \right) \; = \; 0 \;\; , \tag{3.71}$$

and from $\nabla \cdot \vec{j}_{1b} \; = \; 0$, one finds

$$\frac{d}{dr}(\, r j_r \,) \; + \; i j_\theta \; + \; ikr j_z \; = \; 0 \;\; . \tag{3.72}$$

Eqs.(3.70)-(3.72) form a complete set of equations to determine $\vec{j}_{1b}$. Using Eqs.(3.70)-(3.71) to eliminate j_θ and j_z from Eq.(3.72) gives

$$r^2 I_1' j_r' \; + \; j_r \left[r I_1' \; + \; I_1(1 + k^2 r^2) \right] \; = \; ikr \dot{\tilde{I}}_1 (kr J_\theta \; - \; J_z) \;\; ,$$

where primes denote $\frac{d}{dr}$. Using the identity $r^2 I_1'' \; + \; r I_1' \; = \; I_1(1 + k^2 r^2)$, the above becomes

$$r^2 I_1' j_r' \; + \; j_r \left[r^2 I_1'' \; + \; 2 r I_1' \right] \; = \; ikr \dot{\tilde{I}}_1 (kr J_\theta \; - \; J_z) \;\; .$$

The LHS is a perfect derivative, yielding

$$(\; r^2 I_1' j_r \;)' \; = \; ikr \dot{\tilde{I}}_1 (kr J_\theta \; - \; J_z) \;\; . \tag{3.73}$$

Using $J_\theta = -r(1 + k J_{z0})$, $J_z = J_{z0}$ in the RHS of Eq.(3.73) and integrating, yields

$$r^2 I_1' j_r \; = \; \frac{-i \dot{\tilde{I}}_1 r^2}{4} \left[k J_{z0} (2 + k^2 r^2) \; + \; k^2 r^2 \right] \; + \; \text{const.} \;\; .$$

The quantity $r^2 I_1' j_r$ must vanish at $r = 0$ and $r = 1$; this is possible only if

$$\text{const.} \; = \; 0 \;\; , \qquad J_{z0} \; = \; - \frac{k}{2 + k^2} \quad \text{(Bertram s current)} \;\; . \tag{3.74}$$

Inserting Eq.(3.74) into Eq.(3.60) yields

$$\vec{B}_0 \; = \; \left\{ \; 0 \; , \; - \frac{\alpha k r}{2(2 + k^2)} \; , \; B_a \; + \; \frac{\alpha r^2}{2 + k^2} \; \right\} \; + \; \vec{b}_v + \vec{b}_v^* \;\; , \tag{3.75}$$

$$\vec{J}_0 \; = \; \left\{ 0 \; , \; \frac{-2r}{2 + k^2} \; , \; \frac{-k}{2 + k^2} \right\} \;\; . \tag{3.76}$$

The fields $j_{1\theta}$ and j_{1z} can now be found by returning to Eqs.(3.70)-(3.71); the full expression for $\vec{j}_{1b}$ becomes

$$\vec{j}_{1b} \; = \; \frac{\dot{\tilde{I}}_1}{2r(2 + k^2)(\dot{I}_1)^2} \Big\{ \; ikr(1 - r^2)\dot{I}_1 \; , \; (1 - r^2) I_1 - 2kr \dot{I}_1 \; , \; kr(1 - r^2) I_1 + 4r^2 \dot{I}_1 \Big\} \;\; . \tag{3.77}$$

Taking the a-part of Eq.(3.66) (noting that $\vec{b}_1 = \vec{b}_v$ is a-type) yields

$$\nabla \times \left[\vec{j}_{2a} \times \vec{b}_v^* \; + \; \vec{j}_{1b} \times \vec{b}_0 \right] \; = \; 0 \quad . \tag{3.78}$$

Here we are beginning to see that the perturbation scheme can lead to a divergent series. Unless $\vec{j}_{1b}$ happens to be parallel to $\vec{b}_0$, then Eq.(3.78) yields, roughly,

$$|\vec{j}_{2a}| \sim \frac{|\vec{b}_0|}{|\vec{b}_v|} |\vec{j}_{1b}| \quad .$$

For tokamak current-drive, the DC fields must be larger than the oscillating fields [e.g., $\alpha \sim 10$, $B_a \sim 100$ in Eq.(3.75)]. For strong toroidal field strength, the second-order harmonic $|\vec{j}_{2a}|$ is larger than the first-order harmonic $|\vec{j}_{1b}|$ by a factor roughly, of B_a. The trend continues, and from Eq.(3.67) it follows that $|\vec{j}_{3b}|$ is larger than $|\vec{j}_{2a}|$ by a factor, roughly of B_a. The harmonics appear to be growing without bound by factors of $(B_a)^m$.

There is, however, a special case where the series terminates after a single harmonic. Taking the limit $k \rightarrow 0$ gives

$$\vec{J}_0 \; = \; \{0, -r, 0\} \quad ,$$

$$\vec{B}_0 \; = \; \left\{ 0, 0, B_a + \frac{1}{2} \alpha r^2 \right\} \; + \; \vec{b}_v + \vec{b}_v^* \quad ,$$

$$\vec{b}_v \; = \; \frac{1}{2} \{1, i, 0\} \, e^{i(\theta - \tau)} \quad ,$$

$$\vec{j}_{1b} \; = \; \{0, 0, r\} \, e^{i(\theta - \tau)} \; + \; \text{cc} \quad .$$

This is the rigid-rotor solution of the standard rotamak — an *exact* solution of Eq.(3.62) with $\vec{J}_1 = \vec{j}_{1b}$ (note that $\vec{j}_{1b}$ is now exactly parallel to $\vec{b}_0$). Hence, the exact first-order solution consists of only a single harmonic.

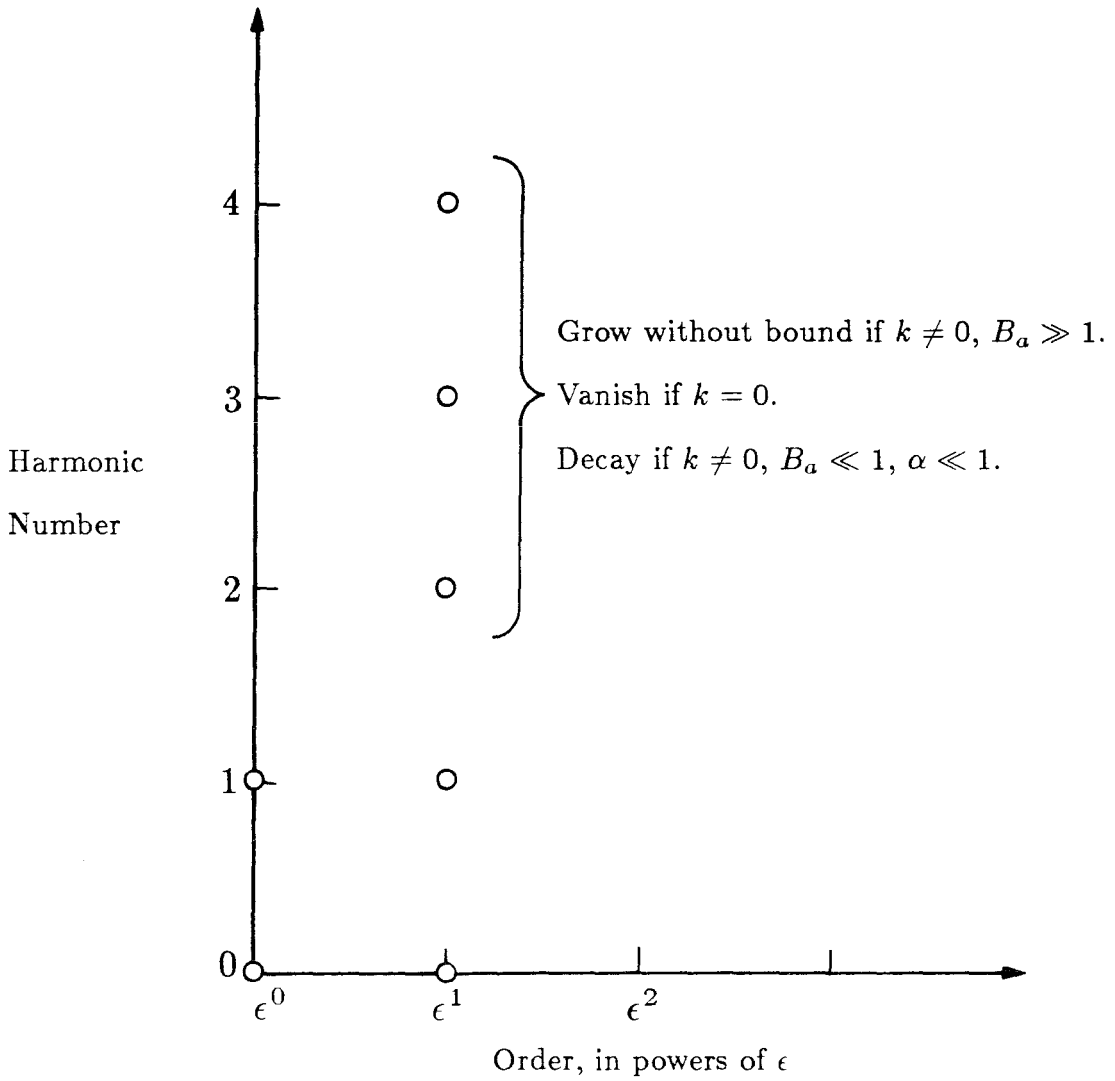

Figure 3.4 Schematic representation of the perturbation scheme. Horizontal axis represents order of perturbation in powers of ϵ; vertical axis represents the harmonic number. Only a DC component and a first-order harmonic appear to zero-order in ϵ. In general, all harmonics are generated to first order in ϵ.

A schematic representation of this perturbation scheme appears in Fig.(3.4). The order of the calculation in powers of ϵ appears on the horizontal axis; the number of harmonics in the solution appears on the vertical axis. To zero order in ϵ, the solution consists of a DC part and a first-order harmonic. To first order in ϵ, all harmonics are needed, in general. The magnitude of each harmonic grows without bound, for large values of B_a, when k is nonzero. However, in the special case $k = 0$, where $\vec{j}_{1b}$ becomes parallel to $\vec{b}_0$, all higher-order harmonics ($m \geq 2$) vanish.

The divergent series indicates that the zero-order solution described by the lemma is not attained as $\epsilon \to 0$. Professor Noel Corngold[42] has given the following analogy to explain this puzzling result. Suppose that we write down the equations needed to describe the water level in a leaky bucket with a small hole in the bottom, of order ϵ. We *insist* on looking for steady-state solutions of the leaky-bucket problem, as we did in the above Hall MHD calculation. If, to zero order in ϵ, we plug up the hole, then we can arrive at only one possible solution — the water level remains constant. If we now reinstate the small hole and wait an infinite amount of time (equivalent to assuming steady state), then the only solution possible is that the water level is zero. Thus, the zero-order solution is a poor approximation of the first-order solution, no matter how small the value of ϵ. Bertram's uniform toroidal current $J_z = -k/(2 + k^2)$ is a "leaky-bucket" solution in the case where $B_a \gg 1$, $\alpha \gg 1$. It should be noted that Bertram's result appears to be valid in the case where $\epsilon \to 0$, $\alpha \to 0$, $B_a \to 0$ (this occurs as the rotating field strength B_ω approaches infinity, holding all other parameters fixed).

3.6 Solution of the System S_1 as $\epsilon \to 0$

In the last section, we investigated the most general DC flux-conserving motion. It was found that the DC zero-order current led to a diverging series in the limit where $\alpha \gg 1$ or where $B_a \gg 1$. We must therefore search for an alternative flux-preserving motion that includes an oscillating component. We begin the analysis of this section by giving analytical and numerical solutions of the system S_1 — the system of ODE's formed by truncating after a single harmonic:

$$\vec{B} = \sum_{m=-1}^{m=+1} \vec{b}_m(r) e^{im\psi} \quad .$$

In the next section, we will address the question of whether the system S_1 is a good approximation to the full system.

In order to avoid writing subscripts, we will let upper-case variables denote steady-state quantities and let lower-case variables represent oscillating quantities. In this notation, the full magnetic field is written as

$$\vec{B} = \{ B_\theta(r)\hat{\theta} + B_z(r)\hat{z} \} + \{ \vec{b}(r)e^{i\psi} + \vec{b}^*(r)e^{-i\psi} \} \quad .$$

The functions $B_\theta(r)$ and $B_z(r)$ are real, whereas the vector $\vec{b}(r)$ is complex. The system S_1 can then be written as

$$\nabla \times \vec{E} = 0 \quad ,$$

$$\nabla \times \vec{e} = -\frac{\partial \vec{b}}{\partial \tau} \quad ,$$

$$\nabla \times \vec{B} = \alpha \vec{J} \quad ,$$

$$\nabla \times \vec{b} = \alpha \vec{j} \quad ,$$

$$\vec{e} = \epsilon\vec{j} + \vec{J}\times\vec{b} + \vec{j}\times\vec{B} \ , \tag{3.79}$$

$$\epsilon\vec{J} + 2\mathrm{Re}[\ \vec{j}\times\vec{b}^{*}\ ] = 0 \quad (\hat{\theta},\ \hat{z}\ \text{only}) \ . \tag{3.80}$$

As discussed in Sec.(3.1), the static electric field (E_θ, E_z) must vanish, leading to Eq.(3.80). The steady radial electric field is given by

$$E_r = \vec{J}\times\vec{B} + 2\mathrm{Re}\left[\vec{j}\times\vec{b}^{*}\right]_r \ .$$

Taking the curl of Eq.(3.79) and using Faraday's law to eliminate $\nabla\times\vec{e}$ yields

$$-\frac{\partial\vec{b}}{\partial\tau} = \epsilon\nabla\times\vec{j} + \nabla\times[\ \vec{J}\times\vec{b} + \vec{j}\times\vec{B}\ ] \ . \tag{3.81}$$

Decomposing Eqs.(3.80)-(3.81) into a-type and b-type components gives,

$$-\frac{\partial\vec{b}_a}{\partial\tau} = \epsilon\nabla\times\vec{j}_b + \nabla\times\left[\vec{J}\times\vec{b}_a + \vec{j}_a\times\vec{B}\right] \ , \tag{3.82}$$

$$-\frac{\partial\vec{b}_b}{\partial\tau} = \epsilon\nabla\times\vec{j}_a + \nabla\times\left[\vec{J}\times\vec{b}_b + \vec{j}_b\times\vec{B}\right] \ , \tag{3.83}$$

$$\epsilon\vec{J} + 2(\ \vec{j}_a\times\vec{b}_b^{*} + \vec{j}_b\times\vec{b}_a^{*}\ ) = 0 \quad (\theta,\ z\ \text{only}) \ . \tag{3.84}$$

So far, the only approximation made is the neglect of higher-order harmonics.

We are now ready to investigate the limit $\epsilon \to 0$ (the limit $\epsilon \to 0$ is implied throughout this section even if not written explicitly). The limit $\delta = 1/\epsilon \ll 1$ (limit of large resistivity) is investigated in Appendix 3.

For $\epsilon \to 0$, two cases arise where the applied vacuum field fully penetrates the plasma cylinder:

• Case (1): $\alpha \to 0$, k = fixed, B_a = fixed. Since $\nabla\times\vec{B} = \alpha J$, it follows that the magnetic field becomes a vacuum field as $\alpha \to 0$. As noted in Sec.(3.1), the parameter α is roughly the ratio of the DC magnetic field to the AC magnetic field.

• Case (2): α = fixed, k = fixed, $B_a \to \infty$. This case is of primary interest for tokamaks, where the resistivity is small ($\epsilon \ll 1$), where the oscillating field is a small fraction of the DC field ($\alpha \gg 1$), and where the toroidal field strength is very large ($B_a \gg 1$). As we will verify self-consistently, the strong axial field excludes all plasma currents from the core of the plasma; the DC and AC currents then reside in a skin layer of width $\sim 1/kB_a$, leaving only the vacuum magnetic fields created by the external coils as $B_a \to \infty$. Bertram[36] has identified a similar skin effect in a slab-geometry calculation.

In either of the cases outlined above, only the vacuum fields appear to lowest order:

$$\vec{b}_a \to \vec{b}_v \ ,$$

$$\vec{b}_b \to 0 \ ,$$

$$\vec{B} \to B_a \hat{z} \ ,$$

where $\vec{b}_v$ is the oscillating vacuum field and $B_a\hat{z}$ is a uniform DC vacuum field. Again, for case (2), we first assume that the vacuum field appears to lowest order and later verify the assumption self-consistently. Eqs.(3.82)-(3.84) then become, to lowest order,

$$-\frac{\partial \vec{b}_v}{\partial \tau} = \nabla \times \left[\vec{J} \times \vec{b}_v + \vec{j}_a \times B_a \hat{z} \right] \ , \tag{3.85}$$

$$0 = \epsilon \nabla \times \vec{j}_a + \nabla \times \left[\vec{j}_b \times B_a \hat{z} \right] \ , \tag{3.86}$$

$$\epsilon \vec{J} + 2\vec{j}_b \times \vec{b}_v^* = 0 \quad (\theta, \ z \text{ only}) \ . \tag{3.87}$$

The term $\epsilon \nabla \times \vec{j}_b$ was dropped in Eq.(3.82), since we are interested in the limit $\epsilon \to 0$. There are two limits taking place simultaneously in Eqs.(3.83)-(3.84): $\vec{b}_b \to 0$ and

$\epsilon \to 0$. The terms that scale with ϵ in Eqs.(3.86)-(3.87) have been retained, whereas the terms that scale with $\vec{b}_b$ have been dropped. For case (1), we are, in effect, taking the limit $\alpha \to 0$ first, before taking the limit $\epsilon \to 0$. The approximation is valid for α sufficiently small, for any fixed value of ϵ. Similarly, in case (2), we are taking the limit $B_a \to \infty$ before taking the limit $\epsilon \to 0$. The approximation is valid for sufficiently large values of B_a, for any fixed value of ϵ.

The role played by $\vec{j}_a$ is quite different from the role played by $\vec{j}_b$. According to Eq.(3.85), the flux-conserving motion consists of a steady current $\vec{J}$ and an oscillating current $\vec{j}_a$. According to Eq.(3.87), the oscillating current $\vec{j}_b$ interacts with the vacuum field to produce the steady current $\vec{J}$. Hence, $\vec{j}_a$ is needed for flux conservation, whereas $\vec{j}_b$ is needed to sustain the steady current against Ohmic dissipation ($\vec{j}_a$ is orthogonal to the vacuum field and does not interact to produce a steady current). The current $\vec{j}_b$ becomes vanishingly small as the Hall Reynolds number approaches infinity. We will find that $\vec{j}_a$ vanishes only of the standard rotamak, where $k = 0$.

For the special case where $\epsilon \to 0$, $\alpha \to 0$, $B_a \to 0$, Eqs.(3.82)-(3.84) become, to leading order,

$$-\frac{\partial \vec{b}_v}{\partial \tau} = \nabla \times \left(\vec{J} \times \vec{b}_v \right) \quad , \tag{3.88}$$

$$0 = \epsilon \nabla \times \vec{j}_a + \nabla \times \left(\vec{j}_b \times \vec{B} \right) \quad , \tag{3.89}$$

$$\epsilon \vec{J} + 2\vec{j}_b \times \vec{b}_v^* = 0 \quad (\theta, z \text{ only}) \quad . \tag{3.90}$$

All lower-case variables are proportional to $e^{i\psi}$ and for the general case where $B_a \neq 0$ Eqs.(3.85)-(3.86) yield

$$ikB_a \vec{j}_a = i\vec{b}_v \left(1 + \frac{J_\theta}{r} + kJ_z \right) + b_{vr} \left(\hat{\theta} \frac{J_\theta}{r} - \frac{d\vec{J}}{dr} \right) \quad , \tag{3.91}$$

$$ikB_a\vec{j}_b \;=\; -\epsilon\left\{\frac{i}{r}j_{az} - ikj_{a\theta}\;,\; ikj_{ar} - j'_{az}\;,\; \frac{1}{r}\frac{d(rj_{a\theta})}{dr} - \frac{i}{r}j_{ar}\right\}\quad . \tag{3.92}$$

From Eq.(3.91), the boundary condition $j_{ar}(r=1)=0$ yields

$$1 \;+\; J_\theta \;+\; kJ_z \;=\; 0\;,\quad (r=1)\quad . \tag{3.93}$$

From Eqs.(3.91)-(3.92), the boundary condition $j_{br}(r=1)=0$ yields

$$\frac{dJ_z}{dr} \;+\; k\left[J_\theta \;-\; \frac{dJ_\theta}{dr}\right] \;=\; 0\;,\quad (r=1)\quad . \tag{3.94}$$

The current $\vec{j}_a$ can be eliminated from the RHS of Eq.(3.92), using Eq.(3.91). The resulting expression for $\vec{j}_b$ can then be substituted into Eq.(3.87) to obtain a second-order, linear equation for the DC currents:

$$x\left[xf(x)J'_\theta\right]' \;-\; J_\theta\left\{\left[xf(x)\right]' \;+\; \frac{B_a^2x^2}{2}\right\} \;=\; 0\;, \tag{3.95}$$

$$x\left[xf(x)J'_z\right]' \;-\; J_z\frac{B_a^2x^2}{2} \;=\; 0\;, \tag{3.96}$$

$$f(x) \;=\; \left[\frac{\dot{I}_1(x)}{2\dot{I}_1(k)}\right]^2\quad ,$$

where $x=kr$ and primes denote $\frac{d}{dx}$.

It is emphasized again that Eqs.(3.95)-(3.96) are valid only if the vacuum fields appear to lowest order, which occurs in either of two cases: (1) $\alpha \to 0$ or, (2) $B_a \to \infty$, $k=$ finite (currents reside in a skin layer).

3.6.1 The Limit $\alpha \to 0$, $k \tilde{<} 1$, B_a = fixed

For values of k somewhat less than unity, the first term in the Taylor expansion for $I_1(x)$ can be substituted into Eqs.(3.95)-(3.96): $\dot{I}_1(x) \approx \frac{1}{2}$, $f(x) \approx \frac{1}{4}$, yielding Bessel function solutions,

$$J_\theta = C_\theta I_1(\gamma r) \ , \tag{3.97}$$

$$J_z = C_z I_0(\gamma r) \ , \tag{3.98}$$

$$\gamma = \sqrt{2} k B_a \ ,$$

where C_θ and C_z are constants. The constants can be determined from Eqs.(3.93)-(3.94), yielding

$$C_\theta = \frac{-I_1}{I_1^2 + k^2 I_0 I_2} \ , \tag{3.99}$$

$$C_z = \frac{-k I_2}{I_1^2 + k^2 I_0 I_2} \ . \tag{3.100}$$

The argument of each Bessel function is γ.

The steady currents become skin currents for large B_a. The skin effect is unusual in that the width of the skin layer depends only on k and B_a — not on the frequency and resistivity. Numerical and analytical solutions are compared in Fig.(3.5).

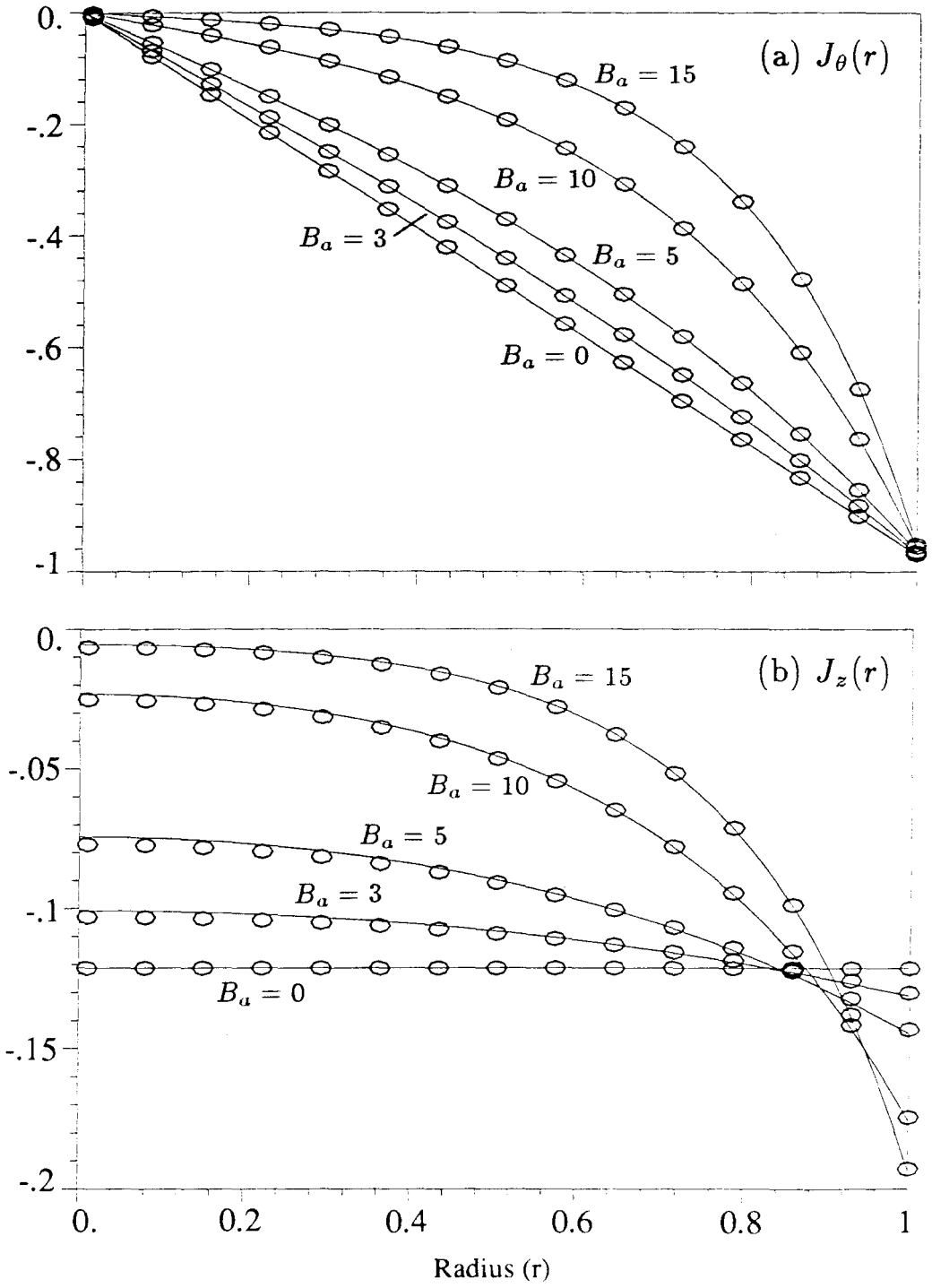

Figure 3.5 Plot of steady current (a) $J_\theta(r)$ and (b) $J_z(r)$ for the case where $\epsilon = 0.01$, $\alpha = 0.1$, $k = 0.25$. Circles represent numerical solutions of the system S_1 with 15 grid points. The solid curve is a plot of the approximate analytical theory.

3.6.2 The limit $\alpha \to 0$, $k =$ fixed, $B_a \to 0$

Here, we expect to reproduce Bertram's result, which was shown in Sec.(3.5) to be valid in this limit (higher-order harmonics decayed away gracefully when $\alpha \ll 1$ and $B_a \ll 1$). To lowest order, the basic equations are now given by Eqs.(3.88)-(3.90). The exact solution to these equations was derived in the analysis leading to Eq.(3.77) in Sec.(3.5). We quote the results here for convenience:

$$\vec{B} = \left\{ 0 \, , \, -\frac{\alpha k r}{2(2+k^2)} \, , \, \frac{\alpha r^2}{2+k^2} \right\} \, , \tag{3.75}$$

$$\vec{J} = \left\{ 0 \, , \, \frac{-2r}{2+k^2} \, , \, \frac{-k}{2+k^2} \right\} \, , \tag{3.76}$$

$$\vec{j}_b = \frac{\epsilon \dot{\tilde{I}}_1}{2r(2+k^2)(\dot{I}_1)^2} \Big\{ ikr(1-r^2)\dot{I}_1 \, , \, (1-r^2)I_1 - 2kr\dot{I}_1 \, , \, kr(1-r^2)I_1 + 4r^2\dot{I}_1 \Big\} \, , \tag{3.77}$$

$$\vec{b}_v = \frac{1}{2\dot{I}_1(k)} \left\{ \dot{I}_1(kr) \, , \, \frac{i}{kr} I_1(kr) \, , \, iI_1(kr) \right\} \, . \tag{3.61}$$

The current $\vec{j}_a$ can be found by returning to Eq.(3.89). However, an expression for $\vec{j}_a$ involving only simple Bessel functions could not be found. Analytical and numerical solutions are plotted in Fig.(3.6).

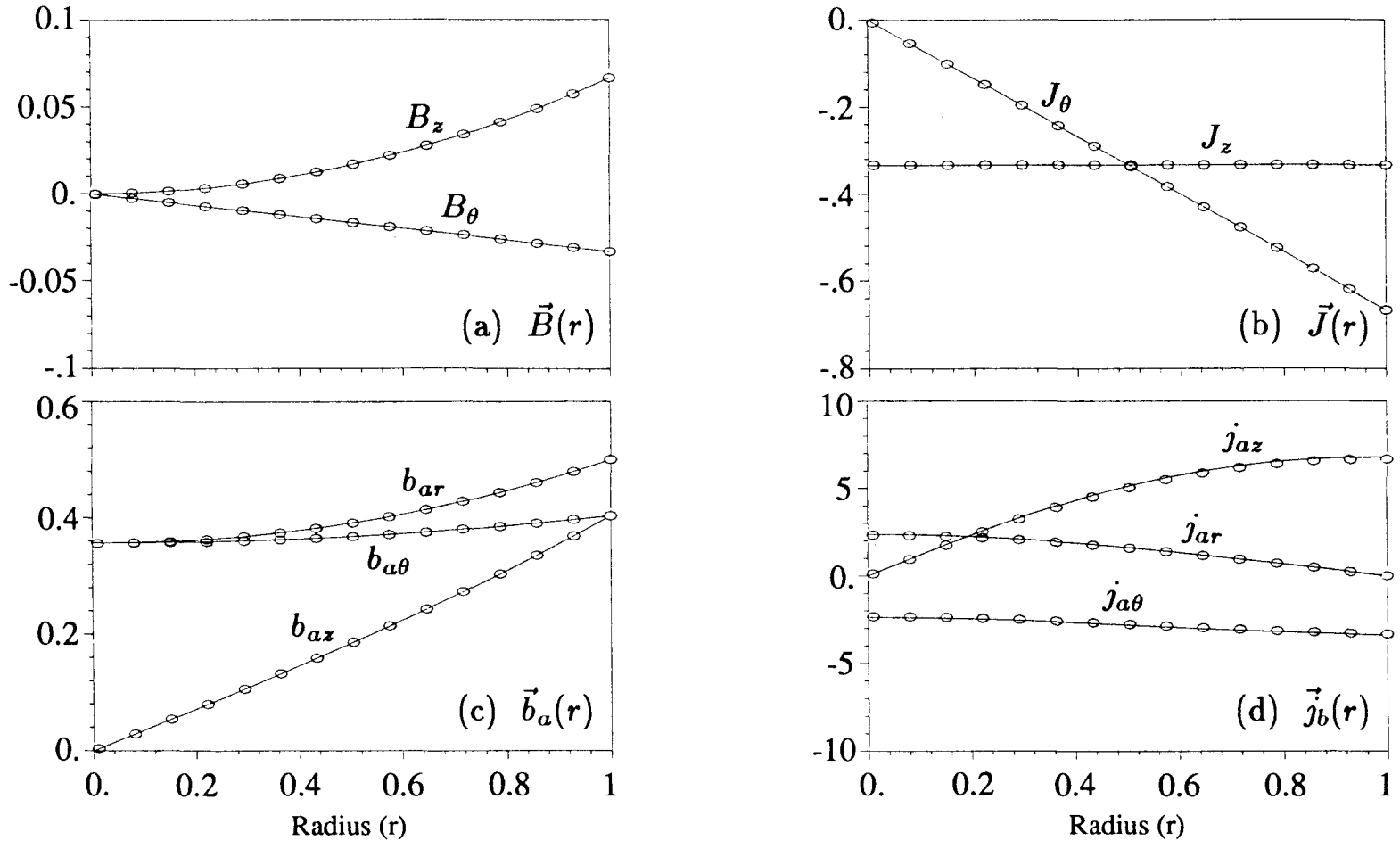

Figure 3.6 Plot of (a) $\vec{B}(r)$, (b) $\vec{J}(r)$, (c) $\vec{b}_a(r)$, (d) $\vec{j}_b(r)$ for the case where $\alpha = 0.2$, $\epsilon = 0.01$, $k = 1$, $B_a = 0$. Circles represent numerical solutions of the system S_1 for 15 grid points. The solid curve is a plot of the approximate analytical solution.

3.6.3 The Limit $\alpha =$ fixed, $k =$ fixed, $B_a \to \infty$

The limiting case $\epsilon \to 0$, $B_a \to \infty$, $\alpha \gg 1$ is of greatest interest for tokamaks where the resistivity is small and where the static toroidal field is large. It was shown in a previous section ($\epsilon \to 0$, $\alpha \to 0$, $B_a \neq 0$) that the driven, steady current resides in a skin layer of width $\sim 1/(kB_a)$. As will be shown here, the skin layer persists for large values of α. The derivation given here will be as simple as possible, providing the most physical insight with the least amount of mathematical detail. As $B_a \to \infty$, it will be assumed that all currents either vanish or that the currents are confined to a skin layer of width $1/(kB_a)$ (all assumptions must be verified self-consistently).

The radial part of Eq.(3.91) gives

$$kB_a j_{ar} \;=\; \left(1 + \frac{J_\theta}{r} + kJ_z\right) b_{vr} \quad .$$

Thus, the radial current j_{ar} is small, scaling as $\sim \frac{1}{B_a}$. Since $j_{ar}(r=1) = 0$, it again follows that,

$$1 + J_\theta + kJ_z \;=\; 0 \quad (r=1) \quad . \tag{3.101}$$

Consider the θ and z components of Eq.(3.91). Of the various terms on the RHS of Eq.(3.91), only the term $-b_{vr}\vec{J}'$ scales with B_a (since there is a boundary layer of width $1/B_a$ near $r = 1$). A reasonable approximation is to let

$$ikB_a j_{a\theta} \;=\; -b_{vr}^{\text{wall}} J_\theta' \quad , \tag{3.102}$$

$$ikB_a j_{az} \;=\; -b_{vr}^{\text{wall}} J_z' \quad , \tag{3.103}$$

where $b_{vr}^{\text{wall}} = b_{vr}(r=1)$.

It was noted above that j_{ar} is small, scaling as $\sim 1/B_a$, and terms involving j_{ar} can therefore be neglected on the RHS of Eq.(3.92). The quantity $j_{a\theta}/r$ can be neglected compared with $j'_{a\theta}$ since, again, the current is confined to a boundary layer of width $1/B_a$. To good approximation, the θ and z components of Eq.(3.92) yield

$$ikB_a j_{b\theta} = \epsilon j'_{az} \ , \tag{3.104}$$

$$ikB_a j_{bz} = -\epsilon j'_{a\theta} \ . \tag{3.105}$$

The radial component of Eq.(3.92) gives

$$kB_a j_{br} = -\epsilon \left(\frac{j_{az}}{r} - k j_{a\theta} \right) \ .$$

The radial current j_{br} is very small, scaling as $\sim \epsilon/B_a$. Using the above expression with Eqs.(3.102)-(3.103) yields the condition,

$$J'_z - kJ'_\theta = 0 \quad (r = 1) \ , \tag{3.106}$$

since j_{br} must vanish at $r = 1$. Finally, Eq.(3.87) yields

$$\epsilon J_\theta + 2 j_{bz} b_{vr}^{\text{wall}\,*} = 0 \ , \tag{3.107}$$

$$\epsilon J_z - 2 j_{b\theta} b_{vr}^{\text{wall}\,*} = 0 \ , \tag{3.108}$$

where the terms involving j_{br} have been dropped since, as noted above, these scale as $\sim \epsilon/B_a$.

The current $\vec{j}_a$ can be eliminated from the RHS of Eqs.(3.104)-(3.105), using Eqs.(3.102)-(3.103). The current $\vec{j}_b$ can then be eliminated from Eqs.(3.107)-(3.108). Carrying out these manipulations and using the fact that $b_{vr}^{\text{wall}} = \frac{1}{2}$, yields

$$J''_\theta - \gamma^2 J_\theta = 0 \ ,$$

$$J_z'' - \gamma^2 J_z = 0 \ ,$$

$$\text{where } \gamma = \sqrt{2}kB_a \ .$$

The driven currents are therefore given by

$$J_\theta = C_\theta e^{\gamma(r-1)} \ , \quad J_z = C_z e^{\gamma(r-1)} \ , \tag{3.109}$$

where the constants C_θ and C_z are determined from Eq.(3.101) and Eq.(3.106). Evaluating these constants is trivial and yields

$$C_\theta = -\frac{1}{1+k^2} \ , \quad C_z = -\frac{k}{1+k^2} \ . \tag{3.110}$$

Analytical and numerical surface contours of $I_z(k, B_a)$ are plotted in Fig.(3.7), where

$$I_z = \int\int J_z \, r dr d\theta \ .$$

All surface contours are normalized in the same way. As expected, the analytical theory is a very good approximation for large values of B_a. Note that the integrated current I_z is insensitive to the value of α for sufficiently large values of B_a (as predicted in the above analysis).

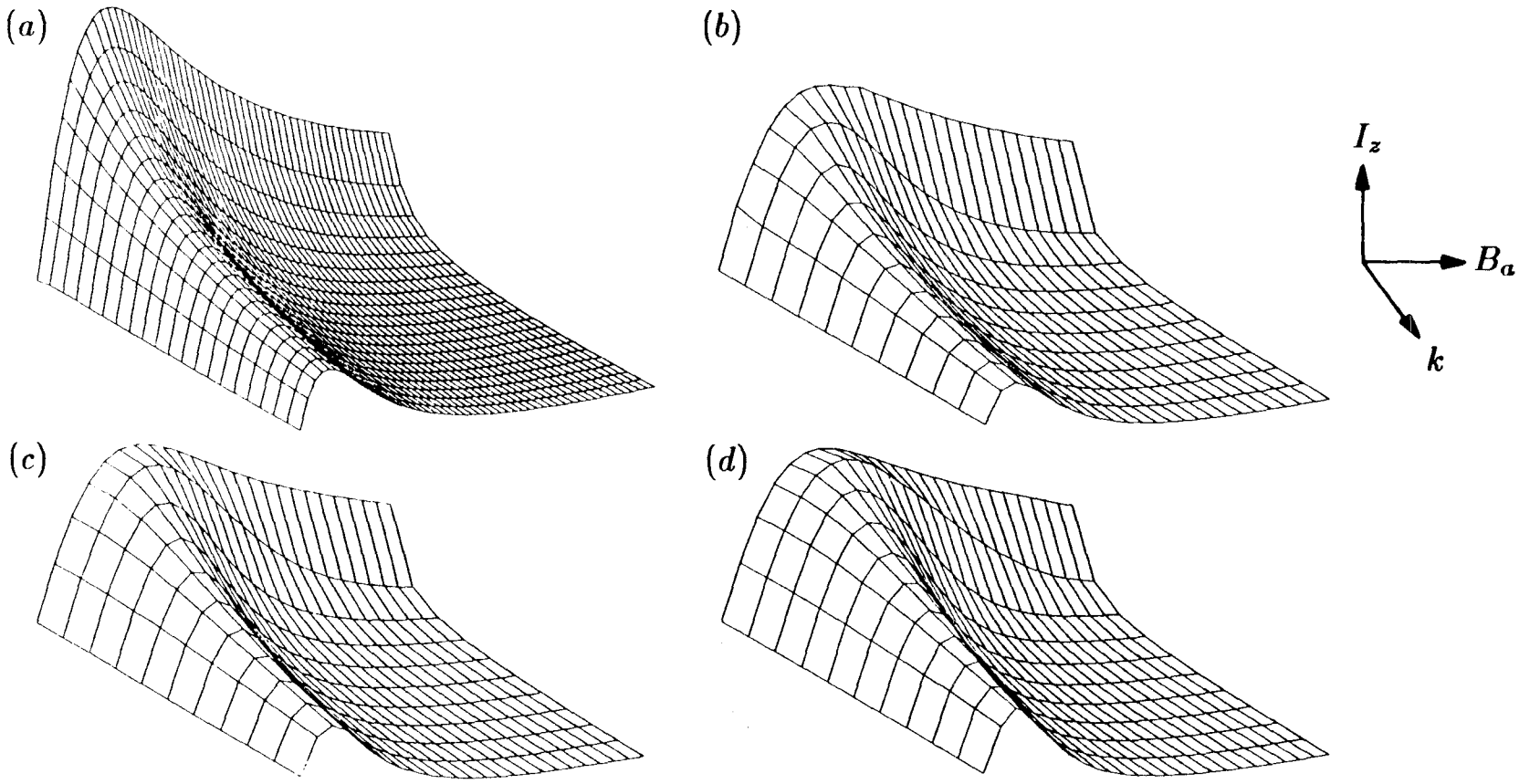

Figure 3.7. Plot of $I_z(k, B_a)$ for (a) approximate analytical theory, (b) $\alpha = 0.1$, $\epsilon = 0.01$ (numerical), (c) $\alpha = 3.0$, $\epsilon = 0.01$ (numerical), (d) $\alpha = 6.0$, $\epsilon = 0.01$ (numerical). All contours are normalized in the same way, and the domain for each contour is $(k = 0.1 \rightarrow k = 5.0)$, $(B_a = 0 \rightarrow B_a = 5.0)$.

3.7 Validity of the System S_1

In the preceding work, the truncated system S_M was formed by including only the first M harmonics in the steady-state solution. The truncation was performed for mathematical tractability, and we hope that solutions of the system S_n will closely approximate solutions of S_{n+1}. We explore the consequences of truncating the system in this section.

Recall that the full system can be cast as a single, nonlinear equation for $\vec{B}$,

$$-\frac{\partial \vec{B}}{\partial \tau} = \epsilon \nabla \times \vec{J} + \nabla \times \left(\vec{J} \times \vec{B} \right) ,$$

$$\text{where } \nabla \times \vec{B} = \alpha \vec{J} .$$

When $\delta = 1/\epsilon \ll 1$, it is not difficult to justify the neglect of higher-order harmonics because the nonlinear term scales with δ and enters the calculation as a perturbation. We are, perhaps, conditioned to think that higher-order harmonics must diminish in strength. This is the case for the ubiquitous weakly nonlinear harmonic oscillator, which is ingrained in the mind of every student of classical mechanics. Furthermore, in the laboratory, we do not expect to see large, second and higher-order harmonics, growing without bound. Nevertheless, the neglect of higher-order harmonics is difficult to justify in the more important regime of low resistivity, $\epsilon \to 0$, since — unlike the weakly nonlinear oscillator — *it is a linear term that enters as a perturbation* . It is therefore surprising that the consequence of truncating the system has received little mention in the literature. It is true that higher-order harmonics are not seen experimentally — but there is no guarantee that our exceedingly simple, fluid-type equation describes what is seen in the laboratory.

A number of rough scaling arguments will be given in this section to assess the magnitude of higher-order harmonics. Analytical and numerical solutions to the system S_1 were given earlier, and we now consider the system S_2:

$$\epsilon\vec{j}_0 \; + \; 2\mathrm{Re}\left\{\vec{j}_{-1} \times \vec{b}_1\right\} \; = \; -2\mathrm{Re}\left\{\vec{j}_{-2} \times \vec{b}_2\right\} \quad , \tag{3.111}$$

$$-\frac{\partial \vec{b}_1}{\partial \tau} \; - \; \epsilon\nabla \times \vec{j}_1 \; - \; \nabla \times \left\{\vec{j}_0 \times \vec{b}_1 \; + \; \vec{j}_1 \times \vec{b}_0\right\} \; = \; \nabla \times \left\{\vec{j}_{-1} \times \vec{b}_2 \; + \; \vec{j}_2 \times \vec{b}_{-1}\right\} \quad , \tag{3.112}$$

$$-\frac{\partial \vec{b}_2}{\partial \tau} \; = \; \epsilon\nabla \times \vec{j}_2 \; + \; \nabla \times \left\{\vec{j}_0 \times \vec{b}_2 \; + \; \vec{j}_1 \times \vec{b}_1 \; + \; \vec{j}_2 \times \vec{b}_0\right\} \quad . \tag{3.113}$$

Subscripts in Eqs.(3.111)-(3.113) denote the harmonic number. If the system S_1 has already been solved, then all fields with subscript -1, 0, or $+1$ are considered known; Eq.(3.113) then gives a linear equation for the second harmonic, $\vec{b}_2$. The system S_1 is recovered if the terms on the RHS of Eqs.(3.111)-(3.112) are dropped; our goal, therefore, is to show that we can neglect the RHS of Eqs.(3.111)-(3.112) to good approximation.

Case of Large Resistivity $\delta = 1/\epsilon \ll 1$

As mentioned above, the neglect of higher-order harmonics is not hard to justify in the limit where $\delta \to 0$. Suppose that we attempt to balance the terms $\epsilon\nabla \times \vec{j}_2$ and $\nabla \times \left(\vec{j}_1 \times \vec{b}_1\right)$ on the RHS of Eq.(3.113), so that $\vec{j}_2 \sim \delta\vec{j}_1 \times \vec{b}_1$. The second harmonic $\vec{j}_2$ is then diminished by a factor of δ. This checks out self-consistently, since the terms $-\frac{\partial \vec{b}_2}{\partial \tau}$, $\nabla \times \left(\vec{j}_0 \times \vec{b}_2\right)$, $\nabla \times \left(\vec{j}_2 \times \vec{b}_0\right)$ in Eq.(3.113) are then all smaller by a factor of δ than the two terms that were originally assumed to dominate.

Case of Small Resistivity: $\epsilon \ll 1$

DC Flux-Conserving Motion

In Sec.(3.6), the current $\vec{J}_0 = \{0, -r(1 + kJ_{z0}), J_{z0}\}$ was shown to be the most general DC flux-conserving motion. A perturbation about this exact zero-order solution was performed starting from the full Hall MHD system, and it was found that higher-order harmonics were *not* important if (1) $k = 0$, or (2) $B_a \ll 1$ and $\alpha \ll 1$. Case (1) corresponds to the standard rotamak and case (2) corresponds to Bertram's[37] solution for the rhythmac with $J_{z0} = -k/(2 + k^2)$.

Case of Small Resistivity: $\epsilon \ll 1$

AC Flux-Conserving Motion

In Sec.(3.7), it was shown that all plasma currents are confined to a skin layer in the limit as $\epsilon \to 0$, $B_a \to \infty$. In this limit, we anticipate a balance between the last two terms on the RHS of Eq.(3.113): $\vec{j}_1 \times \vec{b}_1 \sim \vec{j}_2 \times \vec{b}_0$. Since $\vec{b}_0 \sim B_a$, it then follows that $\vec{j}_2$ is diminished by a factor roughly, of $1/B_a$. This checks out self-consistently since the terms $-\frac{\partial \vec{b}_2}{\partial \tau}$, $\epsilon \nabla \times \vec{j}_2$, and $\nabla \times \left(\vec{j}_0 \times \vec{b}_2\right)$ are then all smaller by a factor, roughly, of $1/B_a$ than the two terms that were originally assumed to dominate.

3.8 Conservation Laws

For steady-state current drive it is of interest to investigate the injection and dissipation of energy, momentum, and magnetic helicity. We begin by deriving three steady-state conservation laws that are satisfied exactly by any solution of the system S_1. One could also derive these conservation laws starting from the full Hall MHD equations; the form of the conservation equations is identical whether one begins from the truncated system or the full system.

Recall that the system S_1 is given by

$$\nabla \times \vec{E} = 0 \quad , \quad \nabla \times \vec{e} = -\frac{\partial \vec{b}}{\partial \tau} \quad ,$$

$$\nabla \times \vec{B} = \alpha \vec{J} \quad , \quad \nabla \times \vec{b} = \alpha \vec{j} \quad ,$$

$$\vec{e} = \epsilon \vec{j} + \vec{J} \times \vec{b} + \vec{j} \times \vec{B} \quad ,$$

$$\epsilon \vec{J} + 2\mathrm{Re}\left(\vec{j} \times \vec{b}^*\right) = 0 \quad (\theta,\ z \text{ only}) \quad .$$

For convenience we introduce the following notation: Primed variables will represent the full field, consisting of a steady vector and an oscillating vector. For example, the full magnetic field is written as

$$\vec{B}' = \vec{B}(r) + \left\{\vec{b}(r)e^{i\psi} + \vec{b}^*(r)e^{-i\psi}\right\} \quad .$$

3.8.1 Energy Conservation and the Poynting Theorem

Taking the divergence of $\vec{E}' \times \vec{B}'$ and using a vector identity gives

$$\nabla \cdot \left(\vec{E}' \times \vec{B}' \right) \; = \; \vec{B}' \cdot \nabla \times \vec{E}' \; - \; \vec{E}' \cdot \nabla \times \vec{B}' \quad .$$

Inserting Faraday's law and Ampere's law into the RHS yields the energy conservation equation,

$$\frac{\partial}{\partial \tau} \left(\frac{1}{2} B'^2 \right) \; + \; \nabla \cdot \left(\vec{E}' \times \vec{B}' \right) \; + \; \alpha \vec{J}' \cdot \vec{E}' \; = \; 0 \quad . \tag{3.114}$$

The Poynting vector $\vec{E}' \times \vec{B}'$ represents a flux of incident energy which is balanced by an increase in mechanical energy, $\vec{J}' \cdot \vec{E}'$, and an increase in magnetic energy, $\frac{\partial}{\partial \tau} (B'^2/2)$.

Taking the time-average and integrating over a plasma cylinder of radius $r = 1$ gives

$$2\mathrm{Re} \left[\vec{e}(r=1) \times \vec{b}^*(r=1) \right]_{\mathrm{radial}} \; + \; \alpha \int_0^1 2\mathrm{Re} \left(\vec{j} \cdot \vec{e}^{\,*} \right) \, r dr \; = \; 0 \quad . \tag{3.115}$$

[Note that the electrostatic field points only in the radial direction so that (1) $\vec{J}(r) \cdot \vec{E}(r) = 0$, and (2) $\vec{E}(r) \times \vec{B}(r)$ has no radial component.] Using Ohm's law,

$$\begin{aligned} 2\mathrm{Re} \left(\vec{j} \cdot \vec{e}^{\,*} \right) \; &= \; 2\mathrm{Re} \left[\vec{j} \cdot \left(\epsilon \vec{j}^{\,*} \; + \; \vec{J} \times \vec{b}^* \; + \; \vec{j}^{\,*} \times \vec{B} \right) \right] \\ &= \; 2\mathrm{Re} \left[\epsilon \vec{j} \cdot \vec{j}^{\,*} \; + \; \vec{J} \cdot \left(\vec{b}^* \times \vec{j} \right) \; + \; \vec{B} \cdot \left(\vec{j} \times \vec{j}^{\,*} \right) \right] \quad , \\ &= \; 2\epsilon \, \vec{j} \cdot \vec{j}^{\,*} \; + \; \epsilon \vec{J} \cdot \vec{J} \; + \; \vec{B} \cdot 2\mathrm{Re} \left(\vec{j} \times \vec{j}^{\,*} \right) \quad . \end{aligned}$$

The last term on the RHS vanishes, since $\mathrm{Re} \left(\vec{j} \times \vec{j}^{\,*} \right) \; = \; 0$. The time-averaged conservation law becomes

$$2\mathrm{Re} \left[\vec{e}(r=1) \times \vec{b}^*(r=1) \right]_{\mathrm{radial}} \; + \; \alpha\epsilon \int_0^1 \left[\vec{J} \cdot \vec{J} \; + \; 2 \, \vec{j} \cdot \vec{j}^{\,*} \right] r dr \; = \; 0 \quad . \tag{3.116}$$

The incident energy flux is balanced by Ohmic dissipation associated with the oscillating current $\vec{j} \cdot \vec{j}^*$ and Ohmic dissipation associated with the steady current, $\vec{J} \cdot \vec{J}$. For current drive one hopes to minimize the amount of AC dissipation, which degrades the current-drive efficiency.

For the case where $\epsilon \to 0$, $B_a \to \infty$, Eqs.(3.102)-(3.103) yield $ikB_a\vec{j}_a = -b_{vr}^{\rm wall}\vec{J}'$ (θ, z, only). The radial component j_{ar} is much smaller and can be neglected. Using $b_{vr}^{\rm wall} = 1/2$ and $\vec{J}' = \sqrt{2}kB_a\vec{J}$ [from Eq.(3.109)] then yields

$$\vec{j}_a \approx \frac{i}{\sqrt{2}}\vec{J} \ . \tag{3.117}$$

From Eqs.(3.104)-(3.105), it follows that $\vec{j}_b$ scales with ϵ and can be neglected here. Using Eq.(3.117), one finds

$$\vec{j} \cdot \vec{j}^* \ \approx \ \vec{j}_a \cdot \vec{j}_a^* \ \approx \ \frac{1}{2}\vec{J} \cdot \vec{J} \ .$$

Hence, the incident energy flux is equally divided between AC and DC dissipation in this limit (Bertam[36] arrived at the same conclusion is his slab-geometry calculation).

3.8.2 Magnetic Helicity Conservation

From Faraday's law, $\nabla \times \vec{E}' = -\frac{\partial \vec{B}'}{\partial \tau}$, and from $\nabla \cdot \vec{B}' = 0$ alone it follows that $\vec{B}'$ and $\vec{E}'$ can be generated from a scalar potential ϕ' and a vector potential $\vec{A}'$,

$$\vec{B}' = \nabla \times \vec{A}' \ ,$$

$$\vec{E}' = -\nabla \phi' - \frac{\partial \vec{A}'}{\partial \tau} \ .$$

The time derivative of the magnetic helicity density $\vec{A}' \cdot \vec{B}'$ yields

$$\begin{aligned}
\frac{\partial}{\partial \tau}\left(\vec{A}' \cdot \vec{B}'\right) &= \frac{\partial \vec{A}'}{\partial \tau} \cdot \vec{B}' + \vec{A}' \cdot \frac{\partial \vec{B}'}{\partial \tau} \ , \\
&= \left(-\vec{E}' - \nabla \phi'\right) \cdot \vec{B}' - \vec{A}' \cdot \nabla \times \vec{E}' \ , \\
&= -\vec{E}' \cdot \vec{B}' - \nabla \cdot \left(\phi' \vec{B}'\right) - \left\{\vec{E}' \cdot \nabla \times \vec{A}' - \nabla \cdot \left(\vec{A}' \times \vec{E}'\right)\right\} \ , \\
&= -2\vec{E}' \cdot \vec{B}' - \nabla \cdot \left(\phi' \vec{B}' + \vec{E}' \times \vec{A}'\right) \ .
\end{aligned}$$

The helicity conservation equation then reads,

$$\frac{\partial}{\partial \tau}\left(\vec{A}' \cdot \vec{B}'\right) + \nabla \cdot \left(\phi' \vec{B}' + \vec{E}' \times \vec{A}'\right) + 2\vec{E}' \cdot \vec{B}' = 0 \ . \qquad (3.118)$$

The helicity density $\vec{A}' \cdot \vec{B}'$ is not gauge-invariant, but the equality given by Eq.(3.118) is valid for any choice of gauge.

A convenient choice for the gauge is to let

$$\phi' = \phi(r) \ ,$$

$$\vec{A}' = \vec{A}(r) + \frac{1}{2}\int_{\tau}^{\tau+\pi} d\tau' \left\{\vec{e}(r) e^{i(\theta + kz - \tau')} + \vec{e}^{\,*}(r) e^{-i(\theta + kz - \tau')}\right\} \ ,$$

or,

$$\vec{A}' = \vec{A}(r) + \frac{\vec{e}(r)}{i} e^{i\psi} + \frac{\vec{e}^{\,*}(r)}{-i} e^{-i\psi} \ ,$$

where

$$\nabla\phi(r) \;=\; -\hat{r}E_r \;\;,$$

$$\nabla\times\vec{A}(r) \;=\; \vec{B}(r) \;\;,\;\; \vec{A}(r) \;=\; A_\theta(r)\hat{\theta} \;+\; A_z(r)\hat{z} \;\;.$$

It is trivial to check that the above vector and scalar fields generate $\vec{B}'$ and $\vec{E}'$.

Since $\vec{A}'\cdot\vec{B}'$ is time-periodic, it follows that $\frac{\partial}{\partial\tau}\left(\vec{A}'\cdot\vec{B}'\right)$ vanishes on time-averaging. The static helicity flux $\phi\vec{B}(r)+\vec{E}(r)\times\vec{A}(r)$ vanishes in the radial direction since $\vec{B}(r)$ has no radial component and since $\vec{E}=\hat{r}E_r(r)$. Taking the time average of Eq.(3.118) and integrating over the plasma cylinder yields

$$2\mathrm{Re}\Big\{\, i\big[\;\vec{e}(r=1)\times\vec{e}^{\,*}(r=1)\;\big]\Big\}_{\mathrm{radial}} \;+\; \int_0^1 2\mathrm{Re}\big(\vec{e}\cdot\vec{b}^{*}\big)\,rdr \;=\; 0 \;\;. \qquad (3.119)$$

The dissipation term can be rewritten, using Ohm's law in the following steps:

$$\begin{aligned} 2\mathrm{Re}\big(\vec{e}\cdot\vec{b}^{*}\big) \;&=\; 2\mathrm{Re}\left[\big(\epsilon\vec{j}\;+\;\vec{J}\times\vec{b}\;+\;\vec{j}\times\vec{B}\big)\cdot\vec{b}^{*}\right] \\ &=\; 2\mathrm{Re}\left[\epsilon\vec{j}\cdot\vec{b}^{*}\;+\;\vec{J}\cdot\big(\vec{b}\times\vec{b}^{*}\big)\;+\;\vec{B}\cdot\big(\vec{b}^{*}\times\vec{j}\big)\right] \\ &=\; 2\epsilon\mathrm{Re}\big(\vec{j}\cdot\vec{b}^{*}\big)\;+\;\vec{J}\cdot 2\mathrm{Re}\big(\vec{b}\times\vec{b}^{*}\big)\;+\;\epsilon\vec{J}\cdot\vec{B} \;\;. \end{aligned}$$

Since $\mathrm{Re}\big(\vec{b}\times\vec{b}^{*}\big)=0$, the steady-state helicity conservation equation becomes

$$2\mathrm{Re}\Big\{i\big[\;\vec{e}(r=1)\times\vec{e}^{\,*}(r=1)\;\big]\Big\}_{\mathrm{radial}} \;+\; \epsilon\int_0^1\Big[2\mathrm{Re}\big(\vec{j}\cdot\vec{b}^{*}\big)\;+\;\vec{J}\cdot\vec{B}\Big]\,rdr \;=\; 0 \;\;. \qquad (3.120)$$

Hence, the incident helicity flux is balanced by A.C. dissipation $\vec{j}\cdot\vec{b}^{*}$ and D.C. dissipation, $\vec{J}\cdot\vec{B}$. For current drive, one is interested in minimizing the A.C. dissipation of helicity.

The helicity dissipation term can be written as

$$2\mathrm{Re}\;\left(\vec{j}\cdot\vec{b}^{*}\right)\;+\;\vec{J}\cdot\vec{B} \;=\; 2\left(\vec{j}_a\cdot\vec{b}_a^{*}\;+\;\vec{j}_b\cdot\vec{b}_b^{*}\right)\;+\;\vec{J}\cdot\vec{B} \;\;.$$

For the case where $\epsilon \rightarrow 0$, $B_a \rightarrow \infty$, the current $\vec{j}_b$ scales with ϵ [Eqs.(3.104)-(3.105)]. Using Eq.(3.117), the helicity dissipation term can be written as,

$$2\mathrm{Re}\left(\vec{j}\cdot\vec{b}^*\right) + \vec{J}\cdot\vec{B} \approx 2\left(\frac{i}{\sqrt{2}}\vec{J}\right)\cdot\vec{b}_v^* + \vec{J}\cdot\vec{B} \ ,$$

where $\vec{b}_a \approx \vec{b}_v$ has been used (recall that the vacuum fields appear to lowest order in this limit). Since $|\vec{B}| \gg |\vec{b}_v|$, it follows that the AC dissipation is much smaller than the DC dissipation term by a factor, roughly, of $1/B_a$. We thus have an example of AC magnetic helicity injection with predominantly DC helicity dissipation in the limit where $\epsilon \rightarrow 0$, $B_a \rightarrow \infty$.

3.8.3 Momentum Conservation and Current-Drive Efficiency

Using Ampere's law and a standard vector identity yields,

$$\begin{aligned} \vec{J}' \times \vec{B}' &= -\vec{B}' \times \frac{\nabla \times \vec{B}'}{\alpha} \quad , \\ &= -\frac{1}{\alpha}\left\{ \nabla \left(B'^2/2\right) - \vec{B}' \cdot \nabla \vec{B}' \right\} \quad . \end{aligned}$$

Since $\nabla \cdot \vec{B}'\vec{B}' = \vec{B}'\nabla \cdot \vec{B}' + \vec{B}' \cdot \nabla \vec{B}'$, the momentum equation reads,

$$\nabla \cdot \left\{ \frac{1}{\alpha}\left[\frac{1}{2} B'^2 \mathrm{I} - \vec{B}'\vec{B}' \right] \right\} + \vec{J}' \times \vec{B}' = 0 \quad . \tag{3.121}$$

The tensor in the curly brackets is the momentum flux associated with the magnetic field — the magnetic component of the Maxwell stress tensor.

Let P_z represent the z-component of the momentum flux entering in the radial direction at $r = 1$. Then from Eq.(3.121),

$$P_z = -\frac{1}{\alpha} B'_r B'_z \quad .$$

Taking the time average then yields,

$$< P_z > = -\frac{1}{\alpha} 2\mathrm{Re}\left(b_r b_z^*\right) \quad , \tag{3.122}$$

where all quantities are evaluated at the plasma/vacuum interface, located at $r = 1$. In the vacuum region just outside the plasma boundary,

$$\begin{aligned} e_z - k e_\theta &= b_r \qquad \left(\text{using } \nabla \times \vec{e} = -\frac{\partial \vec{b}}{\partial \tau} \right) \quad , \\ b_z - k b_\theta &= 0 \qquad \left(\text{using } \nabla \times \vec{b} = 0 \right) \quad . \end{aligned}$$

Inserting the above into Eq.(3.122) yields

$$\begin{aligned} < P_z > &= -\frac{1}{\alpha} 2\mathrm{Re}\left[(e_z - k e_\theta) b_z^* \right] \quad , \\ &= -\frac{1}{\alpha} 2\mathrm{Re}\left[e_z b_z^* - k e_\theta b_z^* \right] \quad , \\ &= -\frac{1}{\alpha} 2\mathrm{Re}\left[e_z (k b_\theta^*) - k e_\theta b_z^* \right] \quad . \end{aligned}$$

Since the time-averaged radial Poynting vector is given by

$$< S_r >= 2\mathrm{Re}\left(e_\theta b_z^* - e_z b_\theta^*\right) \quad ,$$

we arrive at Klima's[11] relation,

$$< P_z > = \frac{k}{\alpha} < S_r > \quad , \tag{3.123}$$

which relates the time-averaged momentum flux and energy flux.

Taking the time average of the z-component of $\vec{J}' \times \vec{B}'$ yields

$$\begin{aligned} \left\langle \vec{J}' \times \vec{B}' \right\rangle_z &= \left\langle \vec{E}'_z - \epsilon \vec{J}'_z \right\rangle \quad , \\ &= -\epsilon J_z \quad , \end{aligned}$$

where Ohm's law, $\vec{E}' = \epsilon \vec{J}' + \vec{J}' \times \vec{B}'$, has been used (note that the electrostatic field only has a radial component). Thus, the time-averaged z-component of Eq.(3.121) yields

$$\langle P_z \rangle_{r=1} = \epsilon \int_0^1 J_z \, r dr \quad .$$

Combining the above with Klima's result [Eq.(3.123)] yields

$$\frac{\int_0^1 J_z r dr}{\langle S_r \rangle} = \frac{k}{\epsilon \alpha} \quad .$$

This expression for the normalized current-drive efficiency is exact and applies to *any* solution of the system S_1. The current-drive efficiency is inversely proportional to both the collision frequency and the phase velocity — a result previously quoted by Bellan[43].

3.9 Comparison With Experiment

Data from two representative $m = 1$ toroidal machines are tabulated in Table 3.1. The experiment of Hotta[16] et al. was performed at the Tokyo Institute of Technology on the TPX-W2 device. The experiment of Dutch and McCarthy[4] (DM) was performed at the Flinders University of South Australia on the rhythmac device. The geometry of these machines is similar: major radius of 25 cm, minor radius of 2.5 cm (Hotta), 5.0 cm (DM). The toroidal mode number (number of times the coils wrap around in the poloidal direction in one trip around the torus) is n=3 (Hotta) and n=4 (DM). In both experiments a DC toroidal current is observed, which is peaked on axis.

In both experiments the collision frequency ν_{ei} is inferred to be in the range of a few hundred Mhz, whereas the applied frequency is 843 kHz (Hotta) and 330 kHz (DM); the electron inertia is therefore unimportant here. The most striking difference in these experiments is the value of Ω_{ci} — the ion cyclotron frequency referred to the static toroidal field. The value Ω_{ci} = 1.56 MHz (Hotta) is well above the applied frequency, and Ω_{ci} = 12 kHz (DM) is well below the applied frequency. As discussed at the beginning of Chapter 3, the ion motion can be ignored if $\omega \gg \Omega_{ci}$ for the general case of nonzero k. Hence, Hotta's experiment falls in the standard MHD regime. Indeed, Hotta claims that his current-drive scheme relies on a compressional Alfven wave — an appropriate assumption, since $\omega \ll \Omega_{ci}$. However, the ion motion is likely to be unimportant in the experiment of DM, where the Hall analysis of Chapter 3 applies.

The MHD analysis of Chapter 2 leads to the prediction,

$$\frac{B_\theta^{\text{driven}}}{B_\omega} \sim \left(\frac{\omega/k}{v_a}\right)^2 \frac{B_\omega}{B_a}$$

[see Eq.(2.42)]. In the experiment of Hotta, $B_\omega/B_a \sim 0.0075$, $\omega/k \sim 4.4 \times 10^5$ m/s, $v_a \sim 4.4 \times 10^5$ — 1.4×10^6 m/s. For $(\omega/k)/v_a \sim 1$, the MHD theory predicts $B_\theta^{\rm driven}/B_\omega \sim B_\omega/B_a \sim 0.0075$, which can be compared to the experimentally observed value of $B_\theta^{\rm driven}/B_\omega \sim 0.67$. The MHD theory is overly pessimistic and underestimates this ratio by a factor, roughly, of 100.

The Hall MHD analysis of Chapter 3 predicts that the current resides in a skin layer of width $(1/\sqrt{2})(B_\omega/B_a)(1/kR)R$ for large values of B_a (where R is the minor radius). For the experiment of DM, $kR \sim 0.8$, $B_\omega/B_a \sim 0.6$, $R = 5$ cm, yielding a skin layer of width ~ 2.7 cm. A skin current was *not* observed in the experiment of DM. However, the value of B_ω was inferred, not measured, and there is some room for error here; whether or not a skin layer is expected here is probably too close to call. Furthermore, skin currents are known to be unstable to magnetic tearing and it is possible that anomalous current penetration is occurring here. In any case, more experimental work is needed to prove or dispute the main conclusions of Chapter 3. In particular, the dependence of the toroidal field should be investigated to determine whether skin currents appear for large B_a.

	Hotta et al.[16]	Dutch and McCarthy[4]
B_a	4000 G	300 G
f	843 kHz	330 kHz
λ	52 cm ($n = 3$)	40 cm ($n = 4$)
Major radius	25 cm	25 cm
Minor radius	2.5 cm	5.0 cm
Ω_{ci}	1.56 MHz (helium)	12 kHz (argon)
B_ω	30 G (measured directly)	150 - 200 G (inferred)
ω_{ce}	84 MHz	420 - 560 MHz
$B_{\text{poloidal}}^{\text{driven}}$	20 G	50 G
Filling Pressure	17.4 mTorr	1 mTorr
Density	$10^{13} - 10^{14}$ cm^{-3}	unknown
	(probe measurements)	
Driven	$\approx$ 200 A	$\approx$ 900 A
Integrated Current		
T_e	Few eV	unknown
	(probe measurements)	
ν_{ei}	Unknown — Probably in the range of a few hundred Mhz	

Table (3.1)

Chapter 4. Summary and Conclusions

The purpose of this thesis was to investigate the possibility of sustaining a steady toroidal current in a tokamak plasma through the nonlinear interaction of small fluid-type fluctuations. A systematic search was made to uncover a viable laminar model of oscillating-field current drive. All of these models were ultimately derived from the two-fluid plasma equations. At low frequencies and long wavelengths, the standard MHD equations provide an adequate approximation to the full two-fluid equations; in this case the $< \vec{u} \times \vec{b} >$ EMF is the dominant current-drive mechanism. At higher frequencies, where the ion motion can be ignored, the $< \vec{j} \times \vec{b} >$ Hall EMF is the dominant current-drive mechanism.

At frequencies for which the standard MHD equations apply, models with azimuthal symmetry were first analyzed. These dynamo models were based on the interaction of a resistive diffusion mode and a compressional Alfven wave. Since the resulting EMF resides in a narrow skin layer near the wall, these models were very sensitive to assumptions made regarding plasma behavior near the wall. Three different models of the plasma/wall interaction were proposed. In the first model, the radial fluid velocity is nonvanishing at the wall so that a finite flux of plasma is delivered to the wall. In a second model, proposed by Liewer et al.[22], a vacuum region exists, separating the plasma from the wall. In this model, the plasma/vacuum interface must quiver in the radial direction, which significantly reduces the resulting EMF; the driven DC poloidal field is restricted to a small fraction of the AC poloidal field. A third model was proposed in which finite pressure was added to the MHD equations. In this case the motion of the plasma/vacuum interface can be eliminated, and yet dynamo action can still occur within a narrow skin layer near

the wall. However, it again was found that the resulting dynamo effect is too weak to be of practical interest. The dynamo action is significant only in the first model, where plasma is created and destroyed at the wall.

Exact solutions of the linearized, pressureless MHD equations with $m = 1$ helical structure were presented. This model offered three potential advantages over the $m = 0$ models described above: (1) Only $m = 1$ modes can have a finite EMF on axis (a consequence of the "regularity rules" given in Appendix 1); (2) the helical structure breaks the high-degree of symmetry that may have precluded dynamo action in earlier models; and (3) the velocity field carries helicity $\vec{u} \cdot \nabla \times \vec{u}$ which is required for dynamo action. Unfortunately, the helical MHD models again predict that the driven DC fields can be only a small fraction of the AC fields. For comparison, in the experimental work of Hotta et al.[16], $m = 1$ MHD activity is induced within a toroidal device producing a net DC current with $B_\theta^{\text{driven}}/B_\omega \sim 0.67$. Although the driven DC field is smaller than the applied field, the ratio is roughly 100 times greater than that predicted by the MHD calculation; it is not known why the theory underestimates the driven current. Hotta appears to be operating at a point where the phase velocity of the applied wave is tuned to match the Alfven velocity of the plasma. Although our theory does not predict any special benefit from operating near the Alfven speed, Hotta's experimental result may point to some sort of beneficial Alfven resonance, which should be explored in future work.

It was found that all standard MHD models result in an EMF that is too weak for practical fusion applications. An antidynamo argument was given, offered by Professor Roy Gould[24], in which the MHD plasma is divided into an infinite number of closed filamentary loops. If the standard MHD Ohm's law is adopted, then the

time-averaged line integral $\left\langle \int_c \vec{J} \cdot d\vec{l} \right\rangle$ taken around any one of these closed filaments must vanish — which implies, at best, a very weak dynamo effect. However, by adding the Hall EMF, the possibility exists of driving a significant current through the interaction of time-periodic fields.

A model based on the Hall EMF $< \vec{j} \times \vec{b} >$ was presented in Chapter 3. This model is a nonzero k analogue of the rotamak, a device that relies on a transverse rotating magnetic field to generate a compact torus. Many significant differences were found between the rotamak and the nonzero k analogue. First, the rotamak can operate at frequencies well below Ω_{ci} (the ion cyclotron frequency referred to the static magnetic field) since, in the idealized geometry where $\frac{\partial}{\partial z} = 0$, the static field decouples from the fluid motion. The DC flux-conserving motion found in the rigid-rotor solution of the rotamak has only a very restrictive analogue for nonzero k; DC flux-conserving motion for nonzero k is possible only when the toroidal field vanishes and when the DC fields are a small fraction of the AC fields. In general, for nonzero k, the flux-conserving motion consists of a DC component and an AC component of roughly equal magnitude, with the current confined to a skin layer for large values of kB_a. The analytical work was compared with the experimental work of Dutch and McCarthy[4]. Although a skin current was not observed, there is not yet enough experimental evidence to support or dispute the conclusions of Chapter 3.

The conservation laws of energy, magnetic helicity, and momentum were considered in detail. For any solution of the Hall MHD system, the incident energy flux is dissipated by the AC fields and the DC fields. For the limit of very small resistivity and large toroidal field strength, the incident energy is equally divided

between AC and DC dissipation (a result first given by Bertram[36]). In the same limit, the incident AC helicity flux is dissipated almost entirely by the DC fields. The current-drive efficiency was calculated exactly using Klima's[11] formula relating energy flux to momentum flux. For any solution of the truncated system S_1, the current-drive efficiency is inversely proportional to both the phase velocity of the applied field and the collision frequency.

Studies of OFCD schemes are still in their infancy. The toroidal devices built to date are small-scale machines with relatively high resistivity, low field strength, and poor energy confinement. The strength of the driven DC fields is typically a fraction of the applied field strength. Nevertheless, the lifetime of these devices is limited not by plasma disruptions, but by the limited duration of the RF generators used to power the external circuitry. From an empirical standpoint, one important principle has been clearly established on these small machines: Maintaining a traveling wave in the toroidal direction results in a net DC current. In contrast, helicity injection experiments, which rely on a standing-wave pattern, have produced no current or have degraded the toroidal current. Standing wave patterns are capable of injecting magnetic helicity, but not momentum. Thus, it is very likely that traveling waves will be employed in future OFCD schemes. However, a great deal of experimental and theoretical work is necessary to assess how the current-drive parameters will scale to fusion reactor conditions.

It was argued in Chapter 3 that the ion motion is likely to be important at frequencies below Ω_{ci} (the ion cyclotron frequency referred to the static magnetic field) for nonzero k. This point of view is not commonly shared by other investigators in this field. The relatively tractable Hall MHD equations were used with

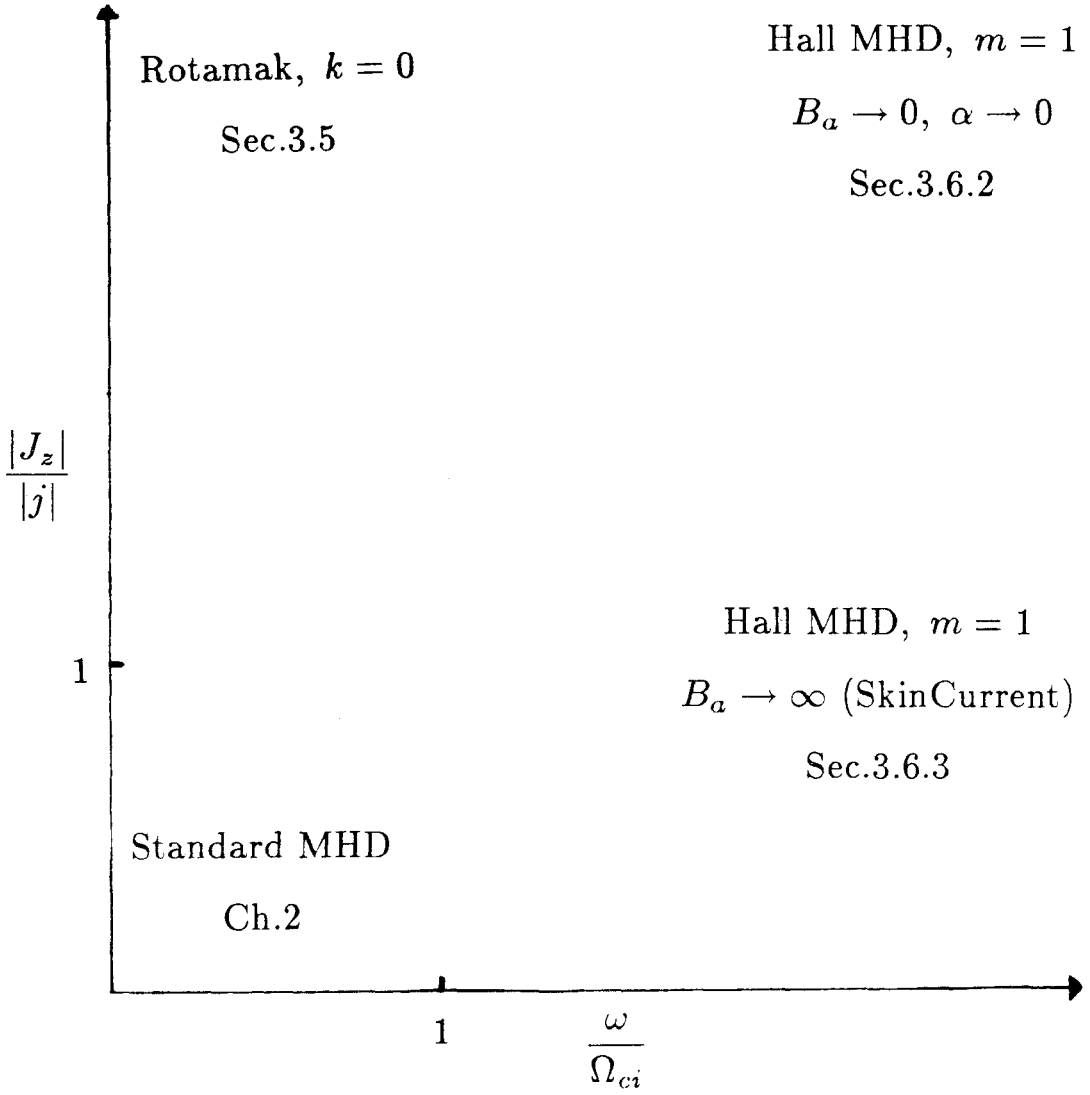

Figure 4.1. Schematic representation of the major results. The Hall MHD equations are valid at frequencies $\omega \gg \Omega_{ci}$ ($\Omega_{ci} = qB_a/m_i$) — except in the case of the rotamak, where the oscillating electric field is in the direction of B_a. A DC flux-conserving motion results as $\epsilon \to 0$ for the case of the rotamak and for the case of the rhythmac (provided that $B_a \to 0$, $\alpha \to 0$). For the rhythmac, all currents are confined to a skin layer as $B_a \to \infty$, with $|J_z|/|j|$ approaching unity.

success to describe the rotamak, and investigators were quick to adopt the same set of equations for nonzero k devices. The Hall MHD equations apply to the rotamak at frequencies well below Ω_{ci} because of the special geometry of the rotamak, where the oscillating electric field is parallel to the static magnetic field. The Hall MHD equations can be used to describe the nonzero k analogue of the rotamak — but only at much higher frequencies, above Ω_{ci}. Such frequencies would be prohibitively high for a fusion plasma. Hence, the analysis of Chapter 3 is likely to be valid for the standard rotamak or for nonzero k devices with relatively low static fields, such as the rhythmac device of Dutch and McCarthy[4].

The major results of this thesis are illustrated schematically in Fig.4.1. As mentioned above, the Hall MHD equations are valid only at frequencies well above Ω_{ci} — except in the case of the standard rotamak, where the oscillating electric field is parallel to the static axial field. The ratio of the strength of the DC axial current to the strength of the oscillating current is always much less than unity in all standard MHD models. The ratio approaches infinity for the case of the rotamak. The ratio also approaches infinity for the case of the rhythmac, in the restricted case where the axial magnetic field is vanishingly small and where the DC magnetic fields are a small fraction of the AC magnetic fields. The rhythmac currents are confined to a skin layer as $B_a \rightarrow \infty$, with the ratio of DC current strength to AC current strength approaching unity.

At toroidal field strengths consistent with fusion reactor conditions, it is likely that the $< \vec{u} \times \vec{b} >$ EMF in Ohm's law will be the dominant, current-drive mechanism. In chapter 2, we searched systematically for OFCD schemes based on the standard MHD equations and departed with a rather pessimistic outlook. It should

be noted, however, that Hotta's[16] experiment has produced currents that are 100 times greater than that predicted by our MHD analysis. Perhaps there are other effects that are outside the scope of our fluid-type models that eventually will be uncovered. In any event, progress in this undertaking, as in any scientific task, will occur through the interplay of careful analysis and experimentation. We look forward to a new body of experimental results soon to come from the new toroidal $m = 1$ device under construction at Caltech.

Appendix 1. Regularity Rules of Ralph Lewis[45]

Consider a smooth vector function $\vec{f}(x,y)$ defined in some domain surrounding the origin in the Cartesian (x,y)-plane. Assume that $\vec{f}$ and all derivatives of $\vec{f}$ with respect to x and y are defined and continuous in this domain. The same vector function can be written as a Fourier series in the cylindrical coordinates (r,θ),

$$\vec{f}(x,y) = \sum_{m=-\infty}^{\infty} \vec{f}_m(r)\, e^{im\theta} \quad ,$$

where the coefficients $\vec{f}_m(r)$ are complex-valued functions of r. Clearly, the coefficients $\vec{f}_m(r)$ cannot diverge as $r \to 0$, since $\vec{f}(x,y)$ is assumed to be well-behaved near the origin. In addition, there are more subtle rules governing the behavior of $\vec{f}_m(r)$ as $r \to 0$, which are fixed solely by the assumption that $\vec{f}$ has smooth derivatives at the origin. These so-called "regularity" rules, given by Ralph Lewis, are useful in analytical and numerical work in cylindrical geometry. Furthermore, the regularity rules demonstrate the important role of $m = 1$ modes in OFCD schemes.

Before treating the case of vector fields, we begin by considering the scalar function $g(x,y)$. All derivatives of $g(x,y)$ with respect to x and y are defined and continuous in a domain surrounding the origin. The function $g(x,y)$ can be written as a Fourier series,

$$g(x,y) = \sum_{m=-\infty}^{\infty} g_m \quad ,$$

where $g_m = (a_0^m + a_1^m r + a_2^m r^2 + \ldots)e^{im\theta}$ (superscripts will be dropped in what follows to reduce clutter). We require that derivatives of g_m must be defined and continuous as $r \to 0$. Noting that

$$e^{im\theta} = [\cos\theta + i\sin\theta]^m = \left[\frac{x}{r} + i\frac{y}{r}\right]^m \quad ,$$

we have

$$g_m = (a_0 + a_1 r + a_2 r^2 + \ldots)(x+iy)^m r^{-m} \quad .$$

The above can also be written as

$$g_m = (a_0 + a_1|z| + a_2|z|^2 + \ldots) z^m |z|^{-m} \quad , \tag{1}$$

where $z = x + iy$ and $|z| = \sqrt{x^2+y^2}$. The k^{th} term in the series given by Eq.(1) is

$$g_m^k = a_k z^m |z|^{k-m} \quad . \tag{2}$$

Suppose that p is a nonnegative integer. We consider the following cases:

Case (1)	$k - m = 2p$,
Case (2)	$k - m = 2p+1$,
Case (3)	$k - m =$ negative integer .

In case (1),

$$g_m^k = a_k z^m |z|^{2p} = a_k (x+iy)^m (x^2+y^2)^p \quad .$$

Thus, g_m^k is a polynomial in x and y, which is analytic everywhere. In case (2),

$$g_m^k = \left\{ a_k z^m |z|^{2p} \right\} |z| \quad ,$$

which does not have smooth derivatives since the term $|z|$ spoils the continuity of the derivatives at the origin. For example, along the line $y = 0$, one has $|z| = |x|$, which has a discontinuous first derivative. Finally, consider case (3). Taking m derivatives of g_m^k with respect to x yields

$$\frac{d^m}{dx^m} g_m^k = a_k m! |z|^{k-m} + \text{other terms} \quad .$$

The term $|z|^{k-m}$ diverges at the origin if $k-m$ is a negative integer.

In summary, the coefficients a_k are nonvanishing only in case (1) where $k-m = 2p$, or when $k = m,\ m+2,\ m+4,\ \ldots$. Thus,

$$g_m = r^m(c_0 + c_2r^2 + c_4r^4 + \ldots)e^{im\theta} \quad . \tag{3}$$

The Bessel function $J_n(x)$, where

$$J_n(x) = x^n \frac{1}{2^n\Gamma(n+1)}\left[1 - \frac{x^2}{2(2n+2)} + \frac{x^4}{2\cdot 4(2n+2)(2n+4)} - \cdots\right] \quad ,$$

is of the form given by Eq. (3). It follows that Fourier-Bessel expansions of the form $\sum c_m J_m(r)e^{im\theta}$ automatically fulfill the regularity conditions as $r \to 0$.

Next, consider the vector function,

$$\vec{A} = \left[a_r(r)\hat{r} + a_\theta(r)\hat{\theta} + a_z(r)\hat{z}\right] e^{im\theta} \quad .$$

Substituting $\hat{r} = \hat{x}\cos\theta + \hat{y}\sin\theta$, $\hat{\theta} = -\hat{x}\sin\theta + \hat{y}\cos\theta$, expanding in exponentials, and rearranging gives

$$\begin{aligned}\vec{A} = {} & \hat{x}\left[i(a_r + ia_\theta)e^{i(m+1)\theta} + i(a_r - ia_\theta)e^{i(m-1)\theta}\right](1/2i) \\ & + \hat{y}\left[(a_r + ia_\theta)e^{i(m+1)\theta} - (a_r - ia_\theta)e^{i(m-1)\theta}\right](1/2i) \quad . \\ & + \hat{z}\left[a_z e^{im\theta}\right]\end{aligned}$$

The $\hat{x}, \hat{y}, \hat{z}$ components now yield three scalar functions, each of which must obey the regularity rules for scalar functions. Applying the regularity rules gives, for $m \geq 1$,

$$a_r + ia_\theta = r^{m+1}(c_0 + c_2r^2 + c_4r^4 + \ldots) \quad , \tag{4}$$

$$a_r - ia_\theta = r^{m-1}(d_0 + d_2r^2 + d_4r^4 + \ldots) \quad , \tag{5}$$

$$a_z = r^m(e_0 + e_2 r^2 + e_4 r^4 + \ldots) \quad .$$

Solving Eqs. (4) and (5) for a_r and a_θ gives,

$$2a_r = r^{m-1}\left[d_0 + (c_0 + d_2)r^2 + (c_2 + d_4)r^4 + \ldots\right] \quad , \tag{6}$$

$$2ia_\theta = r^{m-1}\left[-d_0 + (c_0 - d_2)r^2 + (c_2 - d_4)r^4 + \ldots\right] \quad . \tag{7}$$

Note that the leading terms in Eqs. (6)-(7) are not independent (i.e., $a_\theta = ia_r$ to lowest order) whereas all higher-order terms are independent.

We summarize here the regularity rules for vector and scalar fields.

Regularity Rules

Let $g(r)e^{im\theta}$ represent a scalar field with smooth derivatives at $r = 0$. Then,

$$g(r) = r^m(c_0 + c_2 r^2 + c_4 r^4 + \ldots) \quad . \tag{8}$$

Let $[a_r(r)\ ,\ a_\theta(r)\ ,\ a_z(r)]\, e^{im\theta}$ represent a vector field with smooth derivatives at $r = 0$. Then, for $m \geq 1$ (choosing a different set of constants),

$$a_r = r^{m-1}(\gamma_0 + \gamma_2 r^2 + \gamma_4 r^4 + \ldots) \quad (m \geq 1) \quad , \tag{9}$$

$$a_\theta = r^{m-1}(i\gamma_0 + \beta_2 r^2 + \beta_4 r^4 + \ldots) \quad (m \geq 1) \quad , \tag{10}$$

$$a_z = r^m(\alpha_0 + \alpha_2 r^2 + \alpha_4 r^4 + \ldots) \quad (m \geq 0) \quad .$$

For $m = 0$,

$$a_r = r(\gamma_0 + \gamma_2 r^2 + \gamma_4 r^4 + \ldots) \quad (m = 0) \quad , \tag{11}$$

$$a_\theta = r(\beta_0 + \beta_2 r^2 + \beta_4 r^4 + \ldots) \quad (m = 0) \quad . \tag{12}$$

For $m = 0$, a_r and a_θ scale with r to lowest order and the lowest-order constants are now independent.

Note that a_r and a_θ are nonvanishing at $r = 0$, only when $m = 1$. If, for example, a toroidal current J_z is being maintained by the nonlinear interaction of oscillating fields $< v_\theta b_r >$ or $< j_\theta b_r >$, then the driven current can be finite at the axis only if the oscillating fields have $m = 1$ structure.

Appendix 2. Comment on the Calculation of Dutch and McCarthy[3]

In Ref.(3) it is assumed that all radial currents vanish for the case of nonzero k. This is true for the standard rotamak, because the rotating electric field is strictly in the z direction. It is shown here that the assumption $j_r = 0$ leads to an inconsistency in Ref.(3).

The field quantities in Ref.(3) are divided into a steady part (denoted by upper-case) and an oscillating part (denoted by lower-case). It is assumed initially that $j_r = 0$. It is then argued that $b_\varsigma = 0$ (follows from the $\hat{r}$ component of Ampere's law), $j_\chi = 0$ (follows from $\nabla \cdot \vec{j} = 0$), $J_{0\varsigma} = 0$ [follows from follows from Eq.(3) in Ref.(3)] and $J_{0r} = 0$ (follows from $\nabla \cdot \vec{J}_0(r) = 0$). Thus, $\vec{J}_0$ points only in the $\hat{\chi}$ direction and $\vec{j}$ points only in the $\hat{\varsigma}$ direction.

The $\hat{r}, \hat{\chi}$ and $\hat{\varsigma}$ components of Ohm's law [Eq. (4) in Ref.(3)] are given by

$$e_r + \frac{j_\varsigma B_{0\chi}}{ne} = 0\,, \qquad e_\chi = 0\,, \qquad e_\varsigma + \frac{J_{0\chi} b_r}{ne} = \eta j_\varsigma\,. \tag{1a,b,c}$$

The $\hat{r}$ and $\hat{\varsigma}$ components of Faraday's law are given by

$$k_0 e_\varsigma = -\omega b_r\,, \qquad ik_0 e_r + \frac{2km}{k_0^2 r^2} e_\varsigma = 0\,. \tag{2a,b}$$

Combining Eqs. (1c) and (2a) gives

$$j_\varsigma = \frac{1}{\eta}\Big[\frac{J_{0\chi}}{ne} - \frac{w}{k_0}\Big] b_r\,. \tag{3}$$

Inserting Eqs. (1a) and (2a) into Eq. (2b) gives

$$j_\varsigma = i\Big[\frac{2ne\omega km}{k_0^4 r^2 B_{0\chi}}\Big] b_r\,. \tag{4}$$

According to Eq. (3), j_ς and b_r are in phase [as stated in Ref.(3)], whereas Eq.(4) indicates that j_ς and b_r are 90° out of phase. Thus, Eqs.(3) and (4) can be satisfied if both j_ς and b_r vanish, in contradiction to the solution given in Ref.(3).

Appendix 3. Solution of System S_1 For Large Resistivity

For completeness, solutions of the system S_1 will be given for the limit $\delta = \omega_{ce}/\nu_{ei} \to 0$, the limit of large resistivity. The system S_1 now reads,

$$-\delta\frac{\partial\vec{b}}{\partial\tau} = \nabla\times\vec{j} + \delta\nabla\times\left(\vec{J}\times\vec{b} + \vec{j}\times\vec{B}\right) , \tag{1}$$

$$\vec{J} + 2\delta\mathrm{Re}\left(\vec{j}\times\vec{b}^{*}\right) = 0 . \tag{2}$$

Expanding in powers of δ,

$$\vec{b} = \vec{b}_0 + \delta\vec{b}_1 + \delta^2\vec{b}_2 + \dots ,$$

yields, to lowest order in δ,

$$\nabla\times\vec{j}_0 = 0 , \quad \vec{J}_0 = 0 .$$

Since $\nabla\cdot\vec{j}_0 = 0$ and since $j_{0r} = 0$ at $r = 1$, then it follows that the oscillating current $\vec{j}_0$ must vanish. The zero-order magnetic fields must therefore be vacuum fields, created solely by external currents:

$$\vec{b}_0 = \vec{b}_v = \left\{I_1' , \frac{i}{kr}I_1 , iI_1\right\} ,$$

$$\vec{B}_0 = B_a\hat{z} .$$

To first order in δ, Eq.(1) yields

$$-\frac{\partial\vec{b}_v}{\partial\tau} = \nabla\times\vec{j}_1 , \tag{3}$$

since $\vec{j}_0 = 0$ and $\vec{J}_0 = 0$. To second order in δ, Eq.(2) gives

$$\vec{J}_2 + 2\mathrm{Re}\left(\vec{j}_1\times\vec{b}_v^{*}\right) = 0 . \tag{4}$$

Taking the curl of Eq.(3), noting that $\nabla \cdot \vec{j}_1 = 0$ and $\nabla \times \vec{b}_v = 0$, yields,

$$\nabla^2 \vec{j}_1 \;=\; 0 \;\; .$$

The $\hat{z}$-component of the above gives

$$j_{1z} \;=\; C_z I_1(kr) \;\; , \tag{5}$$

where C_z is a constant to be determined. The $\hat{r}$ and $\hat{\theta}$ components of Eq.(3) read,

$$\frac{i}{r} j_{1z} \;-\; ikj_{1\theta} \;=\; i\frac{d}{d(kr)} I_1(kr) \;\; , \tag{6}$$

$$ikj_{1r} \;-\; \frac{d}{dr} j_{1z} \;=\; -\frac{1}{kr} I_1(kr) \;\; . \tag{7}$$

It is now straightforward to evaluate all components of $\vec{j}_1$. The constant C_z can be found by using the boundary condition $j_{1r}(r = 1) \;=\; 0$. The final expressions for $\vec{j}_1$ and $\vec{J}_2$ are given by

$$\vec{j}_1 \;=\; \left\{ -i\Big(C_z I_1' - \frac{1}{k^2 r} I_1 \Big) \;,\; \frac{1}{k}\Big(\frac{C_z}{r} I_1 - I_1' \Big) \;,\; C_z I_1 \right\} \;\; ,$$

$$\vec{J}_2 \;=\; -\hat{\theta}\frac{2}{r}\left(2C_z r I_1 I_1' - \frac{I_1^2}{k^2} \right) \;-\; \hat{z}\frac{2}{kr^2}\left(r^2 (I_1')^2 + \frac{I_1^2}{k^2} - 2C_z r I_1 I_1' \right) \;\; ,$$

$$\text{where} \;\; C_z \;=\; \frac{1}{k^2}\frac{I_1(k)}{I_1'(k)} \;\; .$$

References

[1] N.J. Fisch, Rev. Mod. Phys. **59**, 175 (1987).

[2]T.H. Jensen and M.S. Chu, Phys. Fluids **27**, 2881 (1984).

[3]M.J. Dutch, A.L. McCarthy, and R.G. Storer, Phys. Rev. Lett. **56**, 1563 (1986).

[4]M. Dutch and A.L. McCarthy, Plasma Physics and Controlled Fusion **28**, 695 (1986)

[5]K.F. Schoenberg, R.F. Gribble, and D.A. Baker, *Oscillating Field Current Drive for Reversed Field Pinch Discharges*, Los Alamos report LA-9161-MS, June 1984

[6]K.F. Schoenberg, C.J Buchenauer, R.S. Massey, J.G Melton, R.W. Moses, A.Nebal, and J.A. Phillips, Phys. Fluids **27**, 548 (1984)

[7]M.K. Bevir and J.W. Gray, *Relaxation, Flux Consumption and Quasi-Steady-State Pinches* Culham Laboratory, Euratom/UKAEA Fusion Association report.

[8]M.K. Bevir and C.G. Gimblett, Phys. Fluids **28**, 1826 (1985).

[9]T.H. Jensen and M.S. Chu, Phys. Fluids **27**, 2881 (1984).

[10]P.M. Bellan, Phys. Rev. Lett. **57**, 2383 (1986).

[11]R. Klima, Plasma Phys. **15**, 1031 (1973).

[12]W.N. Hugrass, I.R. Jones, M.G.R. Phillips, J. Plasma Phys. **26**, 465 (1981).

[13] K. Hirano et al., Phys. Lett. **36A**, 215 (1971).

[14] M.J. Fukuda, Phys. Soc. Japan **45**, 283 (1978).

[15]M.J. Dutch and A.L. McCarthy, *Double Helix Current Drive in the RF Tokamak Device Rythmac*, IAEA report, Kyoto, Japan, 13-20 November 1986.

[16]E. Hotta, Jpn. J. Appl. Phys. **24**, 110 (1985).

[17]J.B. Taylor, Phys. Rev. Lett. **33**, 1139 (1974).

[18]J.M. Finn, Phys. Fluids **29**, 2630 (1986).

[19]H.R. Strauss and D.S. Harned, Phys. Fluids **30**, 164 (1987).

[20]R.A. Nebel, R.A. Scardovelli, K.A. Werley, G.H. Miley, D.S. Harned, H.R. Strauss, D.D. Schnack and Z. Mikic *Modeling and Transport Simulations of Oscillating Field Current Drive in the RFP*, Los Alamos Report LA-UR-86-3349.

[21]P.M. Bellan, Phys. Rev. Lett. **54**, 1381 (1985).

[22]P.C. Liewer, R.W. Gould, and P.M. Bellan, *One-Dimensional Modeling of AC Helicity Injection for Tokamaks* (submitted for publication).

[23]H.K. Moffatt, *Magnetic Field Generation in Electically Conduction Fluids* (Cambridge University Press, Cambridge, England, 1978).

[24]R.W. Gould (private communication).

[25]T.G. Cowling, Mon. Not. Roy. Astr. Soc. **94**, 39 (1934).

[26]K.S. Reidel, Phys. Fluids **29**, 1093 (1986).

[27]Y.P. Pao and W. Kerner, Phys. Fluids **28**, 287 (1985).

[28]T. Ohkawa, *Plasma Current Drive By Injection of Photons With Helicity* (submitted to Comments on Plasma Phys. and Controlled Fusion).

[29]V.S. Chan and T. Ohkawa, *Current Drive in High Density Plasmas With Circularly Polarized Waves* (submitted to Phys. Rev. Lett.)

[30]T. Ohkawa, V.S. Chan, M.S. Chu, R.R. Dominguez, and R.L. Miller, *New Current Drive and Confinement Techniques for Improved Tokamak Operation*, Twelfth International Conference on Plasma Physics, October 12-19,1988, Nice, France.

[31]I.R. Jones, Comments Plasma Phys. Controlled Fusion **10**, 115 (1986).

[32]N.J. Fisch and T. Watanabe, Nucl. Fusion **22**, 423 (1982).

[33]W.K. Bertram, J. Plasma Physics **37**, 423 (1987).

[34]W.N. Hugrass and R.C. Grimm, J. Plasma Physics **26**, 455 (1981).

[35]I.R. Jones and W.N. Hugrass, J. Plasma Physics **26**, 441 (1981).

[36]W.K. Bertram, *Mode-Beating in $J \times B$ Current Drive* (Submitted for publication).

[37]W.K. Bertram, *A Numerical Study of Double-Helix Current Drive For Tokamaks*, (submitted for publication).

[38]W.N. Hugrass, J. Plasma Physics **28**, 369 (1982)

[39]N.A. Krall and A.W. Trivelpiece "Principles of Plasma Physics", International Series in Pure and Applied Physics, McGraw-Hill.

[40]G. Bateman, *MHD Instabilities* The MIT Press, Cambridge, Massachusettes.

[41]W.N. Hugrass, *A General Physical Model for RMF Current Drive* (submitted to Australian Journal of Physics).

[42]Professor N. Corngold (private communication).

[43]P.M. Bellan, *RF Current-Drive Efficiencies Derived Using Klima's Relation* (submitted for publication)

[44]V. Pereyra, Lect. Notes Comp. Sc. **76** 67 (1978).

[45]R. Lewis (private communication).